Issue no. 1 · 2005
ISMRM Edition

MAGNETOM FLASH

www.siemens.com/magnetom-world

Price 10,- EUR

Content

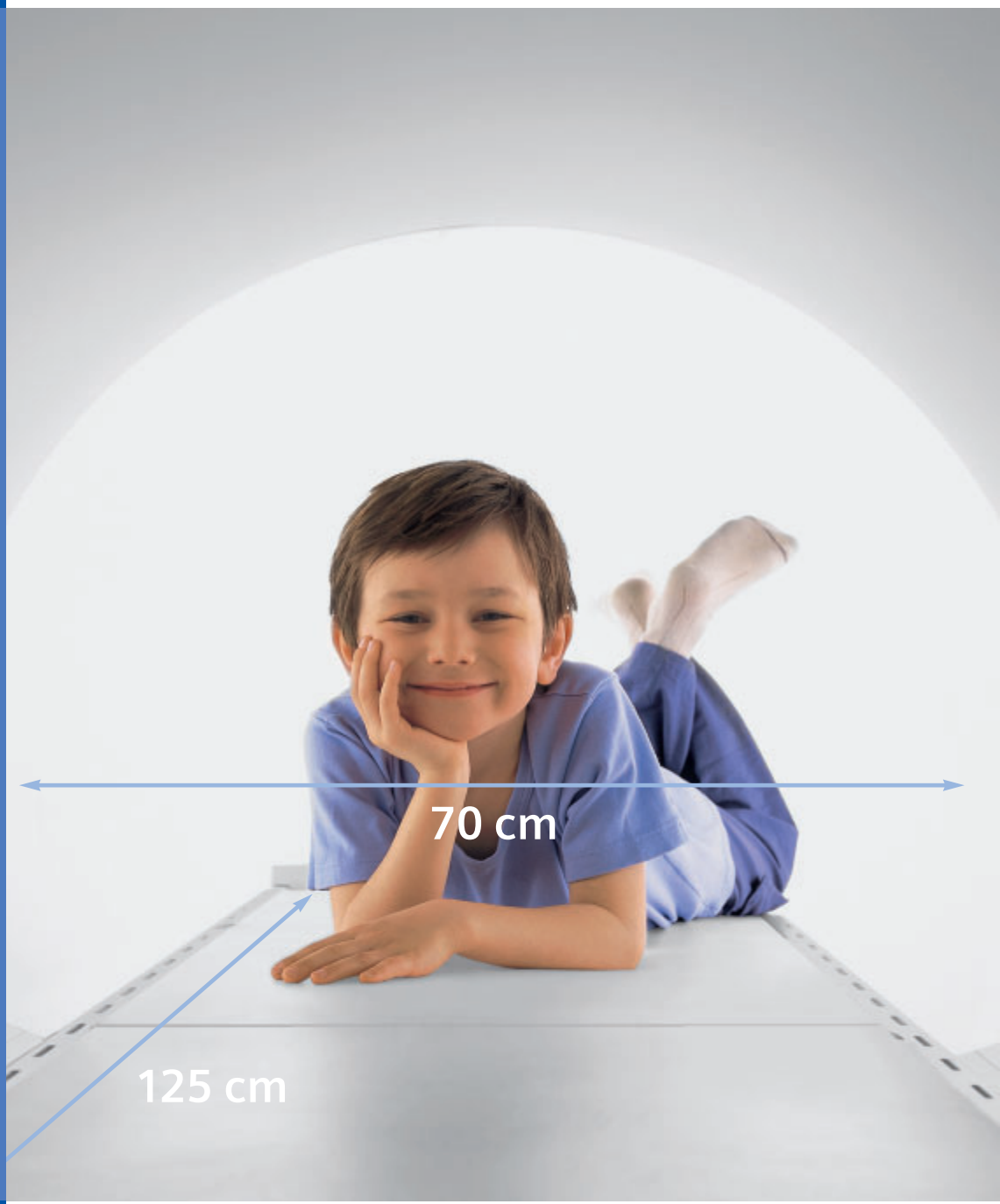

30

SIEMENS
medical

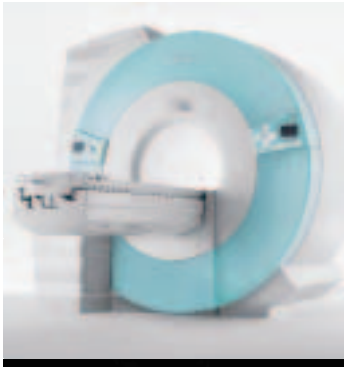

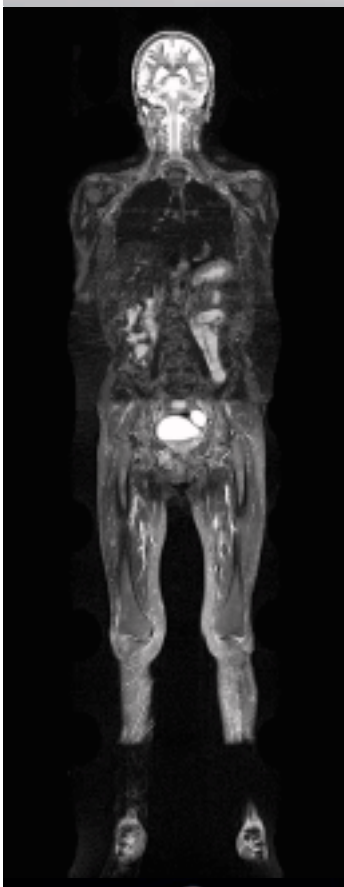

TECHNOLOGY

LIFE

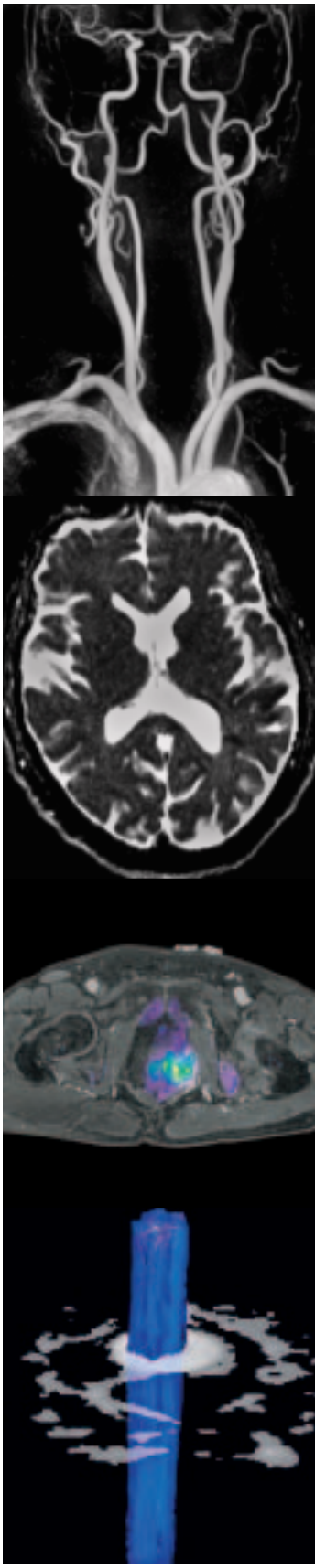

The information presented in MAGNETOM Flash is for illustration only and is not intended to be relied upon by the reader for instruction as to the practice of medicine. Any health care practitioner reading this information is reminded that they must use their own learning, training and expertise in dealing with their individual patients. This material does not substitute for that duty and is not intended by Siemens Medical Solutions to be used for any purpose in that regard.

The drugs and doses mentioned in MAGNETOM Flash are consistent with the approval labeling for uses and/or indications of the drug. The treating physician bears the sole responsibility for the diagnosis and treatment of patients, including drugs and doses prescribed in connection with such use. The Operating Instructions must always be strictly followed when operating the MR System. The source for the technical data is the corresponding data sheets.

MAGNETOM Espree

"It's just like CT"....

We have been hearing this more and more in Erlangen recently. Customer visits for MAGNETOM Espree have caused genuine excitement and almost always the same reaction from potential users: "The dimensions are like CT with its 70 cm patient bore and 125 cm short system."

But at the same time we have been asked some curious questions: "The bore is so large – can I really perform every kind of MR exam with Espree?". The answer: an unequivocal "Yes". Thanks to Tim technology, it is even possible to perform high resolution whole body imaging. In this latest MAGNETOM Flash magazine we include examples from the MR Center Bremen Mitte in Germany and from the University Hospital Basel, Switzerland, together with an interview with Dr. Sally McKinnon from the Turville Bay MRI and Radiation Oncology Center in Madison, USA.

Diffusion

In this issue of MAGNETOM Flash we have two articles from Japan and the U.S. showing the recent developments in body diffusion-weighted imaging.

Dr. Noriatsu Ichiba, from Jikei University Hospital, Tokyo, claims that the future of tumor imaging might belong to whole-body diffusion-weighted imaging with MR. He has already scanned more than 600 patients and has found it very useful to differentiate malignant from benign lesions. He has a name for the MR anatomical images fused with MR diffusion findings: "MR PET Imaging".

Dr. Bachir Taouli shows the preliminary liver diffusion imaging results from New York University. His results are also very promising.

Hong Kong Sanatorium and Hospital

This clinic's routine clinical services have benefited greatly from the MAGNETOM Trio system. The next generation 3T with Tim – to be installed in Hong Kong – will be one of the first in the world. MAGNETOM Flash reports on the fascinating imaging results and the philosophy of the Hong Kong Sanatorium and Hospital's radiology clinic in terms of 3T imaging.

Tim Matrix Modes

Another development in MR technology that works side-by-side with CT is the increased number of RF channels. CT has a larger number of detec-tor rows, producing impressive results through increased speed and higher resolution. MR technology has seen the effect of increasing the number of RF channels (32 with MAGNETOM Avanto) with more elements in array coils, resulting in faster imaging thanks to iPAT, our integrated Parallel Acquisition Technique. Here the Siemens unique Tim technology offers matrix modes, which will enable you to use your coils for either Parallel- or conventional imaging. Other systems require you to invest in dedicated parallel imaging coils in addition to the conventional coils. With Tim you have the flexibility to use up to 76 elements for either conventional or Parallel Imaging, with speeds up to 12 times faster than with conventional techniques. Read more about this revolutionary technology in our Technology section.

Enjoy this issue of MAGNETOM Flash...

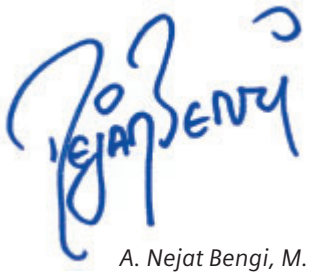

A. Nejat Bengi, M.D.
Editor in Chief

Editorial Team

More Space for You
70 cm (2'1") –
Open Bore MRI

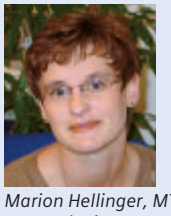

Marion Hellinger, MTRA
MR Marketing-Application Training, Erlangen

Lisa Reid,
US Installed Base Manager, Malvern, PA

Dagmar Thomsik-Schröpfer, Ph.D.
MR Marketing-Products, Erlangen

Antje Hellwich
Associate Editor

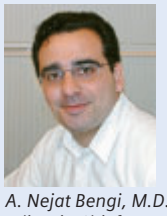

A. Nejat Bengi, M.D.
Editor in Chief

Heike Weh
Clinical Data Manager, Erlangen

Bernhard Baden
Clinical Data Manager, Erlangen

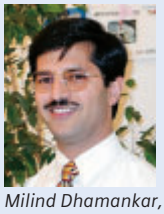

Milind Dhamankar, M.D.
Manager Clinical MR Research Collaborations, Siemens Medical Solutions USA

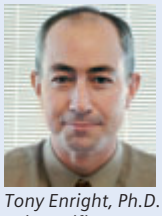

Tony Enright, Ph.D.
Asia Pacific Collaborations, Australia

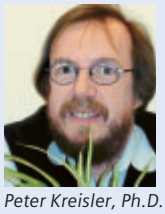

Peter Kreisler, Ph.D.
Collaborations & Applications, Erlangen

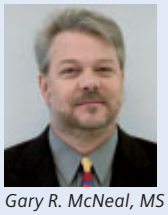

Gary R. McNeal, MS (BME)
Advanced Application Specialist Cardiovascular MR Imaging Siemens Medical Solutions USA

We thank Mr. Lowrence Tallentire for his editorial help.

Case Reports: MAGNETOM Espree 70 cm + 125 cm + 1.5T + Tim

The information presented in these case studies is for illustration only and is not intended to be relied upon by the reader for instruction as to the practice of medicine. Any health care practitioner reading this information is reminded that they must use their own learning, training and expertise in dealing with their individual patients. This material does not substitute for that duty and is not intended by Siemens Medical Solutions to be used for any purpose in that regard.

The drugs and doses mentioned herein are consistent with the approval labeling for uses and /or indications of the drug. The treating physician bears the sole responsibility for the diagnosis and treatment of patients, including drugs and doses prescribed in connection with such use. The Operating Instructions must always be strictly followed when operating the MR System. The source for the technical data is the corresponding data sheets.

Case Report: Wrist

Burckhard Terwey, M.D.
Markus Lentschig, M.D.

MR Zentrum Bremen Mitte
Bremen, Germany

Patient History

70-year-old patient with pain in the right wrist for 4 months, no trauma history.

Image Findings

Scapholunate dissociation due to ligament rupture is visible. There is a narrowing of space between the radius and navicular bone. At around the level of the interarticular disk there is a septated, dilated ganglion. The disk is intact.

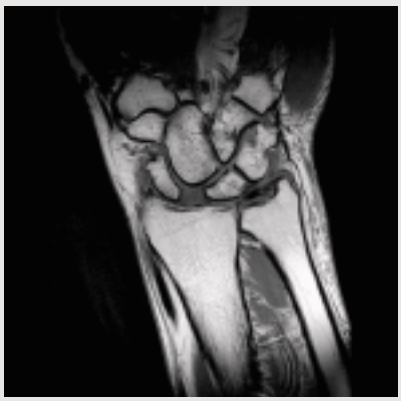

Figure 1 *Spin Echo (se2d), TR: 542 ms, TE: 23 ms, slice thickness: 2.5 mm, matrix: 512, FoV: 130 mm.*

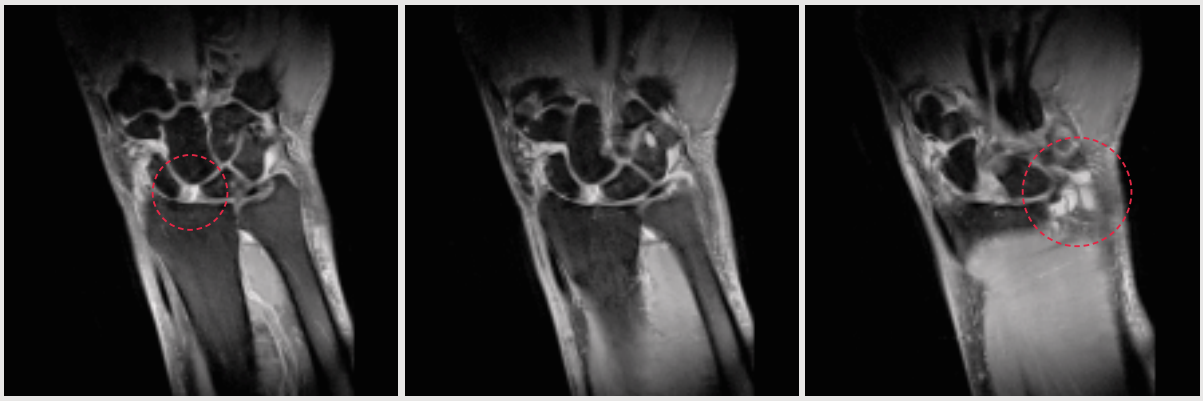

Figure 2 *Turbo Spin Echo (tse 2d) with fat saturation, TR: 3170 ms, TE: 24 ms, sl: 2.5 mm, matrix: 512, FoV: 130 mm.*

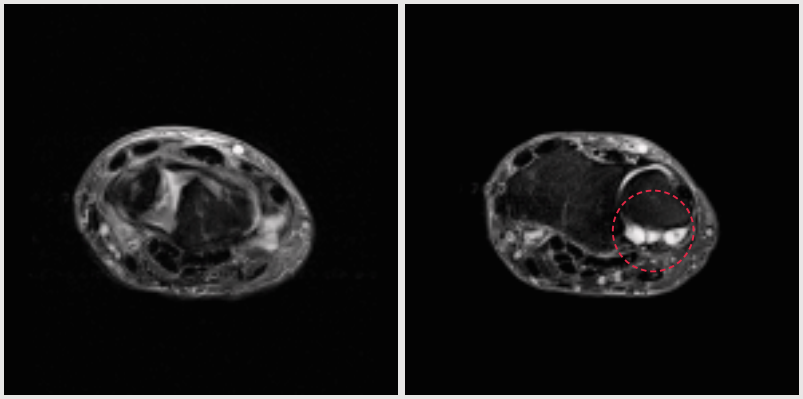

Figure 3 *Turbo Spin Echo (tse 2d), TR: 4770 ms, TE: 84 ms, matrix: 512, FoV: 120 mm.*

Case Report: Neurofibromatosis

Burckhard Terwey, M.D.
Markus Lentschig, M.D.

MR Zentrum Bremen Mitte
Bremen, Germany

Patient History

50-year-old patient with known neurofibromatosis type 1.

Image Findings

In the head images there was no finding of neurofibroma, meningioma or neurinoma. There are post ischemic changes in the right cerebellum.

At the cervical and thoracic levels (cervical 1 – cervical 3, thoracic 4) there are multiple neurinomas. At the lower leg level between the ligaments of the gastrocnemius muscle, extending lower and outer with diameters changing from 1-2 cm, there are neurofibromas. At the thorax wall on the left there is also a node visible.

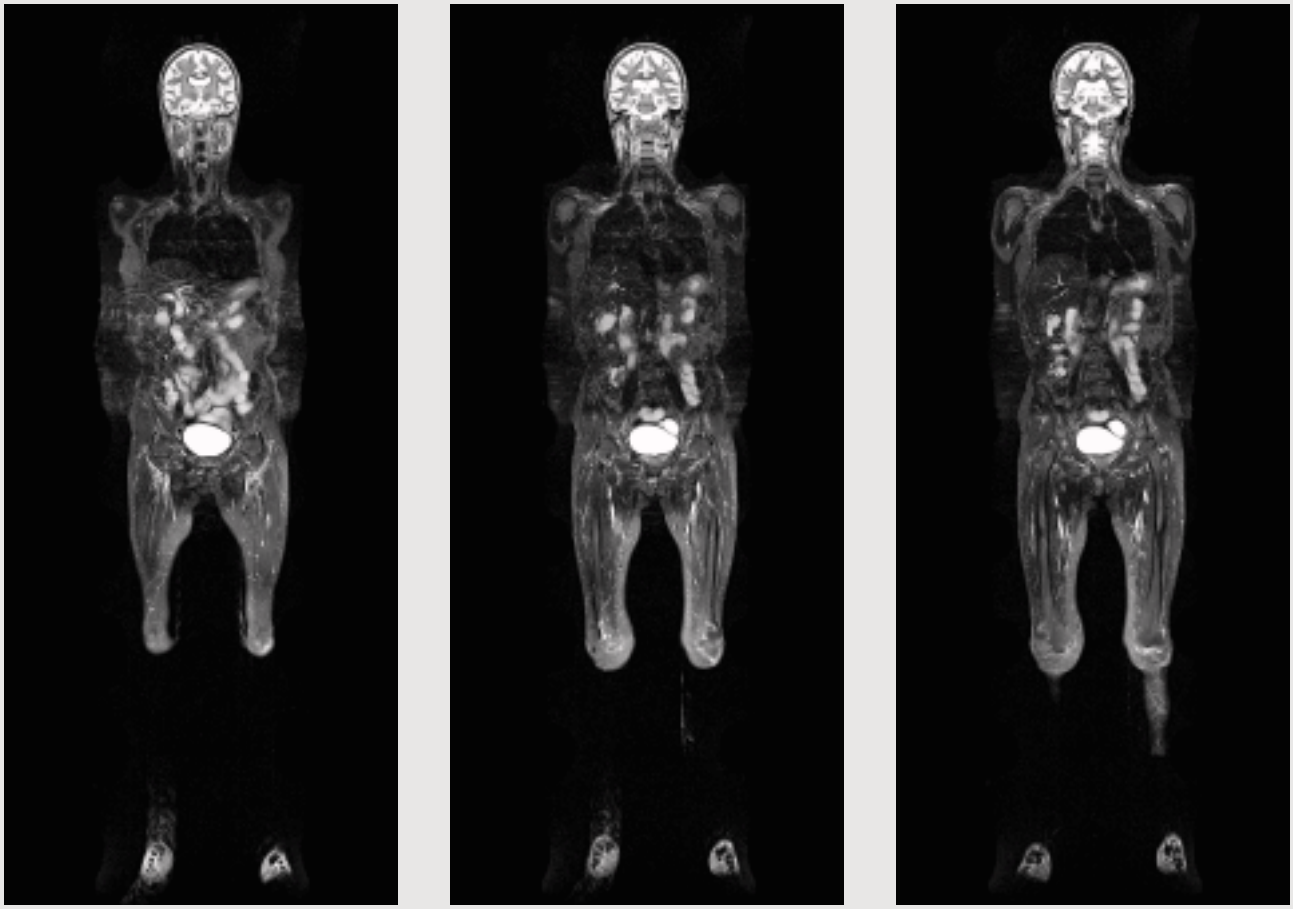

Figure 1 *Turbo Inversion Recovery (tir2d), TR: 5420 ms, TE: 87 ms, slice thickness: 6 mm, matrix: 384, FoV: 400 mm.*

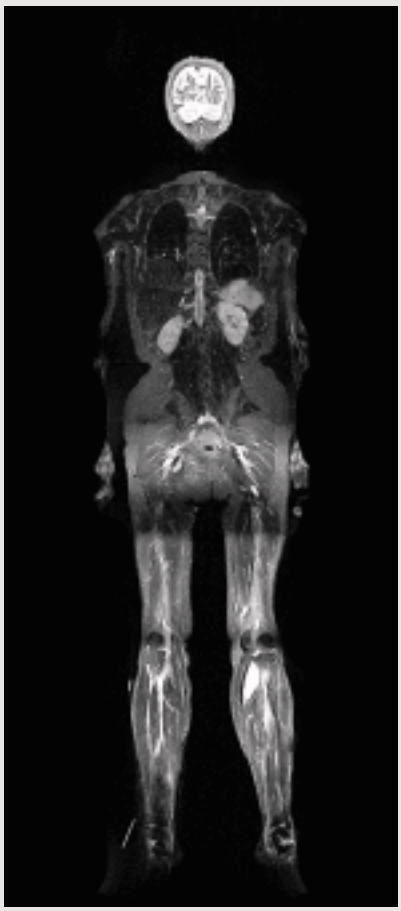

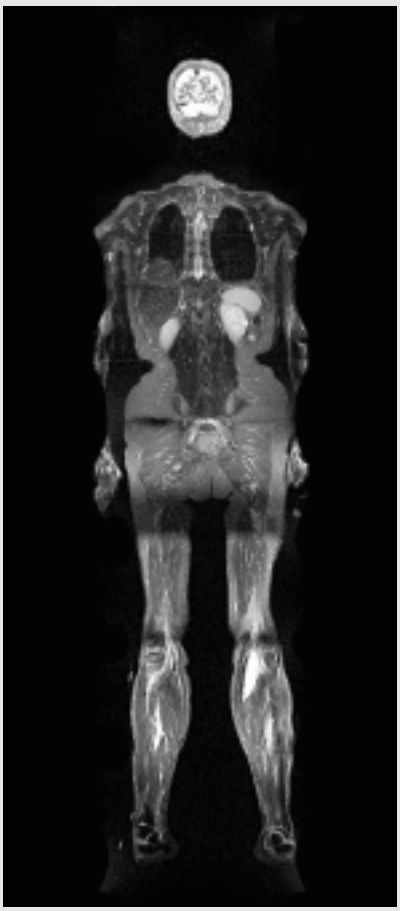

Case Report: Shoulder

Burckhard Terwey, M.D.
Markus Lentschig, M.D.

MR Zentrum Bremen Mitte
Bremen, Germany

Patient History

44-year-old patient who fell from a horse and suffered shoulder dislocation.

Image Findings

After a ventral and caudal dislocation of the shoulder, anterior labral tear and typical Hill-Sachs-Defect with inferior glenoid rim fracture.

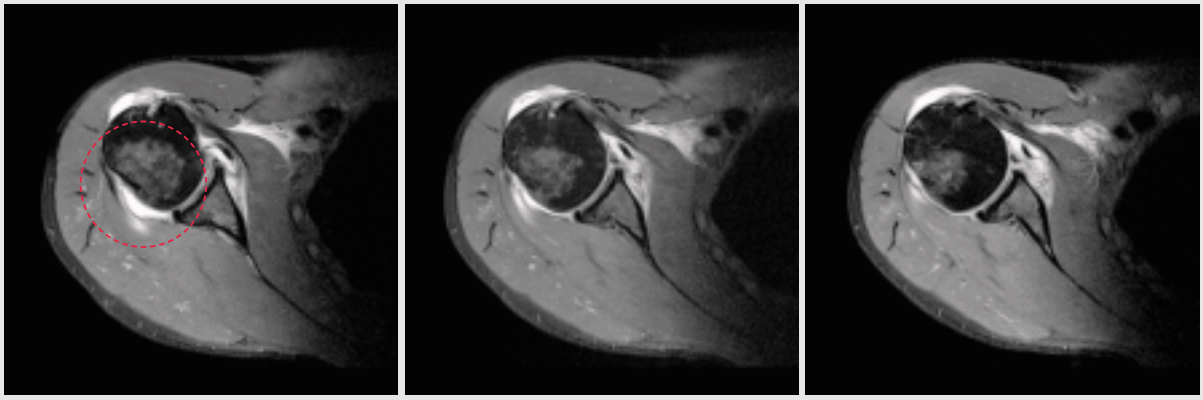

Figure 1 *Turbo Spin Echo (tse2d) with fat saturation, TR: 3670 ms, TE: 41 ms, slice thickness: 3 mm, matrix: 512, FoV: 200 mm.*

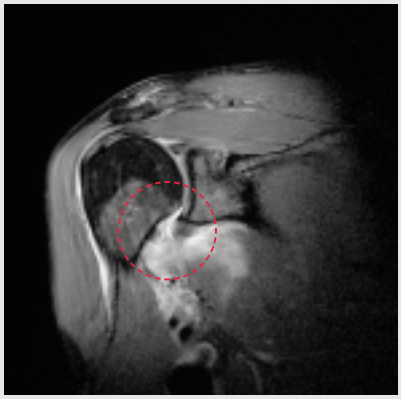

Figure 2 *Turbo Spin Echo (tse2d) with fat saturation, TR: 3800 ms, TE: 41 ms, matrix: 448, FoV: 180 mm.*

Case Report: Prostate Carcinoma

Burckhard Terwey, M.D.
Markus Lentschig, M.D.

MR Zentrum Bremen Mitte
Bremen, Germany

Patient History

65-year-old patient with prostate carcinoma. The question of lymph node infiltration has been asked.

Image Findings

Left lobe prostate carcinoma with extension beyond the prostate capsule and possible infiltration of the seminal vesicle. Local lymph node infiltration is not seen, pelvic bone metastasis is not observed.

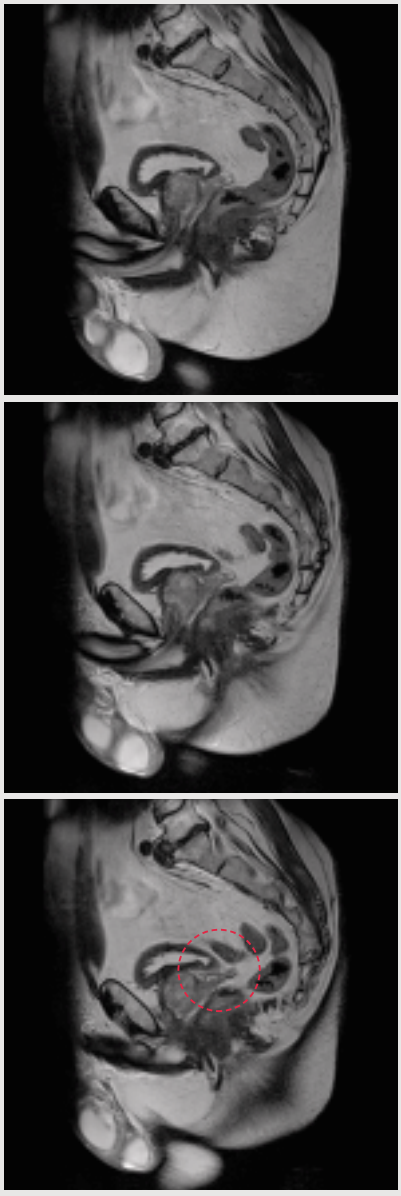

Figure 1 *Turbo Spin Echo (tse2d), TR: 5320 ms, TE: 86 ms, slice thickness: 4 mm, matrix: 512, FoV: 280 mm.*

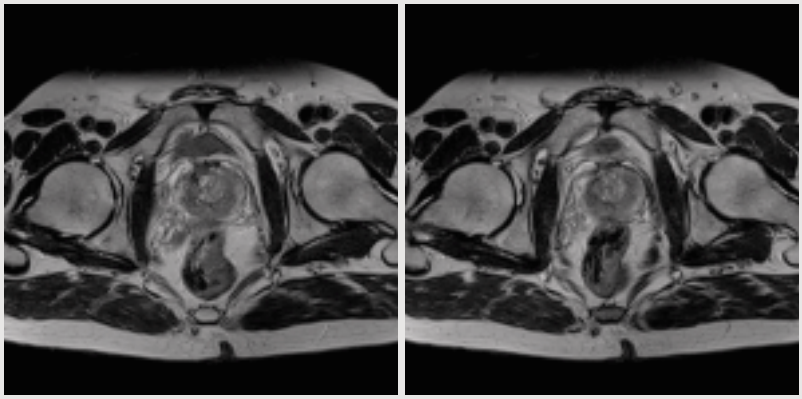

Figure 2 *Turbo Spin Echo (TSE), TR: 5500 ms, TE: 90 ms, slice thickness: 4 mm, matrix: 512, FoV: 280 mm.*

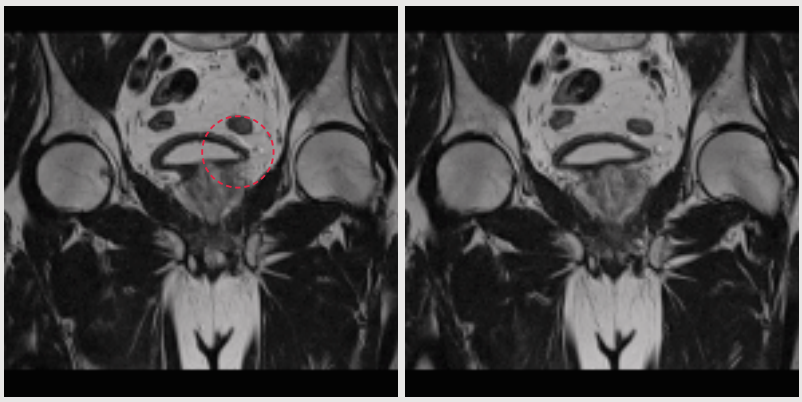

Figure 3 *Turbo Spin Echo (tse2d), TR: 4300 ms, TE: 108 ms, matrix: 512, FoV: 280 mm.*

Case Report: Occipital Infarct

Burckhard Terwey, M.D.
Markus Lentschig, M.D.

MR Zentrum Bremen Mitte
Bremen, Germany

Patient History

70-year-old patient with hemianopsia towards the left for 2 days.

Image Findings

Subacute posterior infarct in right occipital lobe in the posterior cerebral artery feeding zone. Intracranial arteries seem to be normal.

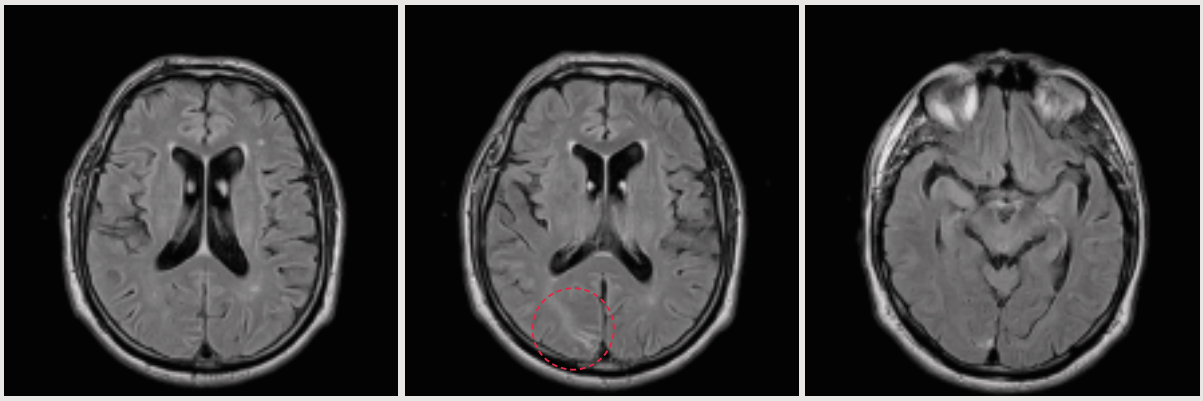

Figure 1 *Turbo Inversion Recovery (tir2d), TI: 2500 ms, TR: 8510 ms, TE: 136 ms, slice thickness: 5 mm, matrix: 256, FoV: 230 mm.*

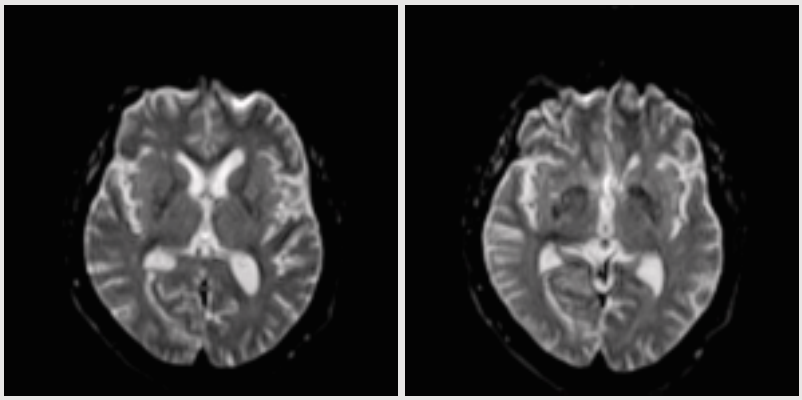

Figure 2 *Echoplanar imaging (ep_b0), TR: 4300 ms, TE: 98 ms.*

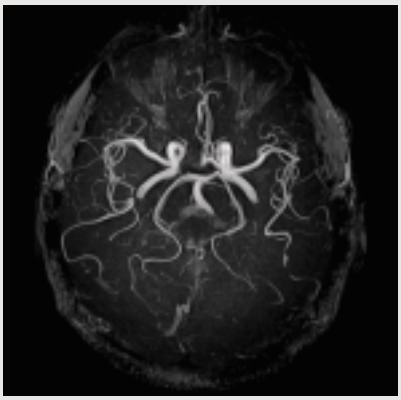

Figure 3 *3D MIP (Maximum Intensity Projection) of 3D Flash (fl3d), TR: 42 ms, TE: 7 ms.*

Case Report: Multiple Sclerosis

Burckhard Terwey, M.D.
Markus Lentschig, M.D.

MR Zentrum Bremen Mitte
Bremen, Germany

Patient History

53-year-old patient with Multiple Sclerosis. There have been disturbances in vision on the left side and there is pain in the left eye with left-sided headache.

Image Findings

Multiple supratentorial demyeleniation foci including paraventricular regions. After gadolinium injection there is enhancement of the left postcentral region and of the left optic nerve.

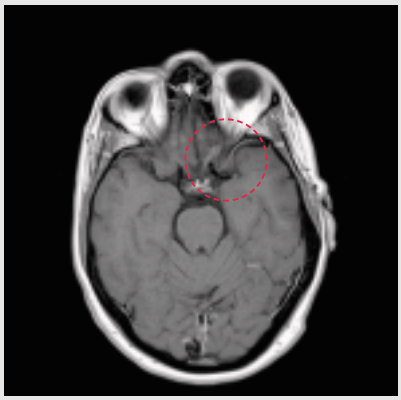

Figure 1 *Spin Echo (se2d) after I.V. contrast, TR: 558 ms, TE: 14 ms, slice thickness: 5 mm, matrix: 512, FoV: 230 mm.*

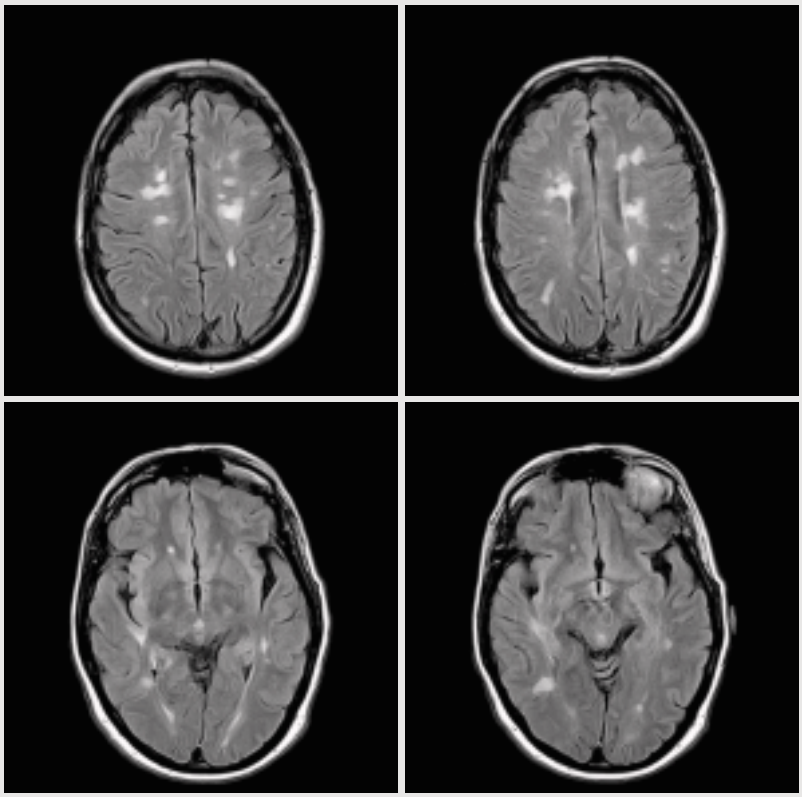

Figure 2 *Turbo Inversion Recovery (tir2d), TI: 2500 ms, TR: 8510 ms, TE: 136 ms, slice thickness: 5 mm, matrix: 320, FoV: 230 mm.*

Case Report: Middle Cerebral Artery Stenosis

Burckhard Terwey, M.D.
Markus Lentschig, M.D.

MR Zentrum Bremen Mitte
Bremen, Germany

Patient History

Left hemiplegia for 40 minutes. There is suspicion of right middle cerebral artery stenosis.

Image Findings

Complete stenosis of the right middle cerebral artery with decreased perfusion of the middle cerebral artery distribution. In diffusion weighted images signal increase of the basal ganglia is observed.

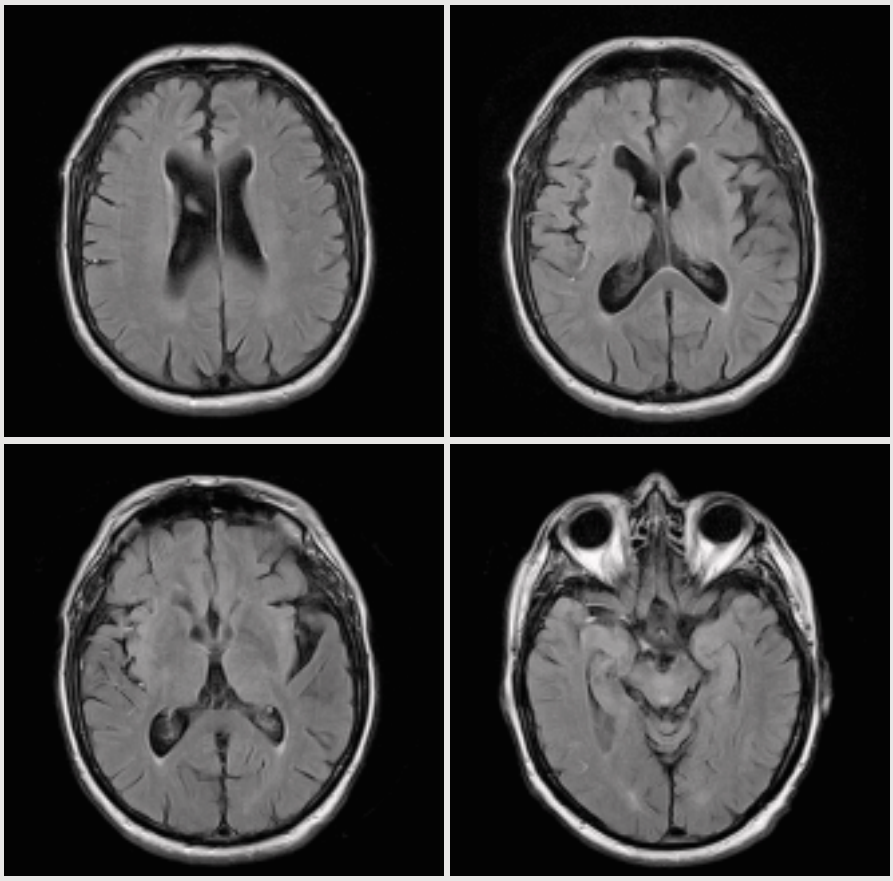

Figure 1 *Turbo Inversion Recovery (tir2d), TI: 2500 ms, TR: 8510 ms, TE: 136, slice thickness: 5 mm, matrix: 256.*

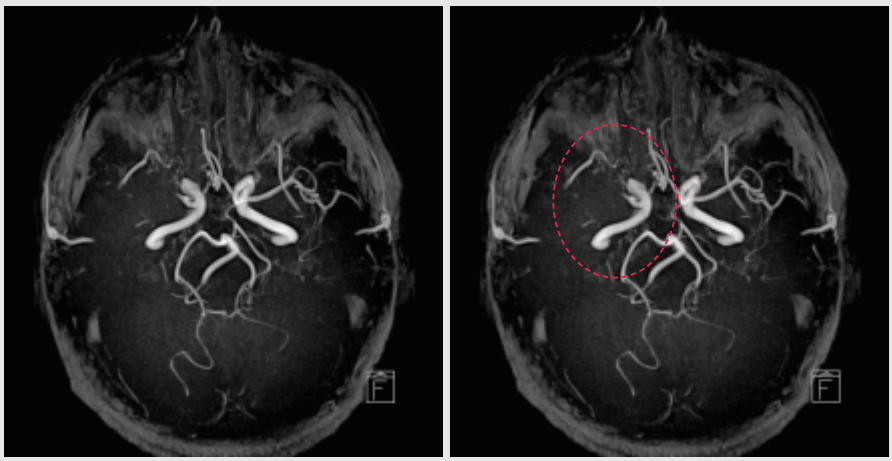

Figure 2 *3D Maximum Intensity Projection (3D MIP) of 3D Flash (fl3d), TR: 42 ms, TE: 7 ms.*

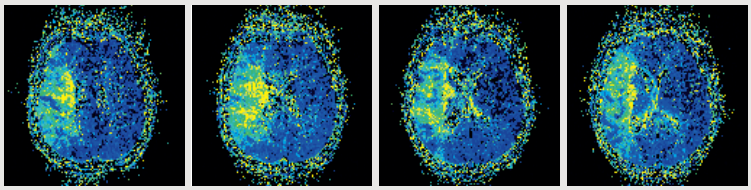

Figure 3 *Time to Peak (TTP) perfusion map.**

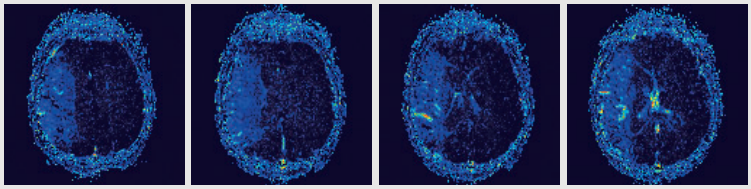

Figure 4 *Relative Cerebral Blood Flow (rel CBF) perfusion map.**

* *The information about this application is preliminary. The application is under development and is not commercially available in the U.S., and its future availability cannot be ensured.*

Case Report: Ankle

Burckhard Terwey, M.D.
Markus Lentschig, M.D.

MR Zentrum Bremen Mitte
Bremen, Germany

Patient History

20-year-old student with pain and swelling of the right ankle joint for almost one month after a sports injury.

Image Findings

Rupture of the anterior and posterior fibiotalar ligament. Bone edema of the medial talus, extensive soft tissue edema.

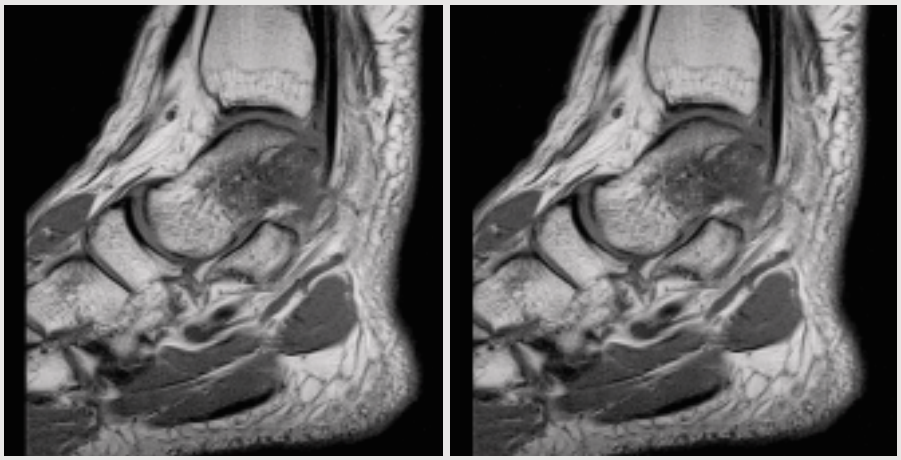

Figure 1 *Spin Echo (se2d), TR: 450 ms, TE: 11 ms, slice thickness: 3 mm, matrix: 512, FoV: 180 mm.*

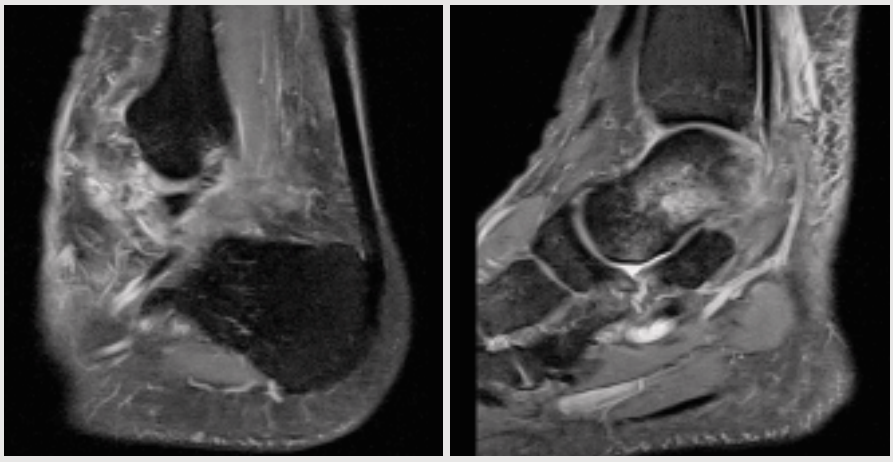

Figure 2 *Turbo Spin Echo (tse2d) with fat saturation, TR: 4950 ms, TE: 30 ms, slice thickness: 3 mm, matrix: 512, FoV: 280 mm.*

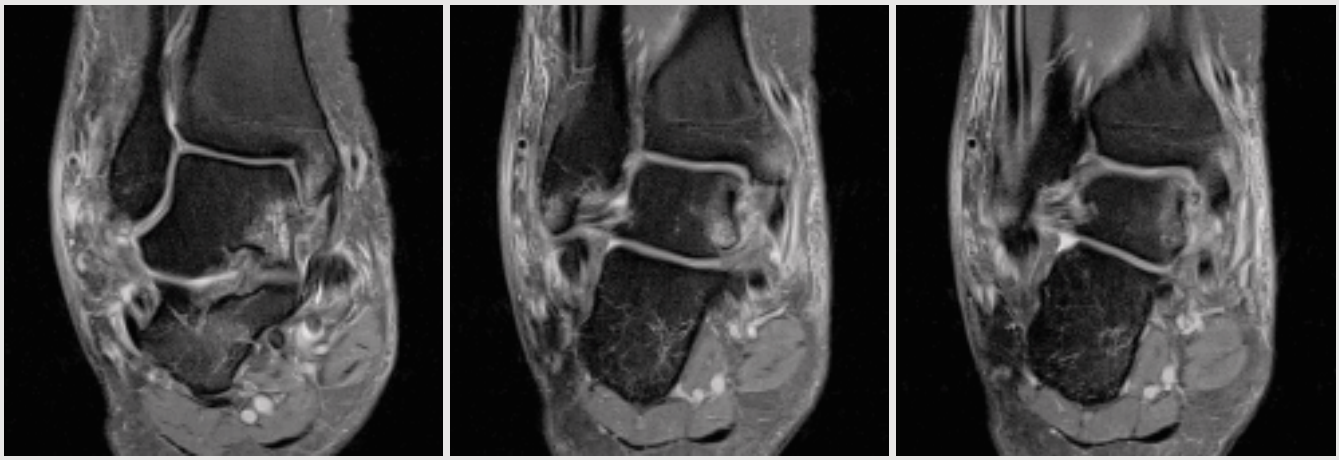

Figure 3 *Turbo Spin Echo (tse2d) with fat saturation, TR: 3600 ms, TE: 36 ms, slice thickness: 3 mm, matrix: 512, FoV: 180 mm.*

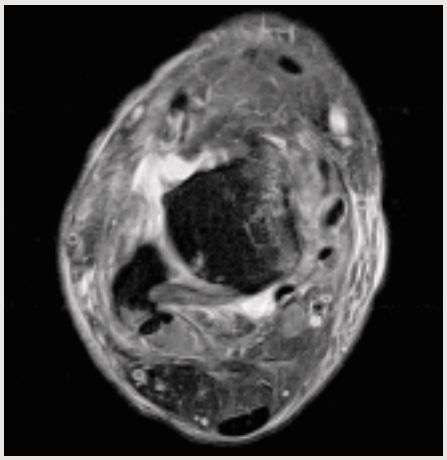

Figure 4 *Turbo Spin Echo (tse2d), TR: 4840 ms, TE: 18 ms, matrix: 512, FoV: 180 mm.*

Case Report: Osteosarcoma

Burckhard Terwey, M.D.
Markus Lentschig, M.D.

MR Zentrum Bremen Mitte
Bremen, Germany

Patient History

21-year-old patient with osteosarcoma, paraplegia after infestation of the spine.

Image Findings

Residual tumor which extends from T6 to T10 located more on the left side and which reaches intraspinally and infiltrates into the spine. There is also a 10 cm mass in the soft tissue on the back of the patient. At the level of Lumbar spine 2 there is a new metastatic lesion of 5 mm.

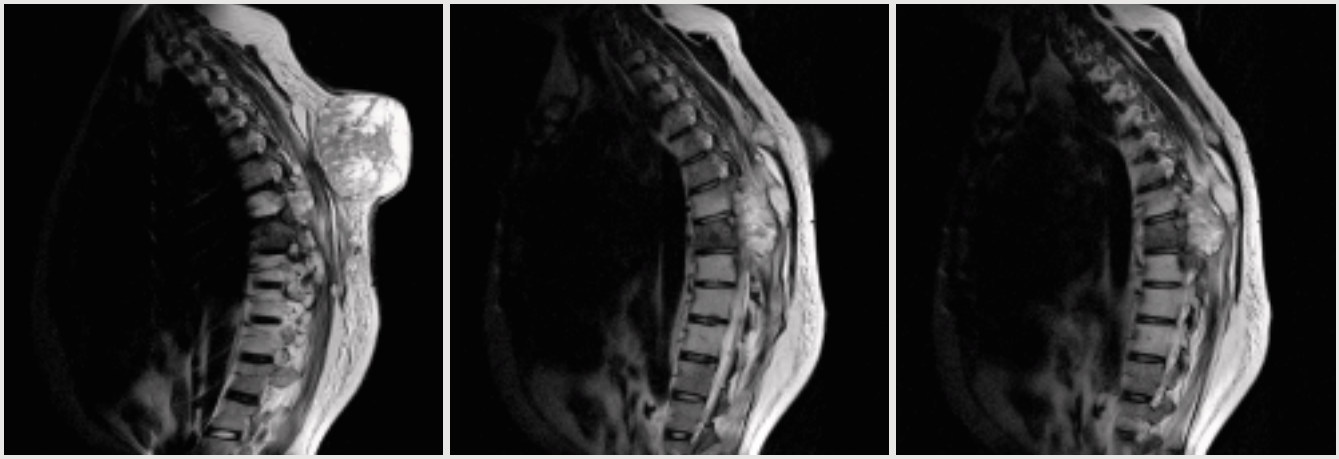

Figure 1 *Turbo Spin Echo (tse2d), TR: 3500 ms, TE: 105 ms, slice thickness: 3 mm, matrix: 512, FoV: 350 mm.*

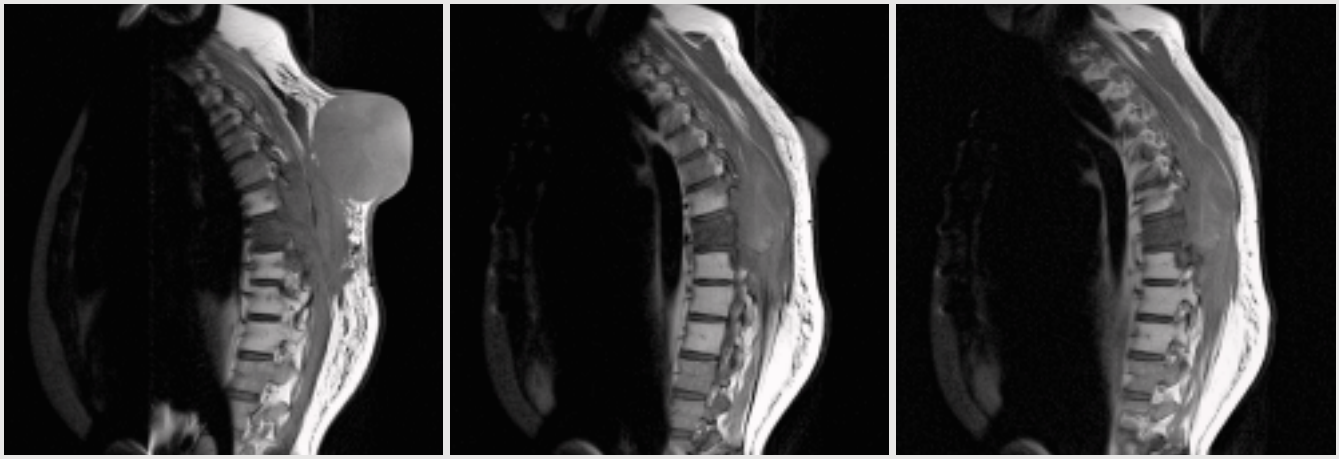

Figure 2 *Turbo Spin Echo (tse2d), TR: 677 ms, TE: 13 ms, slice thickness: 3 mm, matrix: 512, FoV: 350 mm.*

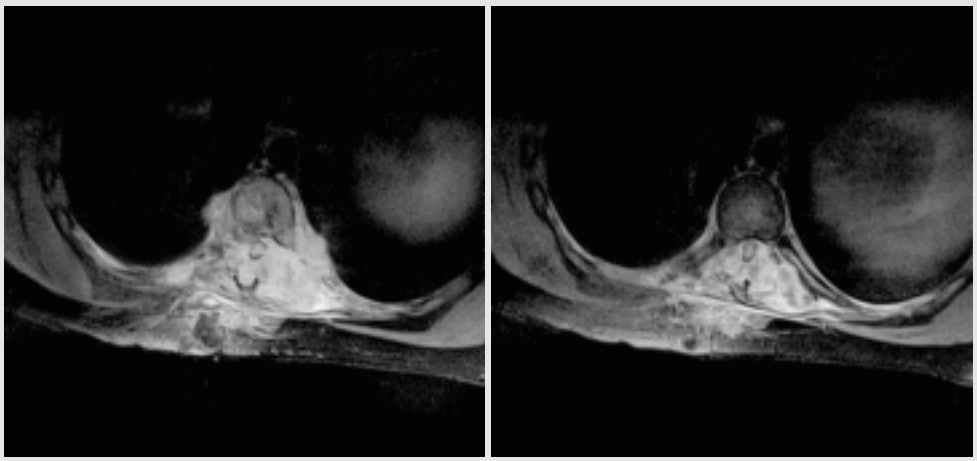

Figure 3 *Turbo Spin Echo (tse2d), TR: 1190 ms, TE: 15 ms, slice thickness: 4 mm, matrix: 512.*

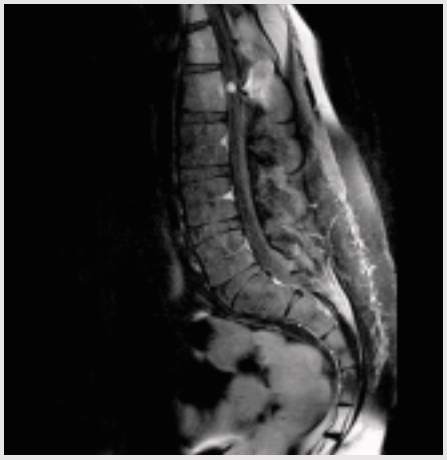

Figure 4 *Turbo Spin Echo (tse2d), TR: 500 ms, TE: 16 ms, slice thickness: 3 mm, matrix: 512.*

Case Report: Sacroiliitis

Burckhard Terwey, M.D.
Markus Lentschig, M.D.

MR Zentrum Bremen Mitte
Bremen, Germany

Patient History

17-year-old patient with extensive back pain radiating to right leg for the last month.

Image Findings

Bilateral sacroiliitis. Lumbar spine is normal.

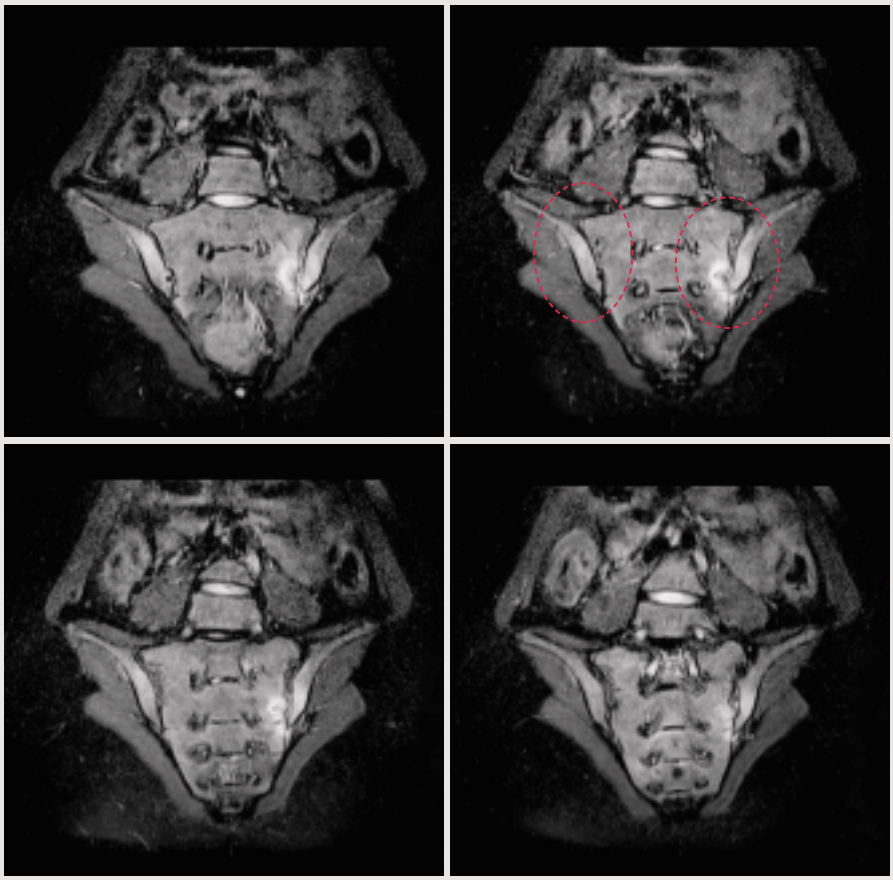

Figure 1 *Turbo Inversion Recovery (tir2d), TI: 160 ms, TR: 5640 ms, TE: 36 ms, slice thickness: 6 mm, matrix: 512, FoV: 380 mm.*

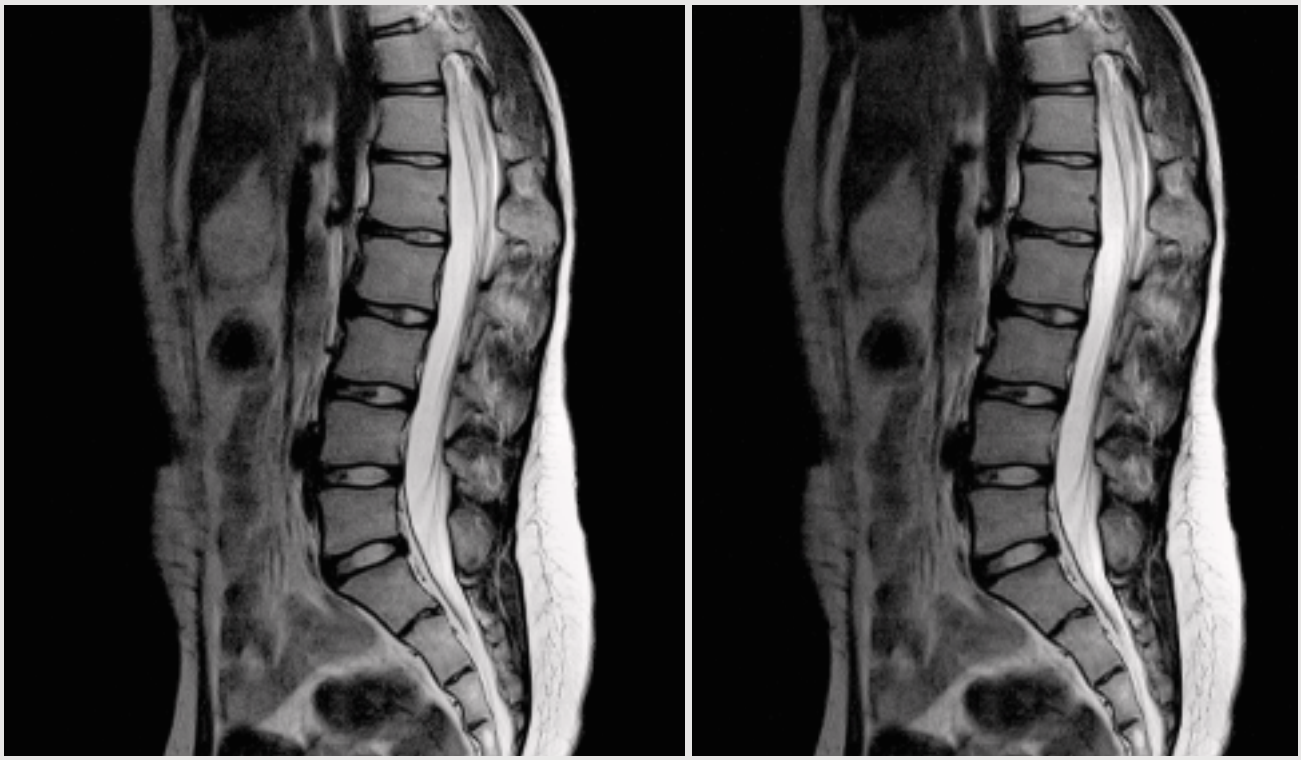

Figure 2 *Turbo Spin Echo (tse2d), TR: 3500 ms, TE: 106 ms, matrix: 512, FoV: 300 mm.*

Case Report: Plasmocytoma

Burckhard Terwey, M.D.
Markus Lentschig, M.D.

MR Zentrum Bremen Mitte
Bremen, Germany

Patient History

25-year-old patient with known plasmocytoma. The patient has recently experienced problems with vision.

Image Findings

1.5 x 1.5 x 2 cm lesion in Clivus which enhances after contrast medium injection. The lesion extends from the optic chiasma to the pons.
The mass is compatible with plasmocytoma infiltration.

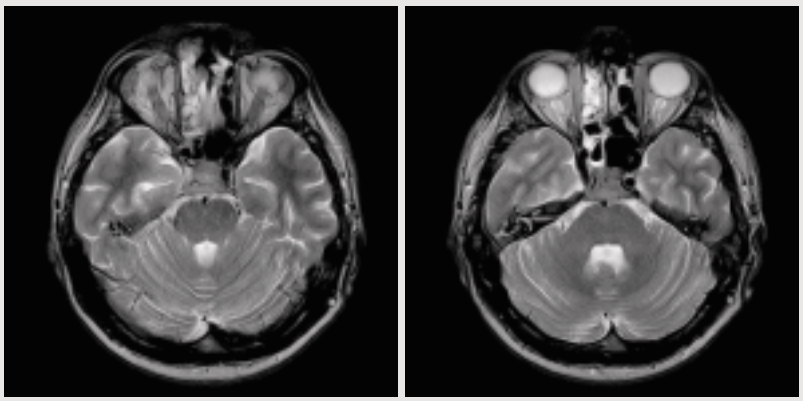

Figure 1 *Turbo Spin Echo (tse2d), TR: 6420 ms, TE: 98 ms, slice thickness: 5 mm, matrix: 512, FoV: 230 mm.*

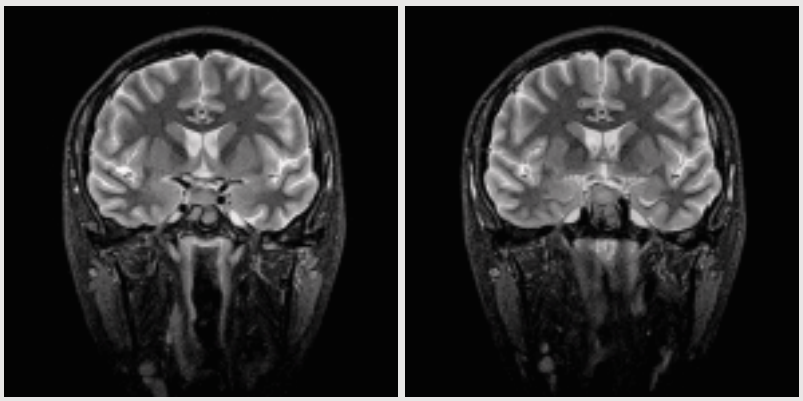

Figure 2 *Turbo Inversion Recovery (tir2d), TI: 130 ms, TR: 8310 ms, TE: 59 ms, slice thickness: 5 mm, matrix: 320, FoV: 230 mm.*

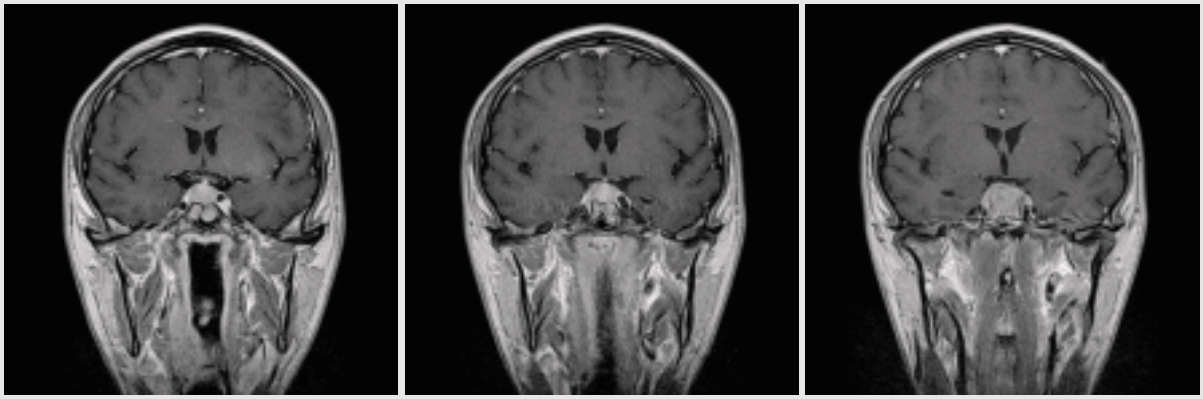

Figure 3 *Turbo Spin Echo (tse2d), TR: 540 ms, TE: 9.7 ms, matrix: 512, FoV: 230 mm.*

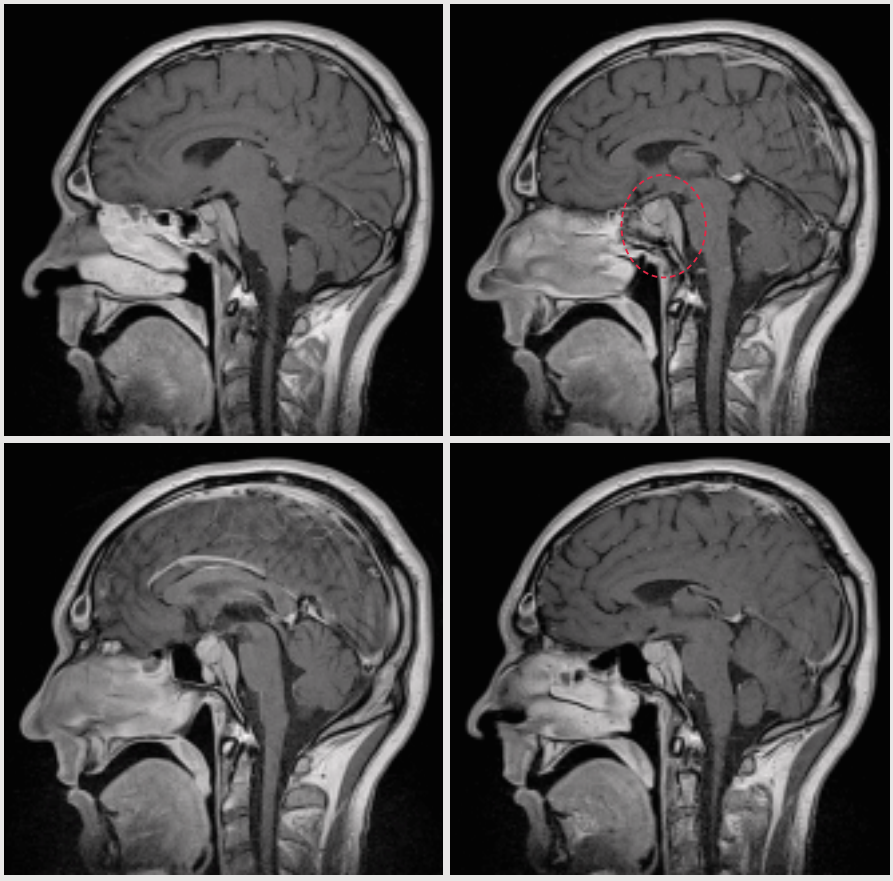

Figure 4 *Spin Echo (se2d), TR: 540 ms, TE: 9.7 ms with I.V. contrast, matrix: 512, FoV: 230 mm.*

Case Report: Knee MRI

Stefan Sonnet, M.D.
Georg Bongartz, M.D.

University Hospital Basel
Dept. of Radiology
Basel, Switzerland

Patient History

36-year-old male patient with Non-Hodgkin's lymphoma has undergone allogeneic stem cell transplantation and is now suffering from severe graft versus host disease of the bowel. High dose steroids are therefore applied. Sudden onset of diffuse pain in both knees. Knee MRI is performed to exclude osteonecrosis.

Findings

A sagittal T2-weighted DESS image through the body of the lateral meniscus demonstrates the normal bowtie appearance and homogeneous dark signal of the lateral meniscus. (Fig. 1). No tear or intrasubstance degeneration was detected. Sagittal TIRM sequence shows a homogeneous dark signal of the tibial and femoral bone marrow without evidence for bone marrow edema (Fig. 2). No osteonecrosis was found. The sagittal T2-weighted DESS through the area of the intercondylar notch reveals a normal anterior (Fig. 3) and posterior cruciate ligament (Fig. 4) with uniform signal.

T1-weighted TSE shows no bone bruise, normal menisci and collateral ligaments (Fig. 5).

Discussion

MRI has a high sensitivity to help detecting bone marrow edema of various etilogies, especially with fat-suppressed TIRM images, providing a high contrast between affected and uninvolved bone marrow. Therefore osteonecrosis, tumorous or infectious pathology was excluded in this case.

Figure 1 *T2-weighted DESS 3D (sagittal), TR: 21.4 ms, TE: 8 ms, slice thickness: 1.8 mm, matrix: 357 x 384, FoV: 161 x 161 mm, flip angle: 25°, BW: 194 Hz/Px.*

Figure 2 *Turbo Inversion Recovery Magnitude – TIRM (sagittal), TI: 160 ms, TR: 4000 ms, TE: 42 ms, slice thickness: 4 mm, matrix: 256 x 320, FoV: 180 x 180 mm, flip angle: 150°, BW: 191 Hz/Px.*

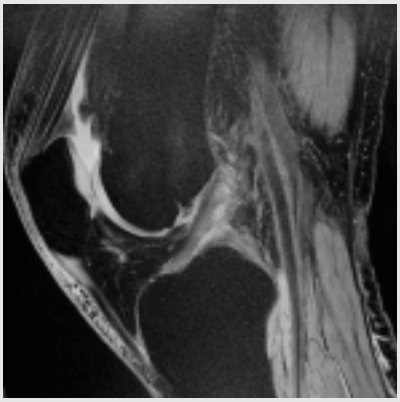

Figure 3 *3D DESS (Dual Echo Steady State).*

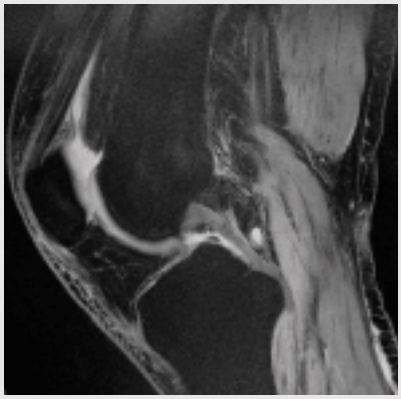

Figure 4 *3D DESS (Dual Echo Steady State).*

Figure 5 *T1-weighted Turbo Spin Echo – TSE (sagittal), TR: 866 ms, TE: 23 ms, slice thickness: 4 mm, matrix: 356 x 448, FoV: 143 x 200 mm, flip angle: 90°, BW: 151 Hz/Px.*

Case Report: Rupture of the Ulnar Disc (TFCC)

Georg Bongartz, M.D.
Annette Merkle

Department of Radiology,
University Hospital Basel
Basel, Switzerland

Patient History

37-year-old female patient without history of trauma. Recurrent pain in the left wrist increasing with workload.

Image Findings

Figure 1 *Coronal T1-weighted acquisition (Spin Echo T1, TR 718 ms, TE 23 ms, FoV 160 x 160 mm; resolution 448 x 358) of the left hand wrist in neutral position. There is a clearly visible cleft in the ulnar disc (triangulate fibroid cartilage complex = TFCC) filled by synovial fluid. The radial adhesion of the TFCC is normally displayed. The carpal bones and the adjacent ulnar and radial bones are of normal structure and signal-intensity.*

Figure 2 *Sagittal slice of a 3D DESS (Dual Echo Steady State) sequence through the outer ulnar part of the TFCC demonstrating increased signal intensity due to edema. (Parameters: DESS T2-weighted, TR 21.4 ms, TE 8 ms, FA 40°, 64 partitions, SL 1.5 mm)*

Discussion

The anatomy of the carpal region is demonstrated in high quality and enables clear diagnosis of ligamentous or cartilaginous pathologies. In this case, the rupture of the TFCC is readily visible even without the application of intra-articular contrast media.

Case Report: Peripheral ceMR Angiography

Deniz Bilecen, M.D.

University Hospital Basel
Basel, Switzerland

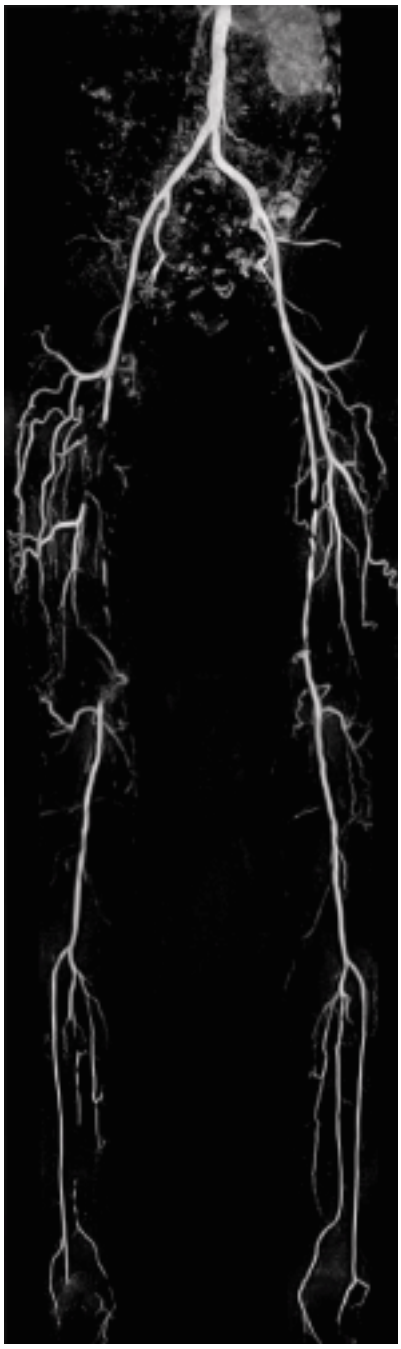

Patient History

83-year-old female with a right-sided critical limb ischemia (Stage III Fontaine). MR angiography for bypass surgery evaluation.

Sequence Details

4-step gadolinium-enhanced high resolution 3D MR angiography of pelvic, thigh and calf station. integrated Parallel Acquisition Technique (iPAT) with GRAPPA. Acceleration factor of 2. 3D FLASH sequence for data acquisition.

Dotarem® (Schering) administration in a biphasic mode (5 ml with injection rate of 1 ml/s; 10 ml with an injection rate of 0.5 ml/s) via an antecubital vein. Bolus timing was based on MR-fluoroscopic finding at aortal level.

T1-weighted MR-contrast, coronal slice orientation, slice thickness 1.5/1.25/1.2/1, TE = 1.2 s;
TA = 13 s/13s/11s/28s;
FoV = 380 mm,
flip angle = 20°.

Image Findings

Aorta and pelvic station: Luminal irregularities of the non-stenotic abdominal aorta. Renal arteries are not clearly visualized. Bilateral patent iliac arteries with mild stenosis of the outlet of the left common iliac artery. Normal findings of the internal iliac artery.

Thigh station: Patent bilateral common femoral artery. Long-distance occlusion of the right superficial femoral artery and segmental occlusions of the deep femoral artery but profound collateral function to the popliteal artery. Multiple stenoses of the left superficial femoral artery. Bilateral patent popliteal artery with mild stenosis.

Calf station: Patent right anterior tibial artery, partially occluded peroneal and posterior tibial artery. Patent left anterior and peroneal artery, partially occluded posterior tibial artery. Patent tibioperoneal trunk. No venous enhancement.

Discussion

To cover the entire peripheral arterial vasculature, a 4-step technique is needed for contrast-enhanced 3D MR angiography. However, fast data acquisition with GRAPPA enables adequate table movement to allow chasing the contrast agent bolus. Good delineation of the arterial vasculature was obtained. No venous overlay occurred. Pre-surgical MR finding was sufficient for femoropopliteal bypass planning.

Case Report: Lumbar Spine

Thomas M. Gluecker, M.D.

**Department of Diagnostic Radiology,
University Hospital Basel
Basel, Switzerland**

Patient History

79-year-old female patient referred from an outside hospital after fenestration and resection of the lumbar disc L4/5. Now new right-sided lumbo-radicular pain L4 and L5.

Examination

Sequence details:
1. T2-weighted TSE sequence, sagittal plane, TR 4690, TE 109, echo train length 15, matrix 384 x 384, FoV 25.9 cm,
slice thickness 4 mm

2. T1 sequence post KM:
a. T1 TSE **axial**, TR 549, TE 18, echo train 3, matrix 192 x 256, FoV 21.9 x 16.4 cm, slice thickness 4 mm
b/c. T1 TSE **sagittal**, TR 577, TE 13, echo train 3, matrix 320 x 320, FoV 25.9 cm, slice thickness 4 mm

Figure 1a

Figure 1b

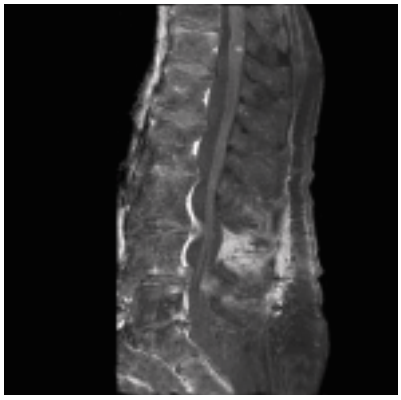

Figure 2b

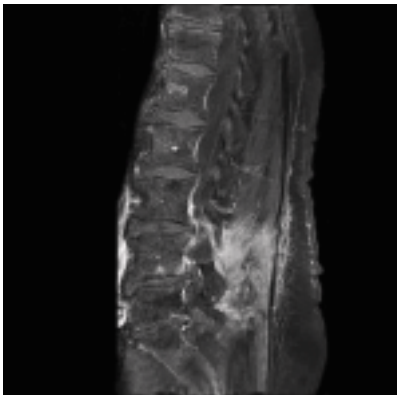

Figure 2c

Image Findings

Residual lumbar hernia L4/5, clearly depicted in the sagittal plane. Axial T1 post contrast images demonstrate post operative changes in the soft tissue posterior to the lumbar spine. At the level of the right neural foramen L4/5 is a 4 mm lesion with peripheral contrast enhancement, consistent with a free fragment. Additionally, at the level of L3/4, large medial hernia clearly demonstrated in the T2 sagittal plane.

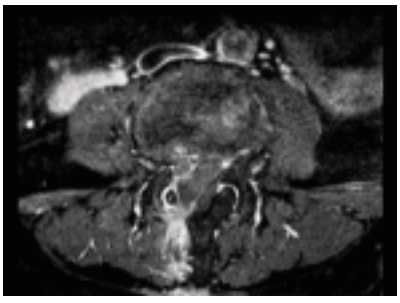

Figure 2a

Case Report: Myocardial Infarction

Jens Bremerich, M.D.[1]
P. Buser, M.D.[2]
Georg Bongartz, M.D.[1]

[1]Department of Radiology,
[2]Department of Cardiology,
University Hospital Basel
Basel, Switzerland

Patient History

67-year-old man with myocardial infarction. Specific question was the extent of myocardial necrosis and scarring.

Image Findings

Figure 1: Parasagittal long axis 2 chamber view shows dilated left atrium (LA) and ventricle (LV) with marked thinning of the myocardium in the apex and anterior wall (arrows). TrueFISP images were acquired on a MAGNETOM Espree scanner with a PAT factor of 2, antegrade ECG gating (RR interval 1155 ms) and retrograde arrhythmia detection.

Figure 2: Short axis view of the heart with the same sequence as figure one. Consecutive 6 mm thick slices of the entire heart were acquired enabling gold standard calculation of the ejection fraction which was markedly reduced (23 %). Moreover, wall thinning was observed in the anterior wall (arrows) of the left ventricle (LV) as already seen on 2 chamber view.

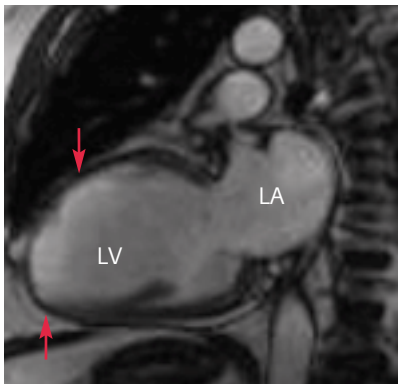

Figure 1

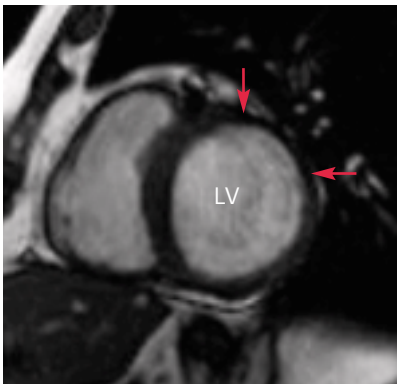

Figure 2

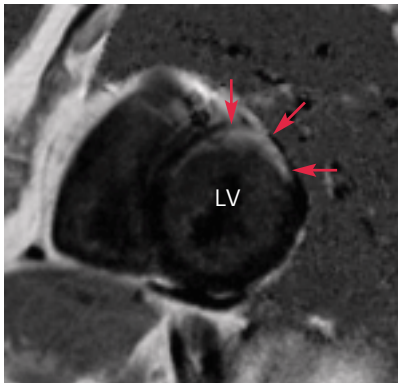

Figure 3

Figure 3: Late enhancement* image acquired in the short axis 15 min after injection of 0.1 mmol Gadolinium with the following parameters: slice thickness = 8 mm, TI = 250 ms, TR = 700 ms, TE = 4.2. The phase sensitive reconstructions of Turbo FLASH images (PSIF) show transmural infarction in the anterior wall (arrowheads).

** The information about protocol for imaging myocardial infarction and viability is preliminary. The product is under development and not commercially available in the U.S., and its future availability cannot be ensured.*

Results & Discussion

The protocol for imaging myocardial infarction and viability* is comprised of cine TrueFISP and late enhancement* Turbo FLASH with phase sensitive reconstruction (PSIR) in three axis: Short axis, long axis 2-chamber view, and long axis 4-chamber view. This protocol enables assessment of wall motion abnormalities, definition of location and transmurality of infarcts, and gold standard calculation of ventricular function.

Case Report: Carotids

Stephan G. Wetzel, M.D.
Christelle Reymann

Department of Radiology,
University Hospital Basel
Basel, Switzerland

Patient History

A 70-year-old patient presented with a sensory deficit of the right hand as the main neurological deficit. A CT scan of the head had been normal at the time of admission. The patient was referred to MR.

Sequence details

Diffusion-weighted imaging:
Axial acquisition, TR 4400 ms, TE 99 ms, 3 averages. FoV read 238 mm, FoV phase 100%, base resolution 192, phase resolution 100%, phase partial Fourier 6/8. Bandwidth 898 Hz/Px. Slice thickness 5 mm, 24 slices, distance factor 20%. PAT mode GRAPPA, acceleration factor PE 2, reference lines PE 40. Diffusion mode: 3-scan trace, b-values 0-500-1000 [s/mm^2].

Contrast enhanced MR Angiography (MRA):
Coronal acquisition, 3D T1-weighted interpolated FLASH sequence, time to centre 6.3 s, 3D centric reordering off. TR 3.9 ms, TE 1.5 ms, FA 30°, bandwidth 410 Hz/Px.
FoV 200 x 300 mm, matrix 192 x 384. 72 partitions, distance factor 20%, effective voxel size 1 x 0.8 x 0.8 mm. PAT mode GRAPPA, acceleration factor PE 2, reference lines PE 70. TA two times 17 s (subtraction). Contrast material (Gadolinium): 1.5 times standard dose.

Placement planning for the contrast enhanced MRA volume with a 2D PC MRA (in three planes). Timing of the scan start based on the bolus arrival time (BAT) as determined with an axial FLASH sequence at the level of the common carotid arteries (scan start: BAT-4 s).

Image findings

Diffusion-weighted images show multiple hyperintense lesions in the territory of the left middle cerebral artery with low ADC values (Figs. 1a-c). The lesions are predominately localized in a cortical localisation, including the postcentral gyrus (Figs. 2a-c). 3D contrast-enhanced MRA showed a middle grade stenosis (30-69%) at the origin of the left internal carotid artery (Fig. 3a). This is better visualized on a targeted MIP reconstruction of the same data set (Fig. 3b).

Results and Discussion

MR imaging with diffusion imaging showed clearly the cause of the neurological symptoms. The degree of stenosis at the origin of the internal carotid artery was in accordance with findings from the Doppler/Duplex-ultrasound examination; a conventional angiography was not performed.

A combined MR examination of the head and neck in patients with TIAs or stroke offers the possibility to visualize parenchymal brain lesions and stenotic lesions of the cervical and intracranial vessels in a highly efficient way. For grading of carotid stenosis, findings from MRA and ultrasound are the primary imaging modalities at our institution, and have supplanted conventional angiography in the vast majority of cases.

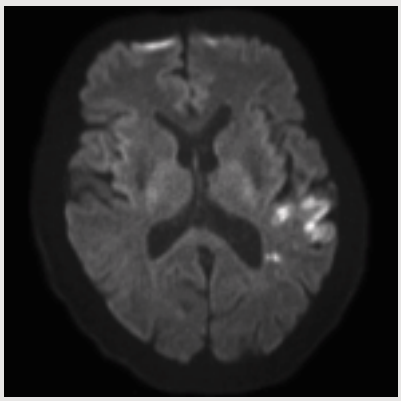

Figure 1a

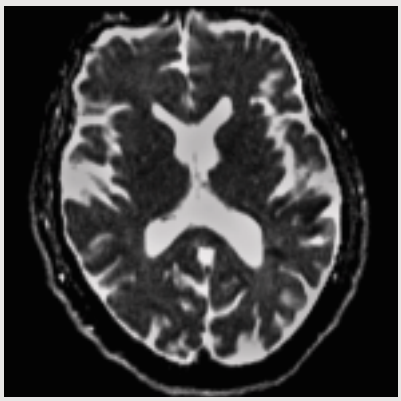

Figure 1b

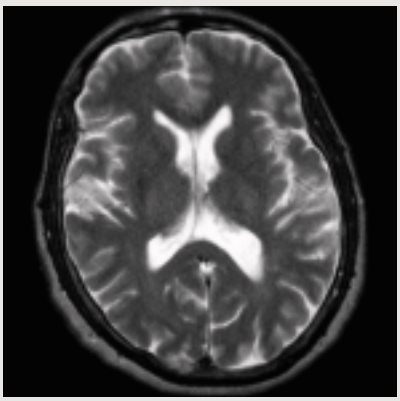

Figure 1c

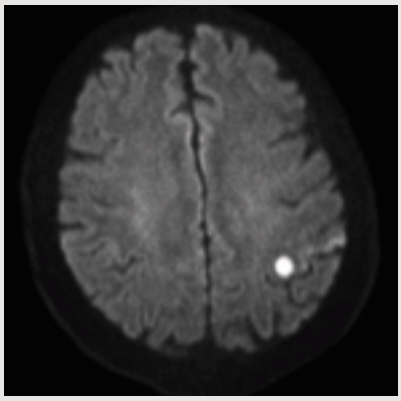

Figure 2a

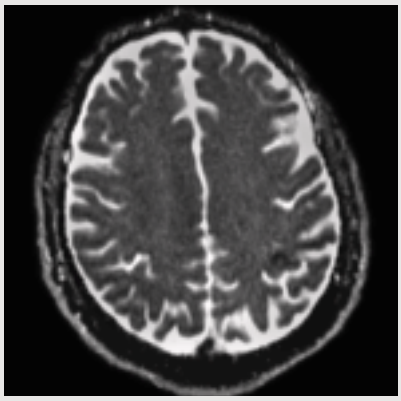

Figure 2b

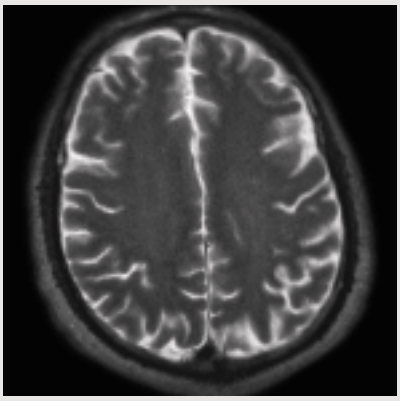

Figure 2c

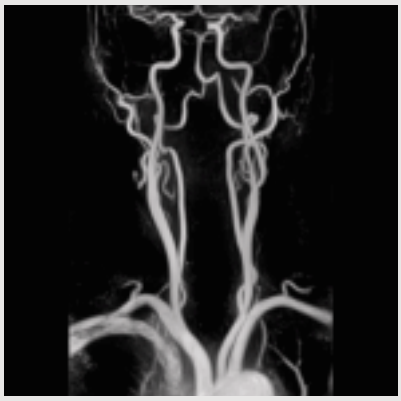

Figure 3a

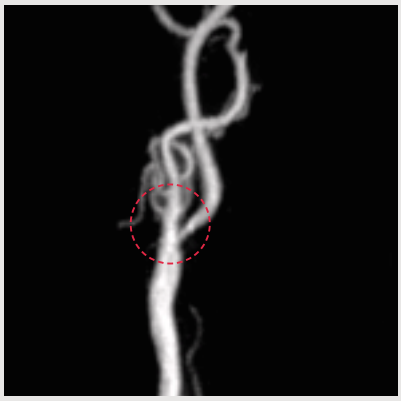

Figure 3b

Case Report: Aortic Aneurysm

Jens Bremerich, M.D.[1]
P. Buser, M.D.[2]
Georg Bongartz, M.D.[1]

[1]Department of Radiology,
[2]Department of Cardiology,
University Hospital Basel
Basel, Switzerland

Patient History

81-year-old man with a history of graft repair after aneurysm of ascending aorta and aortic arch in 1999. Previous MR studies showed normal dimensions of ascending aorta and aortic arch, but aneurysm of the anastomosis distal to the left subclavian artery with maximal lumen diameter of 5 cm.

Image Findings

Figure 1: Maximum intensity projection (MIP) of the aorta shows aneurysm of the brachiocephalic trunk (arrowhead) and at the anastomosis distal to the left subclavian artery (double arrow). 3D MR angiography was acquired during injection of 0.15 mmol/kg Gadolinium @ 2 ml/s, TR/TE were 3.1/1.3 ms, with a PAT factor of 2, acquisition time was 21 s.

Figure 1

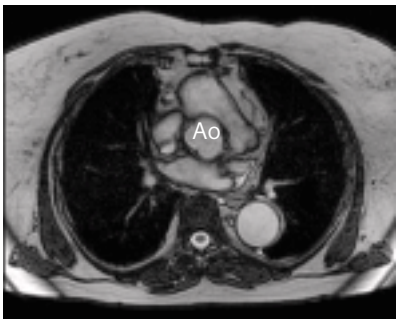

Figure 2

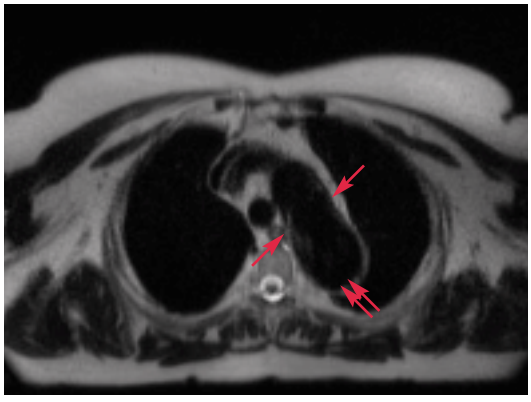

Figure 3

Figure 2: Axial segmented TrueFISP image at the level of the aortic root shows normal anatomy and dimension of the aortic valve (Ao). Flip angle was 80°, PAT factor 2, TR/TE were 248/1.5 ms.

Figure 3: Axial HASTE image at the level of the distal anastomosis (arrow) with aneurysm (double arrow). TR/TE were 1000/85 ms, slice thickness was 5 mm, acquisition time 0.53 s.

Results & Discussion

Dimensions of the aneurysm of the brachiocephalic trunk (2.2 cm) and the anastomsis (5 cm) were unchanged compared to the previous examination. Conservative treatment was continued.

Clinical Experience: Turville Bay MRI Center

Improving Results for Large and Claustrophobic Patients

Antje Hellwich

Siemens AG
Medical Solutions
Magnetic Resonance Division,
Customer Care Manager,
Erlangen, Germany

Sally McKinnon, M.D.

Large and claustrophobic patients pose a special set of challenges in the MRI suite, with implications for imaging efficiency, profitability, and standard of care. It's a significant problem that is becoming more critical for imaging centers every day.

Turville Bay MRI and Radiation Oncology Center in Madison, Wisconsin, USA knows this all too well. "More than 15 percent of our patients are either large or claustrophobic or both, and the problems seem to be escalating," comments Phyllis Nelson, Turville Bay's executive director. She notes that the two issues go hand in hand because large patients often feel particularly confined in the small MRI bore.

For Turville Bay, the only option was an unhappy compromise in image quality and patient care, while workflow and profitability suffered due to missed appointments, scheduling difficulties, long exam prep times, and aborted procedures.

"Basically, we were struggling with a trade-off. These patients were either imaged in our 0.3T low-field open MRI with lower image quality or in a closed MRI two percent of the time under sedation – which brings its own set of problems. We had been waiting a long time for a solution," said Patricia Ethridge, technical director for the center in 2004. Essentially, Turville Bay had been waiting for Siemens MAGNETOM Espree for years. It simply hadn't been invented.

Things changed in October 2004, when the first MAGNETOM Espree was installed at Turville Bay. We spoke with Dr. Sally McKinnon, M.D., chief radiologist at Turville Bay to hear about her experience from half a year with MAGNETOM Espree and MAGNETOM Symphony side by side.

Flash: **What was the major reason behind your decision to buy MAGNETOM Espree ?**

McKinnon: In the first place we wanted to be able to better accommodate our patient population because of the large number of larger patients – larger meaning greater than 250 lbs. – in our outpatient setting.

We have the 1.5T Symphony with Quantum gradients and to accommodate our largest patients we had been using a 0.3T open system from another vendor. But we were increasingly dissatisfied with the image quality of the open MRI. Even though the Quantum required patient sedation in many cases, we preferred the closed 1.5T system and the open MRI had been severely under-utilized.

The Espree maximizes open space with a CT like design while delivering the image quality of a 1.5T system. In most cases patients enter the 4-foot-long Espree bore feet-first, yielding a far more comfortable experience than head-first imaging. Most important, with the 70-centimeter bore it can easily accommodate large patients.

Flash: **Since when has the MAGNETOM Espree been operational in your clinic?**

McKinnon: Around October for early customer site. Roughly around mid-December starting with patients and with reimbursement for the examinations

Flash: **How many patients have been scanned to date? Have you faced any problems?**

McKinnon: A conservative guess would be 4 times more than this time last year.

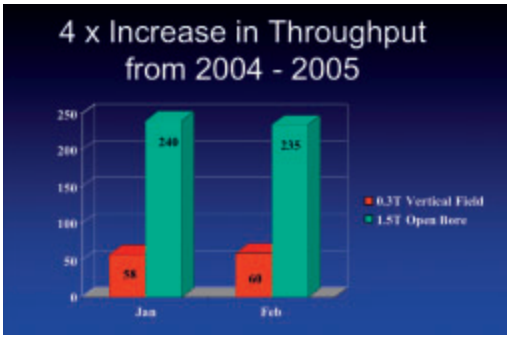

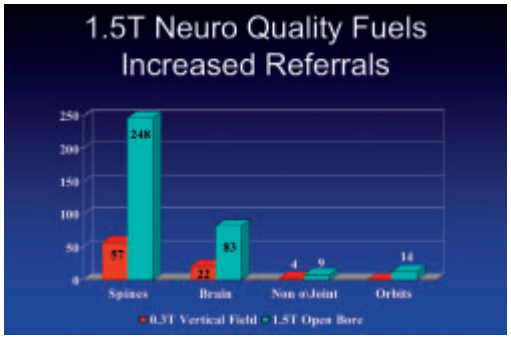

We have scanned 475 patients in the first 2 months of 2005, mostly spine and brain imaging. We have had very few problems and have found the image quality obtained from the Espree to be very similar to that of the Symphony. As we tend to scan more difficult or very large patients on the Espree, this sometimes will affect the image quality. From a clinical perspective, there is only so much you can do with physics to get signal-to-noise on really large patients (greater than 350 lbs). The great news is that we can now scan these patients at 1.5 T, a substantial improvement over our low field open scanner. The ability to provide 1.5 T service for these difficult patients has been extremely well received by our referring physicians.

Flash: **What is the reaction of the patients being scanned?**

McKinnon: The Espree has been very well received by our patients. In fact, patients who have had scans on both the Espree and the Symphony, more often than not, requested follow-up exams to be performed on the Espree. Large patients, who have had limited or no access to MRI for diagnosis, are extremely pleased that they now have an MRI option. Other patients, who have mild claustrophobia, are actually willing to try the exam without sedation once they see the openness of the scanner. Patients having an MRI for the first time generally leave with a better than expected experience. As Turville Bay is an outpatient imaging center, these factors have made scheduling patients easier and have increased our scanner usage and throughput.

Flash: **Was it easy for the technologists to get used to MAGNETOM Espree?**

McKinnon: Yes, because the Symphony Quantum and the Espree have the same user interface. We already had IPA™, the Siemens coil concept at the Quantum, but Tim [Total imaging matrix] virtually eliminates the need for coil repositioning and patient repositioning during the exam.

Flash: **How has MAGNETOM Espree affected your daily clinical routine?**

McKinnon: Can we strike this question?!...

Flash: **Why?**

McKinnon: Because we have gotten busier. It has enabled us to do more patients, which has its pros and cons of course.

Flash: **What applications have you been performing on MAGNETOM Espree?**

McKinnon: Routine head, neuro, abdomen, orthopedics imaging is good. It is what you would expect from a 1.5T system. As I said there are some limits on extremely large patients regarding signal-to-noise. But at least we are now able to get a quality image. Our brain and ortho scans have been accelerated using iPAT [integrated Parallel Acquisition Technique]. However, we haven't used iPAT very much to this point for our larger patients because of the SNR decreases associated with iPAT.

As to angiography, we perform brain MRAs on the both the Espree and the Symphony routinely. However, we have an established lower extremity protocol for the Quantum that we are happy with. To this point, we just have not had the need to optimize it on the Espree. The same is true for thorax-abdomen-pelvis combinations which are possible at the Espree with the Tim technology, but this is routine at the Quantum.

I have had at least a dozen calls from physicians asking how do we use the Espree in our clinical practice. And my answer is always that we try to utilize the Espree for the routine "bread and butter" type exams. We tend to reserve the Espree for our first time patients, mildly claustrophobic, larger patients and keep the MAGNETOM Symphony available for the more complicated procedures. This way we are able to completely utilize both systems.

Flash: **What would be your advice to other potential users in the radiology community?**

McKinnon: MAGNETOM Espree is an Open system with the exact strength and quality of 1.5T. It's a great "workhorse" type scanner for routine imaging. It is a fantastic addition to an existing high-field system. Having both systems has allowed us to split our workload very well. The ability to provide 1.5T service for difficult, large or claustrophobic patients has been extremely well received by our patients and referring physicians.

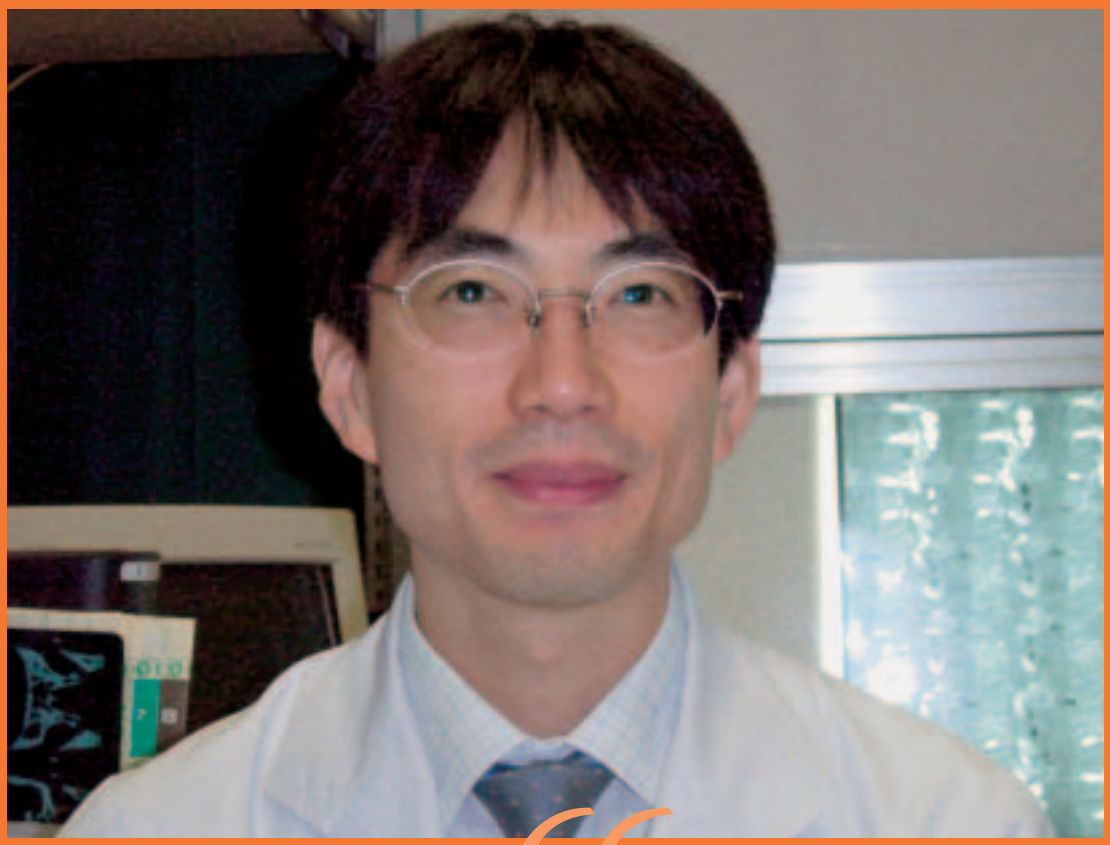

There is the potential for diffusion tumor imaging to replace Positron Emission Tomography in the whole body tumor imaging. Tim and MAGNETOM Avanto enable us to use diffusion imaging for every tumor patient in our clinic and to date we have scanned over 600 patients using this technique. The results are extremely encouraging.

Dr. Noriatsu Ichiba, Jikei University Hospital, Tokyo, Japan

User's Report on MAGNETOM Avanto with Total imaging matrix (Tim)

Noriatsu Ichiba, M.D.
Kunihiko Fukuda, M.D.

Department of Radiology
The Jikei University School of Medicine
Tokyo, Japan

Introduction

Siemens MAGNETOM Avanto 1.5T with Total imaging matrix (Tim) technology – capable of performing high resolution whole-body examination – has been in service since 21 June 2004 in our hospital. In this article, we will discuss our experience and future prospects of this first Tim system in Japan.

1. Total imaging matrix (Tim)

Tim is an entirely new MRI concept that allows true whole-body MR imaging. The most striking feature is the combination of up to 76 coil elements and up to 32 RF channels to create one "matrix," allowing for a total FoV of up to 205 cm. This enables whole-body imaging with surface coil-like higher signal to noise ratio (SNR), or it allows the user to "select exams, not coils." Coil elements are arranged in the X-, Y-, and Z-axis directions, which enables Parallel Imaging in all three directions. Thanks to these features, it is now possible to perform a high resolution whole-body MRI in a relatively short time.

* *The information about this application is preliminary. The application is under development and is not commercially available in the U.S., and its future availability cannot be ensured.*

2. Improvements offered by MAGNETOM Avanto

In addition to the Tim technology, the Avanto has improved magnetic field homogeneity and higher gradient strength (max. 45 mT/m) and slew rate (200 T/m/s). Now local imaging can achieve high spatial resolution and short acquisition time – detailed examination by high resolution whole-body MRI becomes a practical option. The improved homogeneity also allows the routine use of diffusion-weighted images with less distortion not only in the head but also in other areas of the body, which are very useful for the detection and characterization of mass lesions. Cine imaging is readily available, providing dynamic information in a short time. Thus patient throughput is greatly increased – an average of 550 examinations per month after the installation of MAGNETOM Avanto. The fact that examinations of emergency cases such as acute stroke* can be done more quickly also contributes to the improved throughput.

As for the operation of the imaging equipment, the operator is freed from the need for patient repositioning, coil changes or manual table movement in the scanner room during the examination, saving considerable effort. If there are any unexpected findings during the examination, we can easily change the imaging area on the console and perform additional imaging without significant increase in examination time.

The examination of all body areas, except for the head, can be done in feet-first position, which is a plus for claustrophobic patients.

In pediatric imaging, sedation of the child is often required. AudioComfort™ reduces the acoustic noise and prevents the sedated child from waking during the examination. This reduces the interference with the schedule of other patients, and thus reduces the risk of mixing up patients.

3. Clinical applications

I) Whole-body applications

(a) Whole-body MRA
The MAGNETOM Avanto system, in standard configuration, is capable of performing true whole-body MRA from head to toe, taking advantage of the maximum FoV of 205 cm (Fig. 1). This is useful for the evaluation of vasculitis such as arteriosclerosis obliterans and Takayasu's disease. Our whole-body MRA protocol consists of 4 segments. Each has a FoV of 400-500 mm, scan time of 8 seconds to capture the first pass of contrast agent.

(b) Whole-body imaging of bone marrow diseases
Recently, studies showing that whole-body MRI imaging using STIR technique is superior to bone scintigraphy in detecting bone metastases and multiple myeloma have been reported and are receiving attention. Our MAGNETOM Avanto is capable of performing high contrast whole-body bone imaging in a short time by the combination of high-SNR surface coils and Parallel Imaging technique. We use enhanced 3D FLASH subtraction images in addition to conventional STIR images (Fig. 2). Diffusion-weighted images (b=1000) with less distortion are also very useful in lesion detection, providing high sensitivity comparable to enhanced 3D FLASH images (Fig. 3). The highly sensitive whole-body bone imaging appears to eliminate the need for bone scintigraphy.

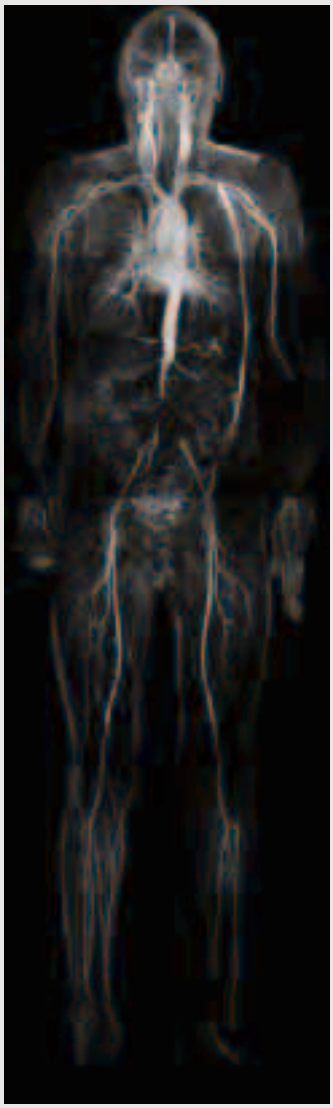

Figure 1 *Whole-body MR Angiography (MRA).*

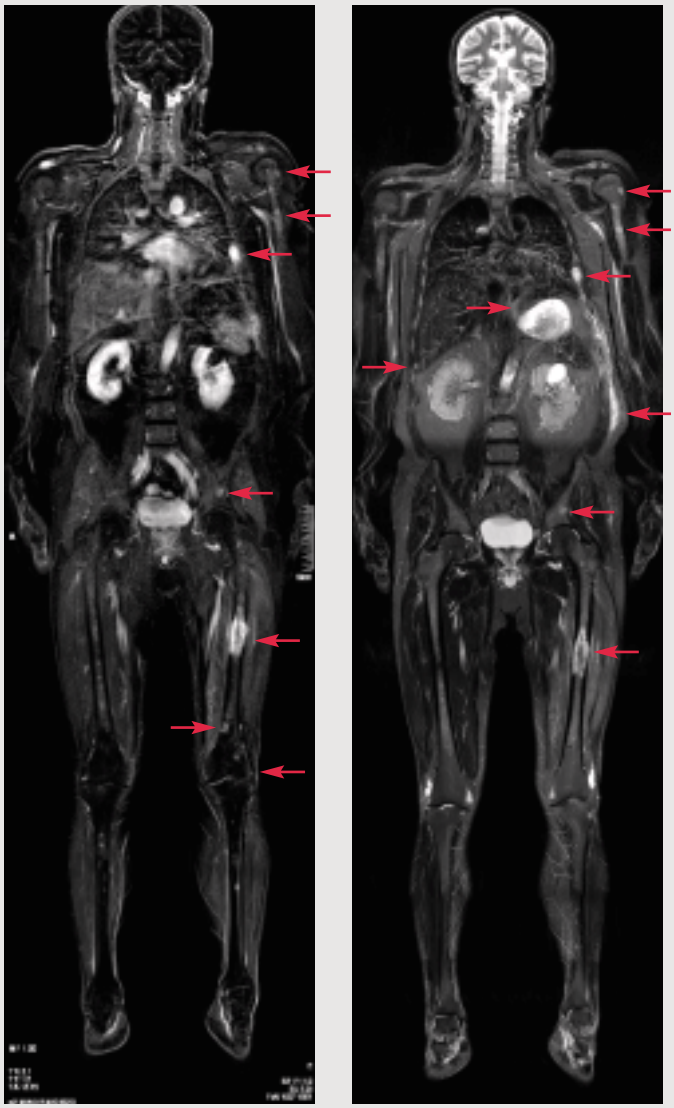

Figure 2 *Whole-body imaging.*

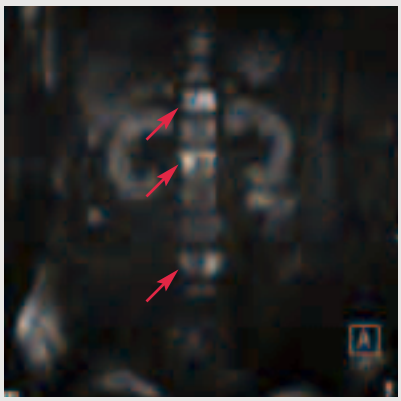

Figure 3 *Diffusion-weighted imaging.*

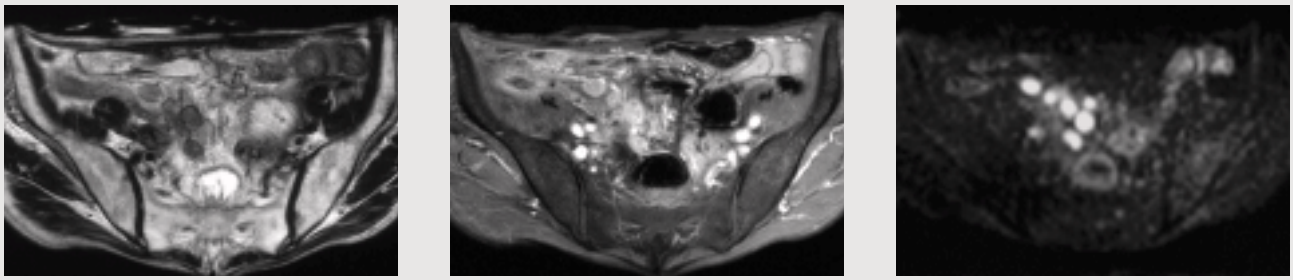

Figure 4 *Lymph node metastases can be seen better using diffusion-weighted imaging.*

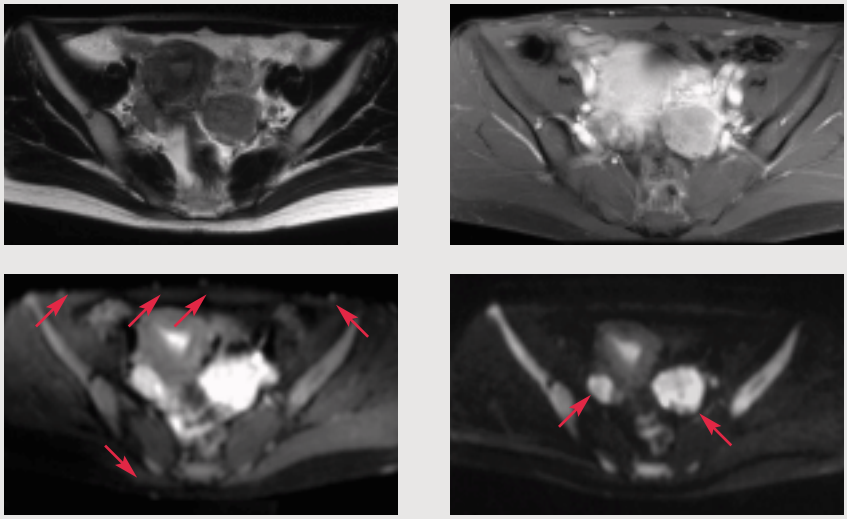

Figure 5 *Distant metastases can be evaluated using diffusion-weighted imaging.*

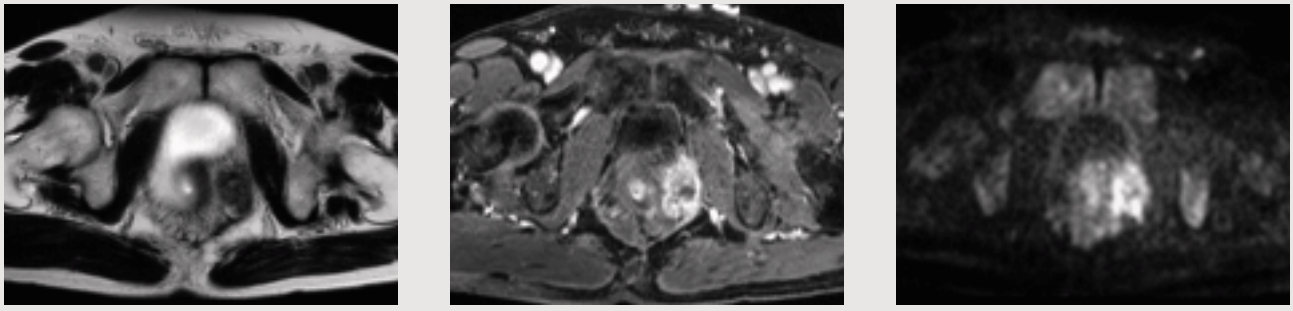

Figure 6 *Recurrence of rectal cancer proven with diffusion-weighted imaging.*

(c) Staging and evaluation of treatment response of malignant tumors
Whole-body imaging with MDCT (Multi Detector CT) or PET (Positron Emission Tomography) is widely performed for the staging and evaluation of treatment response of malignant tumors. However, additional MRI or bone scintigraphy is performed for the imaging of the central nervous system and the bone/ soft tissue. Whole-body MRI using a conventional MR scanner has the disadvantage of long imaging time, while it has relatively high detection sensitivity. Now our system can perform whole-body imaging in a relatively short time (approximately 50 minutes including enhanced imaging). In addition, diffusion-weighted images with significantly improved quality allow diagnoses of metastases in lymph nodes (Fig. 4), distant metastases (Fig. 5) and bone metastases, postoperative evaluation of recurrence (Fig. 6) and assessment of the degree of tumor differentiation. Our experience suggests that the MAGNETOM Avanto's whole-body MRI might replace PET in tumor detection.

(d) Whole-body imaging of multiple muscle disorders and arthritis
Identification of the affected muscles in patients with myopathies (systemic muscle disorders), such as muscular dystrophy and polymyositis, is important in understanding the course of the disease. Whole-body CT imaging is performed for this purpose. Whole-body MRI now allows quantitative as well as qualitative assessments of the muscles of the entire body without X-ray exposure. This has a great clinical significance.

Now it is also possible to examine more than one affected joint in a patient with polyarthritis in one session. This is useful for understanding the progression of the disease and follow-up. Another advantage of the simultaneous assessment of multiple joints is that it can reduce the dose of gadolinium contrast agent required for evaluation of rheumatoid arthritis activity.

II) Local applications

(a) Central nervous system
Routine imaging consisting of brain MRI and head-neck MRA can be done within 10 minutes. Diffusion-weighted images, which we use frequently, have less distortion thanks to improved magnetic field homogeneity and Parallel Imaging technique.

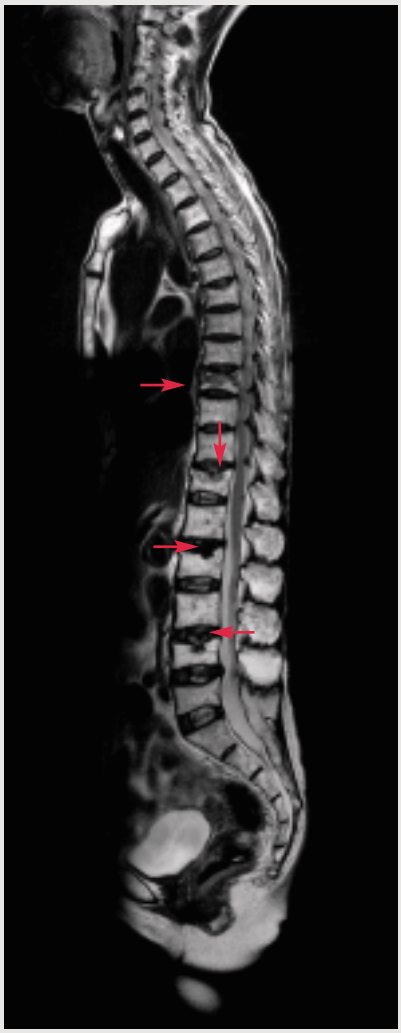

Figure 7 *Whole-spine imaging with MAGNETOM Avanto.*

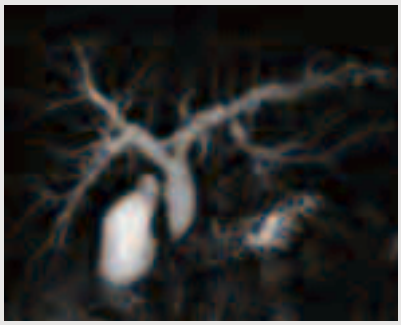

Figure 8 *MR Cholangiography (MRCP)*

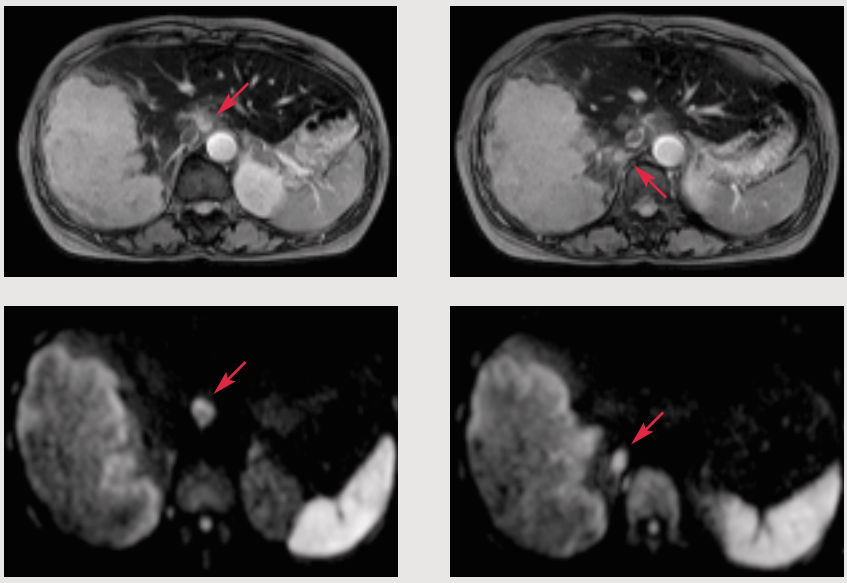

Figure 9 *Diffusion-weighted imaging allows to detect liver tumors better than the SPIO-MRI (SPIO = superparamagnetic iron oxide).*

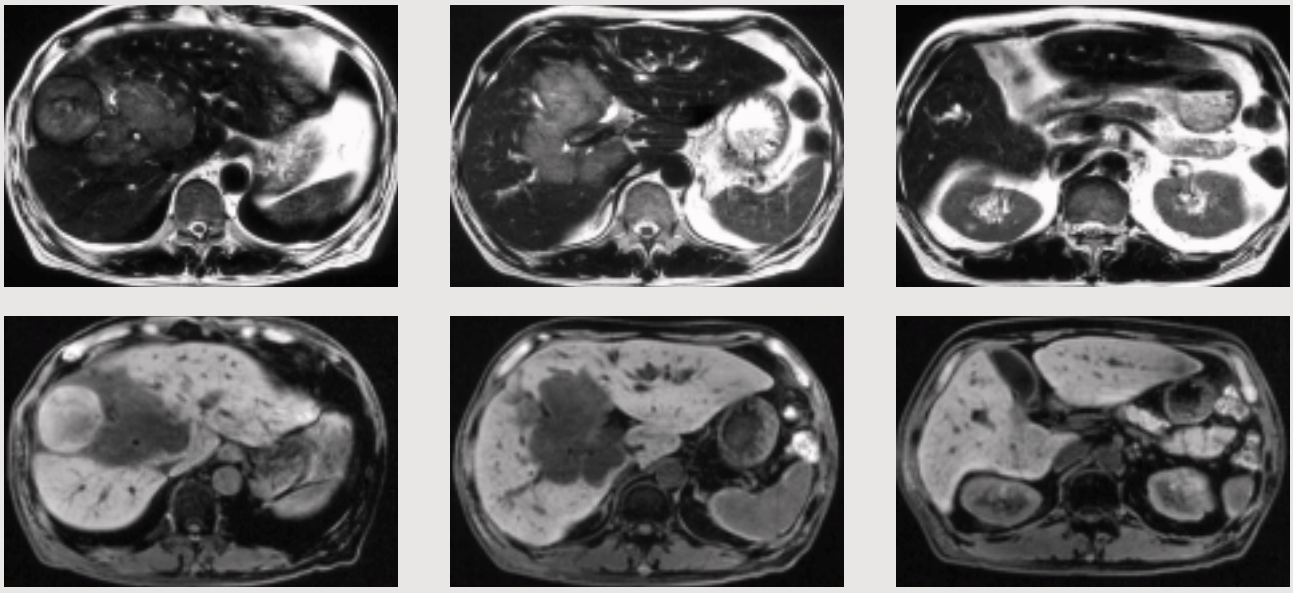

Figure 10 *Compared to dynamic MRI with contrast medium, diffusion-weighted images show recurrent tumor after TAE (Trans Arterial Embolization) better.*

3D-MRDSA, which is considered useful for diagnosis of vascular malformation, can be performed at approximately 1.5 seconds per frame.

In imaging of the spine that extends in the cranio-caudal direction, the use of Siemens' unique Parallel Imaging algorithm or GRAPPA reduces the imaging time. Thus whole-spine imaging in a patient with multiple vertebral compression fracture or disseminated lesions in the central nervous system can be done in approximately 10 minutes (Fig. 7).

(b) Thoracic area
Application of MRI to pulmonary masses has been limited to those with relatively large diameters. Now the MAGNETOM Avanto can visualize nodules with diameters of 5 mm or larger. However, nodules with diameters of 5 mm or smaller are not visualized on diffusion-weighted images (b = 1000). This is an issue that requires further study.

The usefulness of HASTE MRI in the detection of pulmonary nodules has been reported. We expect that the use of PACE technique (discussed later) will further improve this kind of detection and characterization.

We also expect that high resolution MRI will be used for characterization of pulmonary lesions such as diffuse pulmonary disease.

(c) Abdominal area
Prospective Acquisition and Correction (PACE) is a respiratory triggering technique that uses a navigator echo to monitor the position of the diaphragm. 2D-PACE is available on MAGNETOM Avanto. We routinely use respiratory triggered 3D-MRCP using 2D-PACE, which can produce images with isotropic voxels of 1 mm (Fig. 8).

Dynamic study of the abdominal parenchymatous organs using 3D VIBE can now be done in a shorter time and a higher resolution. We can scan each phase of the liver study in 14 seconds and obtain 2-mm-thick slices.

SPIO-enhanced MRI has sensitivity comparable to CTAP in the detection and characterization of liver masses. And the Avanto's diffusion-weighted imaging (b = 50, 1000) has a detectability of liver masses equal to or higher than the SPIO-MRI (Fig. 9). While SPIO-MRI can only detect intrahepatic lesions, diffusion-weighted imaging can detect any metastases with high sensitivity and therefore is useful for evaluation of recurrence. In post-TAE follow-up of patients with hepatocellular carcinoma, recurrent tumor is not likely to be missed, even if it is a poorly differentiated tumor that tends to be poorly enhanced and difficult to identify by dynamic studies (Fig. 10).

In the case of bladder tumors, diagnosis of the depth of invasion has a great impact on the treatment strategy. Previously, the depth of

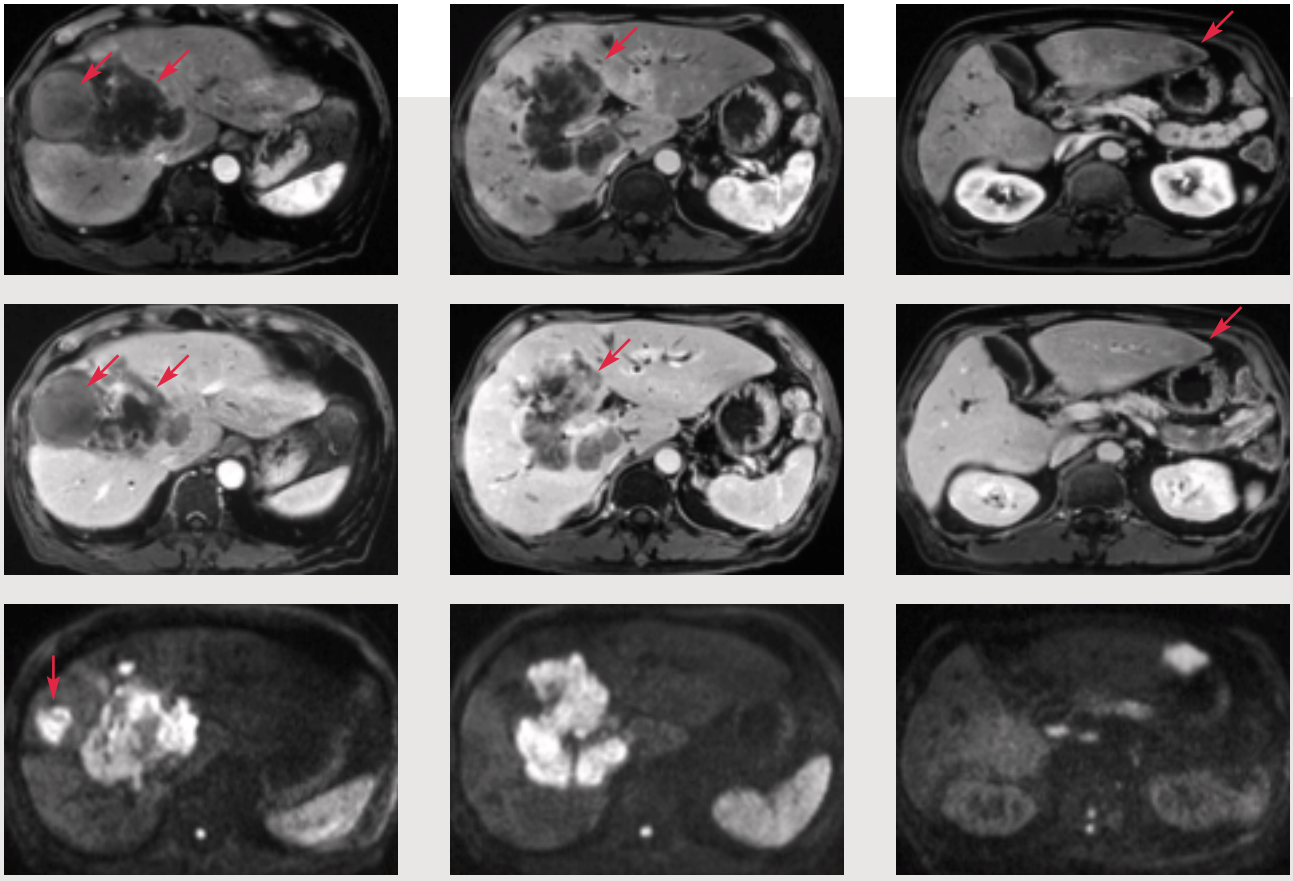

Figure 10 *Compared to dynamic MRI with contrast medium, diffusion-weighted images show recurrent tumor after TAE (Trans Arterial Embolization) better.*

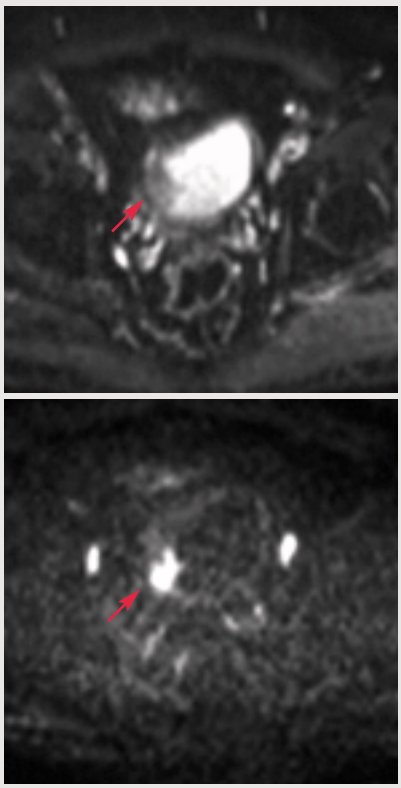

Figure 11 *Urinary bladder wall DWI shows that the thickened wall contains tumorous tissue.*

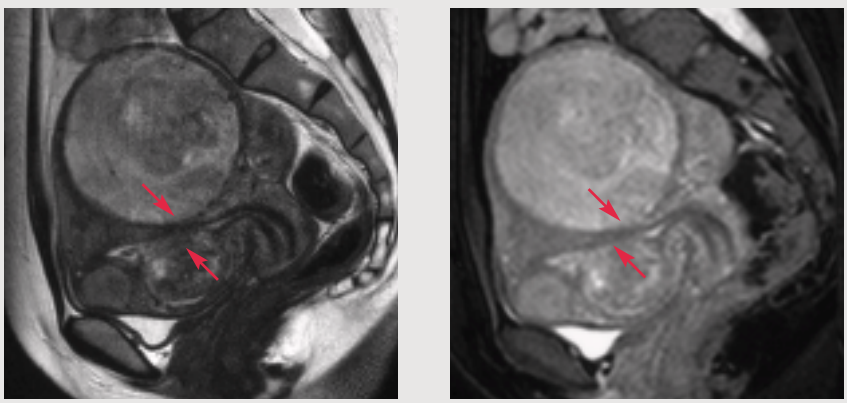

Figure 12 *Visualization of utrine myoma with TrueFISP and HASTE.*

invasion has been determined by T2-weighted images and dynamic studies. However, these methods cannot differentiate between the tumor and reactive fibrosis, it may result in overdiagnosis. Diffusion-weighted imaging may selectively visualize tumorous tissues in the bladder wall with thickening (Fig. 11).

TrueFISP offers fast imaging with high SNR even for thin slices. By using sequential TrueFISP imaging, movements of the gastrointestinal tract can be observed, almost in real time. This is useful in identifying the cause of ileus and localizing the area of adhesion. Thin slice TrueFISP sagittal images, which we routinely use, are superior to T2-weighted and HASTE images in visualizing the relation between uterine myoma and the surroundings (Fig. 12).

(d) Joints
Visualization of the detailed anatomical structure of a certain joint requires a dedicated surface coil, while evaluation of bone marrow lesions can be done using a whole-body surface coil. Since MAGNETOM Avanto allows simultaneous use of surface coils for a joint and whole-body coverage, we can first obtain high resolution images of a certain joint using a dedicated surface coil, and then perform examinations of other joints over the entire body.

In imaging of the joints of the upper limbs, we can obtain images with good quality even if the imaging is performed with the arms at the sides, or the joint to be imaged is in off-center position.

(e) Pediatrics
AudioComfort reduces the acoustic noise during imaging by up to 30 dB. Therefore, as in case of adult patients, we can use acoustically noisy TSE and fast GRE imaging for sedated children.

4. Practical issues in clinical use

At ECR 2004, usefulness of whole-body MR imaging, the initial purpose of developing the Avanto, was reported. Now the whole-body MR imaging becomes a practical option. There will be further discussion, whether it is superior to whole-body PET/CT imaging. In our country, MRI is likely to be recognized as detailed examination, only a limited number of hospitals perform whole-body MR imaging. However, due to the fact that MRI can evaluate the internal organs and bone/soft tissues simultaneously, without X-ray exposure, and offer diffusion-weighted imaging that has a sensitivity equal to or higher than contrast enhanced imaging, MRI is expected to play the leading role in whole-body imaging in the future.

According to the current medical fee schedule, the medical fee for MRI of whole body or multiple body regions is equal to that of the MRI of only one specific region. However, when Diagnosis Procedure Combination (DPC) comes into effect, the fees for whole-body scans on multiple modalities will be bundled into a single payment, therefore, if the multi-modality whole-body imaging is replaced by a single whole-body MRI, it is very advantageous to hospitals. From the viewpoint of overall health economics, whole-body MRI is expected to significantly reduce healthcare expenditures because it can eliminate the need for expensive nuclear medicine examinations and reduce the dose of contrast agent.

On the other hand, in fact, costs for MR equipment, image processing equipment, data storage equipment, and human resources are high. For radiologists who interpret MR images, interpretation of large amounts of high resolution images is a burden, very similar to what has happened with the advent of MDCT. However, unlike MDCT that simply increases the amount of information, diffusion-weighted images help to prevent missing important information and improve the interpretation efficiency. In spite of the large amount of images, more than 20 films per patient, interpretation is not as stressful as initially expected.

Diffusion-weighted images must be interpreted with careful attention to various pitfalls. We must not blindly believe the information that appears on the images. The capability and limitation of diffusion-weighted imaging will be demonstrated as further knowledge is gained in the future. At this moment, it is recommended to carefully refer to conventional T1-weighted and T2-weighted images.

Conclusion

With the advent of MAGNETOM Avanto with Tim technology, it is now possible to obtain high resolution whole-body images in a short time. Whole-body MRI is now a practical option. Moreover, the quality of diffusion-weighted images is remarkably improved; the accuracy of staging and characterization of the lesion is significantly improved as well. In the future, a new concept of diagnostic imaging will be created through the comparison with other modalities. Whole-body MRI is on its way to become an ideal examination tool with less physical and economic burdens on patients.

Acknowledgement

We are deeply grateful to our radiological technologists Hisashi Kitagawa and Takayuki Kishi for their support in preparing this report.

Diffusion-Weighted MR Imaging for Diagnosis of Liver Metastases

Bachir Taouli, M.D.

**Department of Radiology,
NYU Medical Center,
New York, USA**

Liver metastases are the most frequently encountered malignant lesions, most frequently related to colorectal, lung and breast carcinomas. Diagnosis of liver metastases can be obtained with ultrasound (which suffers from limited sensitivity), CT and MR imaging before and after intravenous contrast injection. In some instances, metastases can be difficult to differentiate from benign lesions such as hemangiomas or focal nodular hyperplasias (FNH), and therefore an accurate method of characterization is necessary to avoid unnecessary treatments and anxiety for patients. In addition, in patients with known liver metastases undergoing surgical resection, an accurate detection of metastases is necessary for the surgical planning.

Diffusion is the thermally induced motion of water molecules in biological tissues, called Brownian motion. With the addition of motion probing gradient (MPG) pulses, magnetic resonance imaging (MRI) – by means of the apparent diffusion coefficient (ADC) measurement – is currently the best imaging technique for in vivo quantification of the combined effects of capillary perfusion and diffusion.

Diffusion-weighted imaging (DWI) is possible by using diffusion gradients on each side of the 180° pulse when using single-shot Spin Echo echoplanar imaging (EPI) sequences, using various b-values. The b-value represents the diffusion factor (measured in s/mm^2) and represents the strength of the diffusion gradients. The ideal b-value for lesion characterization is a trade-off between signal attenuation and perfusion contamination, this is generally possible using b-values between 300-1000 s/mm^2 for liver imaging. Pure diffusion images are obtained when using b-values > 1000 s/mm^2, however images will be limited by signal loss.

The ADC (measured in mm^2/s) represents the slope of the curve of signal intensity vs. b-value, and is calculated using the following formula: ADC = (-1/b) Log S1/S0; where b = diffusion factor, S_0 = signal intensity (SI) for b= 0 (before application of diffusion gradient), S_1 = SI after application of diffusion gradient.

The primary application of diffusion-weighted imaging has been in brain imaging. With the advent of EPI technique, DWI of the abdomen has become possible with fast imaging times minimizing the effect of gross physiologic motion from respiration and cardiac movement. DWI can be used to detect and characterize liver lesions (including malignant lesions), and also for treatment follow-up.

Protocol used in our institution

At NYU medical center, for DWI of the liver, we use breath-hold single shot EPI sequences on 1.5T (MAGNETOM Sonata and MAGNETOM Avanto), using CP array surface coils, a pulse trigger to minimize artifacts from heart beating [1]. We use a short TR (1300 ms) to decrease the acquisition time, and the shortest possible TE (approximately 50-70 ms. depending on the b-value) close to the T2 of the liver (which is approximately 50 ms at 1.5T). We use parallel imaging (GRAPPA 2) in order to decrease distortion artifacts, acquisition time as well as to get the shortest possible TE [2]. The matrix size is 128 x 128, with a large FoV in order to decrease ghosting artifacts, and a slice thickness of 7-8 mm. We use typically b-values of 0-50-500-1000 s/mm^2.

Role of DWI for detection of liver lesions

There is limited data on the use of DWI for lesion detection. For example, a recent study from the Netherlands [3] showed that DWI with small b-values < 50 s/mm^2 giving black-blood images can potentially replace the routine Turbo Spin Echo T2 for lesion detection. Fig. 1 shows images in a normal volunteer using small diffusion gradients.

DWI for characterization of liver lesions and diagnosis of liver metastases

DWI represents a potential new tool for the characterization of liver metastases, and differentiation of benign from malignant liver lesions. DWI is non invasive, requires no contrast injection, and can be performed within a breath-hold.

Most of previous studies have used DWI to characterize liver lesions, and have shown that benign lesions – such as liver cysts and hemangiomas – show higher ADCs than malignant lesions – such as hepatocellular carcinomas and metastases [4-8]. This is likely related to free water motion in benign lesions, and restricted water motion in the presence of tumor. However, ADC values are often variable from a study to another, partially related to different equipment and different b-values. ADCs tend to be larger when using small b-values, because the signal attenuation due to diffusion plays only a minor role in that case, and ADC values are contaminated by microperfusion. When higher b-values

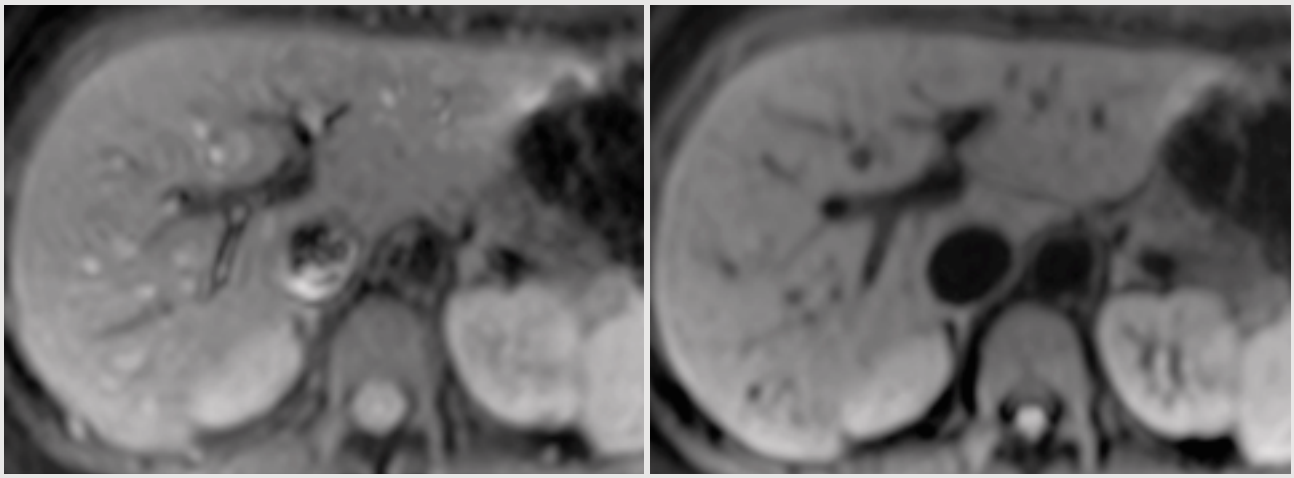

Figure 1a Figure 1b

Figure 1 (a, b) *Diffusion-weighted images in a 31-year-old normal volunteer. Single-shot EPI images without application of a diffusion gradient (b = 0 s/mm²) and after application of a small diffusion gradient of b = 50 s/mm² (b, black-blood image). Note complete vessel darkening on b. This allows easier detection of liver lesions which will not attenuate at this small b-value.*

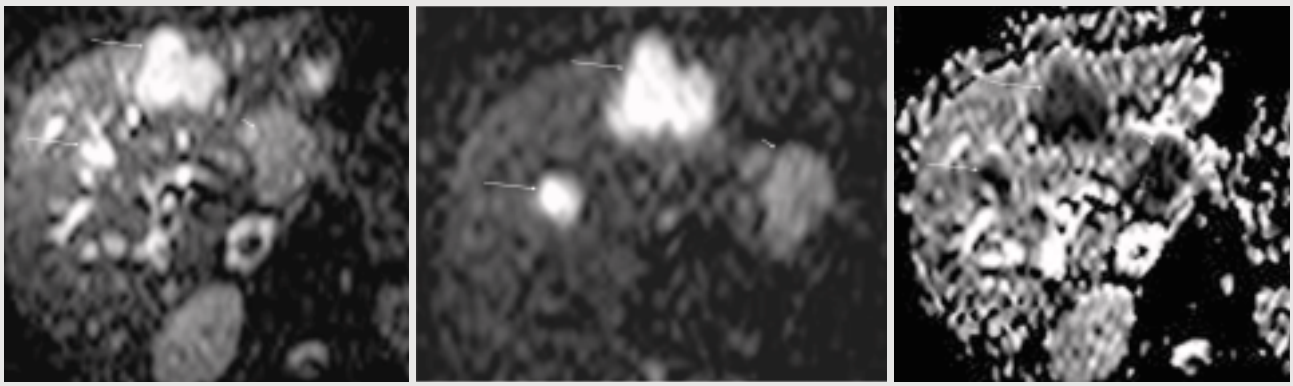

Figure 2a Figure 2b Figure 2c

Figure 2 (a-c) *33-year-old man with liver metastases from pancreatic islet cell tumor. Diffusion-weighted images obtained using single-shot EPI for b = 0 s/mm² (a) and b = 500 s/mm² (b), without parallel imaging, show metastases of the right and the left liver lobes (long arrows) in high signal, with no attenuation at b = 500 s/mm². The primary tumor is located in the pancreatic head (short arrow). These lesions can be easily confused for hemangiomas. ADC measured on the mapping image (c) was very low (0.5 x 10^{-3} mm²/s).*

are used, ADCs tend to decrease, in relation with less perfusion contamination. We showed in a previous study [8] a significant difference between ADCs of benign and malignant lesions ($2.45 \pm 0.96 \times 10^{-3}$ and $1.08 \pm 0.50 \times 10^{-3}$ mm²/s for b = 0 and 500 s/mm²; respectively, $p < 0.001$). The mean ± SD ADCs ($\times 10^{-3}$ mm²/s) of the different groups of lesions were: metastases 0.94 ± 0.60, hepatocellular carcinomas 1.33 ± 0.13, FNH / adenomas 1.75 ± 0.46, hemangiomas 2.95 ± 0.67 and cysts 3.63 ± 0.56 [8]. Using a threshold ADC value of 1.5×10^{-3} mm²/s, we were able to differentiate benign from malignant lesions with 84% sensitivity and 89% specificity. Potential limitations will include necrotic and cystic metastases, where ADC might be elevated, and the diagnosis will then rely on post-contrast images. Fig. 2 and 3 show examples of patients with liver metastases.

DWI for follow-up of treated liver metastases

DWI can potentially be used to follow treated metastases, whether using systemic or local chemotherapy (transarterial catheter chemoembolization), or local treatment (such as radiofrequency or cryoablation). A recent study has shown the usefulness of DWI over routine contrast-enhanced MRI for prediction of hepatocellular carcinoma necrosis in cirrhotic patients [9]. An animal study has also shown a good correlation between response to therapy and ADC changes [10, 11].

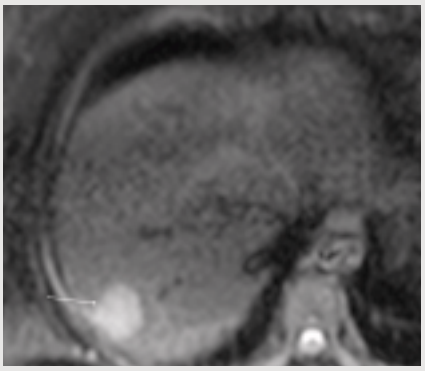

Figure 3a

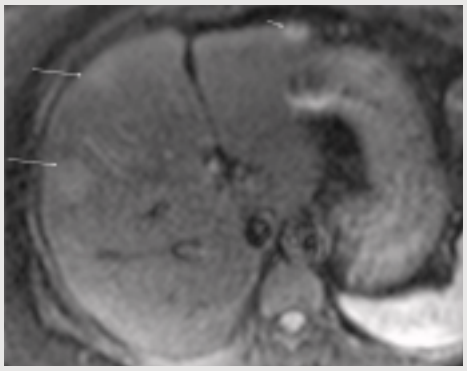

Figure 3b

Figure 3(a-e) *34-year-old patient with liver metastases from colon cancer. Diffusion-weighted images obtained with single-shot EPI and parallel imaging, b-values of 0 (a, b) and b = 500 s/mm² (c, d) show multiple hyperintense liver lesions, with no attenuation on diffusion-weighted images. In particular, there is a sub-centimeter lesion in the lateral left lobe (short arrow) not seen on the routine axial TSE T2 (e) images.*

Future improvements in image quality

3T technology will be potentially able to provide better image quality in relation with improved signal. However, susceptibility and distortion artifacts with EPI sequences may also be increased [12].

Conclusion

DWI allows functional imaging of liver lesions and liver disease. The acceptance of DWI into routine practice will be parallel to the new developments in sequences and also to the improved experience of the radiologists in this area.

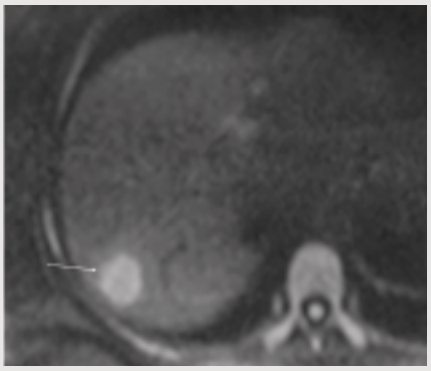

Figure 3c

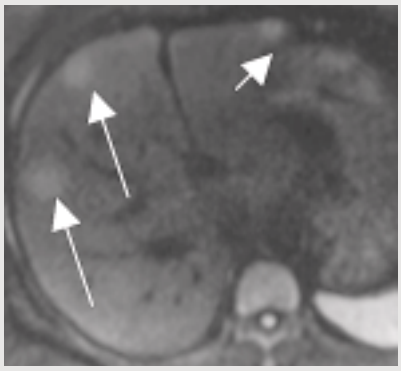

Figure 3d

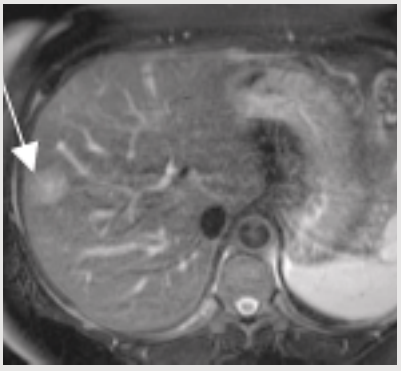

Figure 3e

References

[1] *Murtz P, Flacke S, Traber F, van den Brink JS, Gieseke J, Schild HH. Abdomen: diffusion-weighted MR imaging with pulse-triggered single-shot sequences. Radiology 2002; 224:258-264.*

[2] *Taouli B, Martin AJ, Qayyum A, et al. Parallel imaging and diffusion tensor imaging for diffusion-weighted MRI of the liver: preliminary experience in healthy volunteers. AJR Am J Roentgenol 2004; 183:677-680.*

[3] *Hussain SM, De Becker J, Hop WC, Dwarkasing S, Wielopolski PA. Can a single-shot black-blood T2-weighted spin-echo echo-planar imaging sequence with sensitivity encoding replace the respiratory-triggered turbo spin-echo sequence for the liver? An optimization and feasibility study. J Magn Reson Imaging 2005; 21:219-229.*

[4] *Muller MF, Prasad P, Siewert B, Nissenbaum MA, Raptopoulos V, Edelman RR. Abdominal diffusion mapping with use of a whole-body echo-planar system. Radiology 1994; 190:475-478.*

[5] *Namimoto T, Yamashita Y, Sumi S, Tang Y, Takahashi M. Focal liver masses: characterization with diffusion-weighted echo-planar MR imaging. Radiology 1997; 204:739-744.*

[6] *Kim T, Murakami T, Takahashi S, Hori M, Tsuda K, Nakamura H. Diffusion-weighted single-shot echoplanar MR imaging for liver disease. AJR Am J Roentgenol 1999; 173:393-398.*

[7] *Ichikawa T, Haradome H, Hachiya J, Nitatori T, Araki T. Diffusion-weighted MR imaging with single-shot echo-planar imaging in the upper abdomen: preliminary clinical experience in 61 patients. Abdom Imaging 1999; 24:456-461.*

[8] *Taouli B, Vilgrain V, Dumont E, Daire JL, Fan B, Menu Y. Evaluation of liver diffusion isotropy and characterization of focal hepatic lesions with two single-shot echo-planar MR imaging sequences: prospective study in 66 patients. Radiology 2003; 226:71-78.*

[9] *Kamel IR, Bluemke DA, Ramsey D, et al. Role of diffusion-weighted imaging in estimating tumor necrosis after chemoembolization of hepatocellular carcinoma. AJR Am J Roentgenol 2003; 181:708-710.*

[10] *Roth Y, Tichler T, Kostenich G, et al. High-b-value diffusion-weighted MR imaging for pretreatment prediction and early monitoring of tumor response to therapy in mice. Radiology 2004; 232:685-692.*

[11] *Herneth AM, Guccione S, Bednarski M. Apparent diffusion coefficient: a quantitative parameter for in vivo tumor characterization. Eur J Radiol 2003; 45:208-213.*

[12] *Kuhl CK, Textor J, Gieseke J, et al. Acute and subacute ischemic stroke at high-field-strength (3.0-T) diffusion-weighted MR imaging: intraindividual comparative study. Radiology 2005; 234:509-516.*

Body Diffusion Experience with Over 600 Patients

Noriatsu Ichiba, M.D.
Kunihiko Fukuda, M.D.

Department of Radiology
Jikei University Hospital
Tokyo, Japan

Introduction

Diffusion MR imaging has been up to now used mostly in the head. By detecting water motion over small distances, it is now routinely performed and enables the diagnoses of an acute stroke*.

In our institution, we have been very interested in the potential of the technique applied to imaging of the body, pelvis and organs other than the brain. Indeed, there have been several reports in the literature that diffusion MRI in the body can indicate the malignancy of lesions.

Methods

There are today many discussions about technical aspects regarding the optimal way to perform body diffusion. Our institution works with a MAGNETOM Avanto and we have been performing body diffusion using a single-shot EPI sequence with a PAT factor of 2.

Initially, we performed free-breathing and respiratory triggered scans to compare them. Now, however, respiratory triggering is mainly used. The parameters of the free-breathing scan are as follows: TR of 3500 ms, TE of 65 ms, slice thickness of 5 mm, 128 x 64 matrix with zero-fill interpolation, 40 slices, and scan time of 3:30 minutes. The parameters of the triggered scan are as follows: respiration cuff placed on the abdominal wall, TR of 1500 ms, TE of 65 ms, slice thickness of 5 mm, 128 x 64 matrix with zero-fill interpolation, 12 slices, and scan time of 3-4 minutes depending on the patient's breathing.

Low (50) and high (1000) diffusion b-values are typically investigated.

The total time for an examination of a specific anatomical segment is 15-20 minutes. A whole abdominal examination consists of T1-weighted, T2-weighted and diffusion-weighted images and can be done in the same period of time. Slice thickness of DWI is usually 6 mm.

** The information about this application is preliminary. The application is under development and is not commercially available in the U.S., and its future availability cannot be ensured.*

Clinical Cases

Case 1: 58-year-old male with lung cancer (squamous cell carcinoma)

The T2-weighted image showed a mass lesion in the left lower lobe (LLL) adjacent to the pleura with a small amount of pleural effusion (Fig. 1). The mass was shown as a mixed high signal area on the STIR image (Fig. 2). With diffusion imaging, the corresponding area showed a ring-like high signal intensity on DWI with b = 1000 (Fig. 3) and very low signal intensity on ADC map (Fig. 4). These DWI findings helpfully suggested that the lesion was a lung cancer.

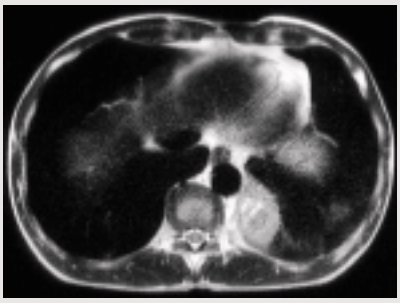

Figure 1 *T2-weighted image*

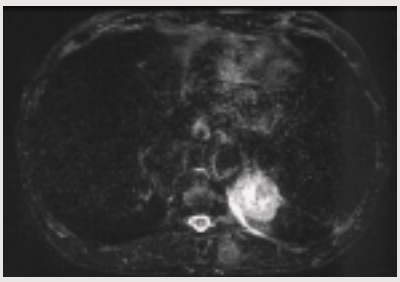

Figure 2 *Short TI Inversion Recovery – STIR image*

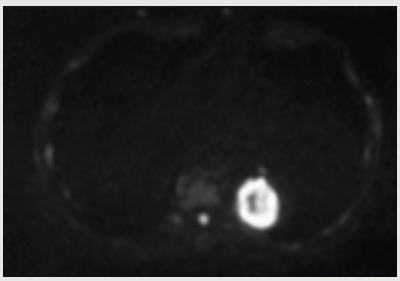

Figure 3 *Diffusion-weighted image – DWI (b = 1000)*

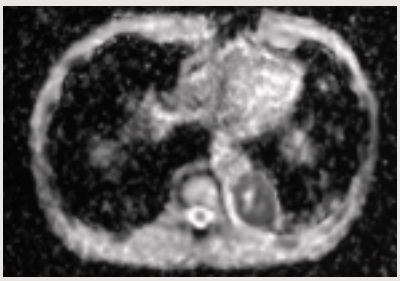

Figure 4 *ADC map*

Case 2: 70-year-old male with chronic empyema with chest pain

There was a left chronic empyema with a pleural mass lesion (Figs. 1-3). The empyema showed high signal on both T1-weighted image and T2-weighted. The pleural mass showed low signal on T1-weighted, high signal on T2-weighted and very well enhanced on the post-enhanced image; these features were compatible with malignant lymphoma. In diffusion imaging (Figs. 4, 5), while both the empyema and the mass showed high signal on DWI with b = 50, only the mass showed high signal on DWI with b = 1000. Additional metastatic nodules can be seen on DWI. With these findings from diffusion images, we came to the conclusion that the mass was of malignant origin. Further tests confirmed the diagnosis of Non-Hodgkin lymphoma.

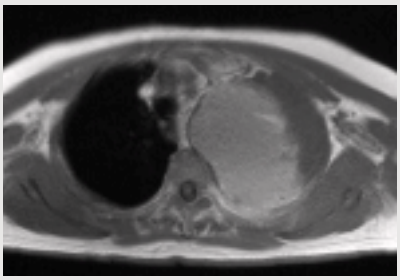

Figure 1 *T1-weighted image*

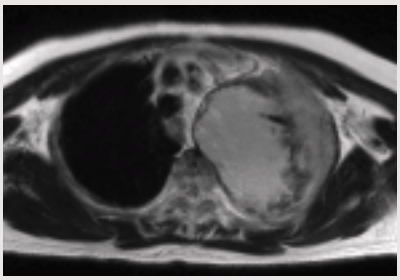

Figure 2 *T2-weighted image*

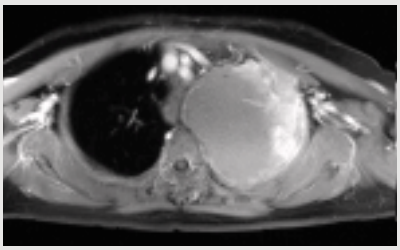

Figure 3 *Post-enhanced image*

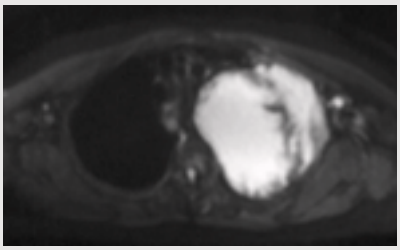

Figure 4 *Diffusion-weighted image – DWI (b = 50)*

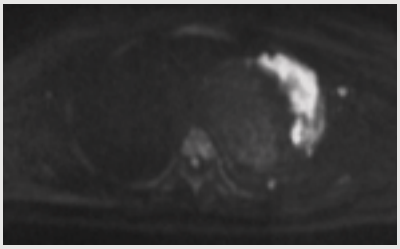

Figure 5 *Diffusion-weighted image – DWI (b = 1000)*

Case 3: 58-year-old male with hepatocellular carcinoma (HCC) after lipiodol TAE (Trans Arterial Embolization)

Figures 1-4 show a round hepatic mass with a capsule in the right lobe. The mass showed high signal on the fat suppressed (FS) T1-weighted; this finding was compatible with HCC after lipiodol TAE. A bizarre recurrent tumor was seen adjacent to the mass. In dynamic study (Figs. 5-8), the recurrent mass showed gradual enhancement pattern, proving to be poorly differentiated adenocarcinoma. An intrahepatic metastatic tumor in the left lateral segment also showed gradual enhancement. DWIs with b = 1000 (Figs. 9, 10) clearly show the recurrent tumor and intrahepatic metastatic tumor as bright lesions, as well as residual viable component in the primary lesion.

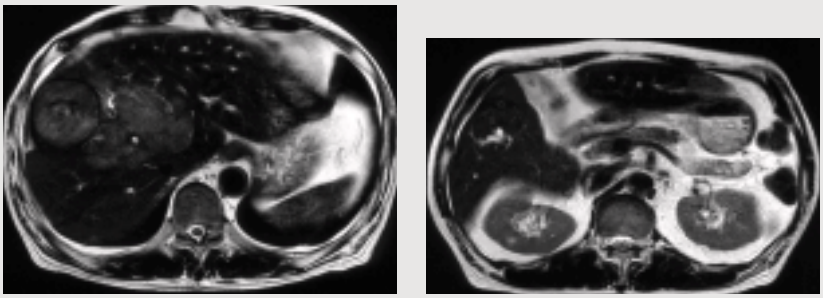

Figure 1, 2 *T2-weighted images*

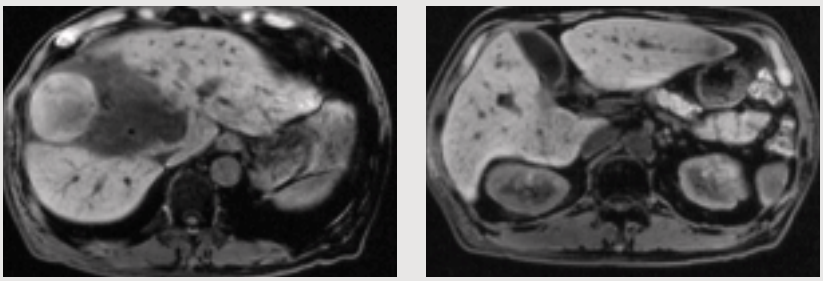

Figure 3, 4 *Pre-contrast 3D VIBE (Volume Interpolated Breathhold Examination) with fat saturation.*

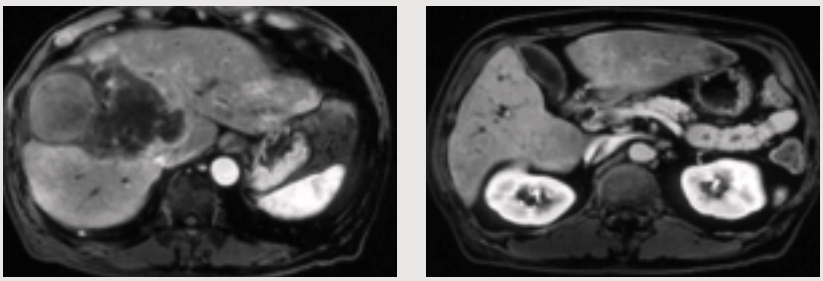

Figure 5, 6 *Early phase of dynamic study (3D VIBE with fat saturation).*

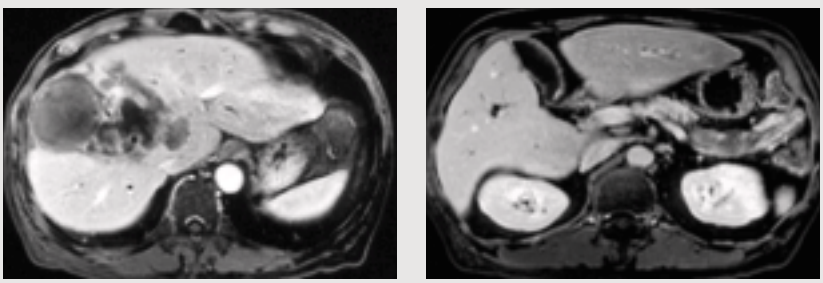

Figure 7, 8 *Delayed phase of dynamic study.*

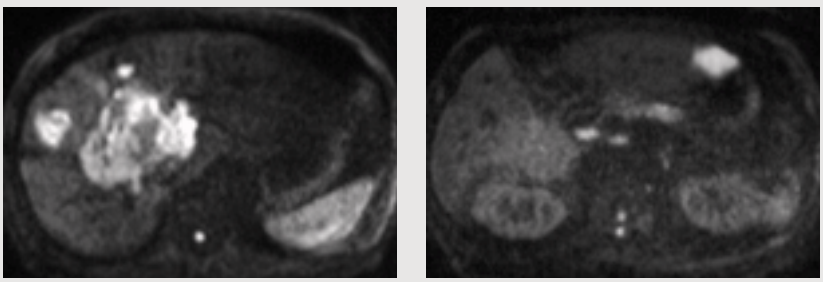

Figure 9, 10 *Diffusion-weighted image – DWI (b = 1000)*

Case 4: 35-year-old male with renal cell carcinoma

Figures 1-3 show a round mass with a capsule in the lower pole of the left kidney, which showed mild enhancement after administration of contrast medium. The lesion showed very high signal on DWI (b = 1000), proved to be renal cell carcinoma (Fig. 4). There was no evidence of metastasis. Our experience has shown that DWI eliminates the need for contrast medium in evaluation of primary and metastatic tumors in such patients.

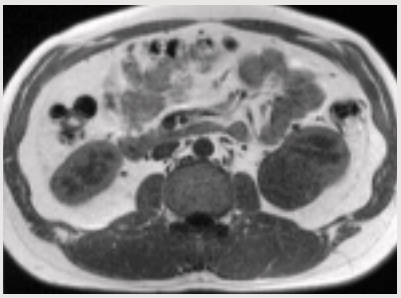

Figure 1 *T1-weighted image*

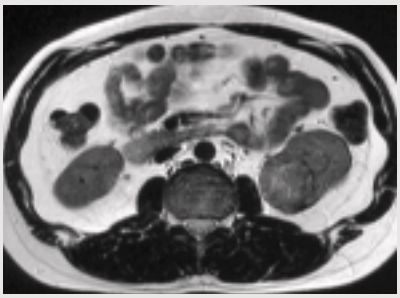

Figure 2 *T2-weighted image*

Figure 3 *Post-enhanced 3D VIBE (Volume Interpolated Breathhold Examination) with fat saturation.*

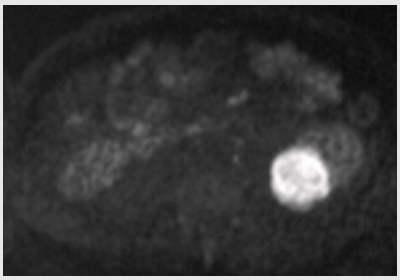

Figure 4 *Diffusion-weighted image – DWI (b = 1000)*

Case 5: 39-year-old female with left ovarian tumor

Figures 1-4 show a round mass lesion in the left adnexa with various components including fat; proving to be ovarian dermoid. The high-signal component within the mass was consistent with the epidermoid component shown on DWI (b = 1000), and the finding of a high-signal component in the right ovary was consistent with hemorrhagic cyst (Figs. 5-7). A benign lesion such as epidermoid and hemorrhagic cyst shows bright signal on DWI due to its viscosity and/or density, so this is a diagnostic pitfall. Abnormal protrusion of the endometrium that can be seen in the right uterine wall as a bright structure, proves to be endometrial carcinoma. From the findings that the metastatic nodules in the right adnexa showed high signal on DWI but low signal on T2-weighted, and the endometrial carcinoma showed high signal on DWI (Fig. 8, b = 3000), it is suggested that advanced endometrial carcinomas could easily be missed without DWI.

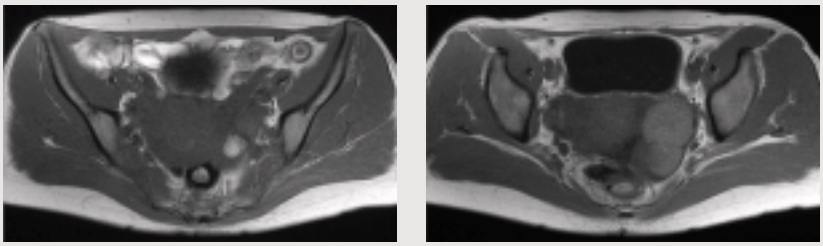

Figure 1, 2 *T1-weighted images*

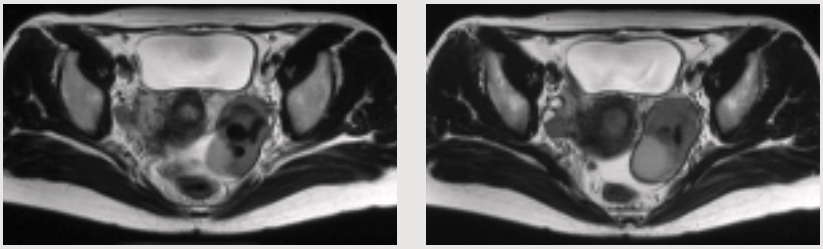

Figure 3, 4 *T2-weighted images*

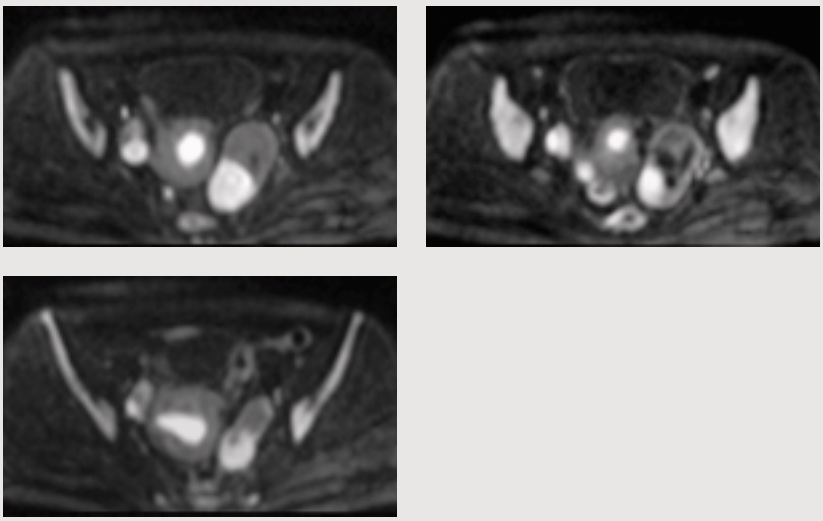

Figure 5-7 *Diffusion-weighted images – DWI (b = 1000)*

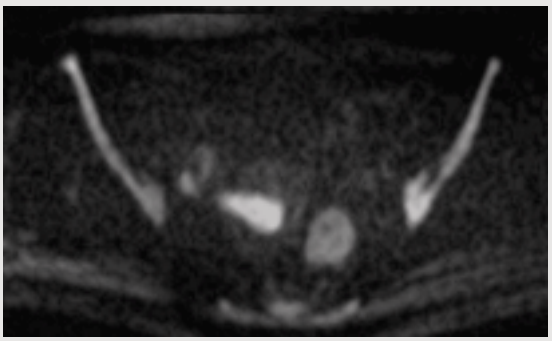

Figure 8 *Diffusion-weighted image – DWI (b = 3000)*

Case 6:
36-year-old female whose PAP smear result was Class V

There were no remarkable malignant tumors in the uterus, but a huge intramural myoma was seen on sagittal images (Figs. 1-4). Careful observation of the DWI (b = 1000) showing a bright region in the uterine cervix (Fig. 5) revealed that a cervical cancer in the portio vaginalis has been missed on the sagittal FS TrueFISP image.

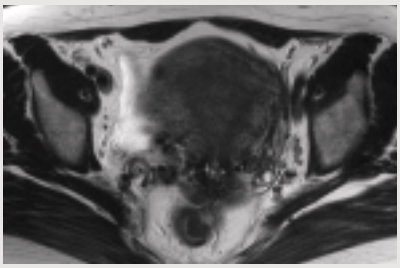

Figure 1 *T1-weighted image*

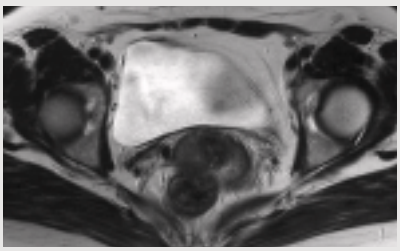

Figure 2, 3 *T2-weighted images*

Figure 4 *TrueFISP (Fast Imaging with Steady Precession) with fat saturation.*

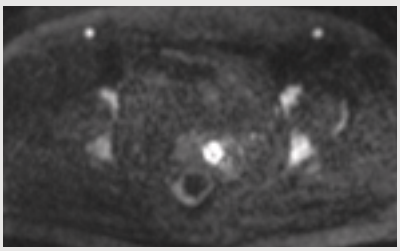

Figure 5 *Diffusion-weighted image – DWI (b = 1000)*

Case 7:
50-year-old female, post-operative state of ovarian cancer, with an elevated tumor marker level

There was no remarkable evidence of recurrent tumors on T2-weighted and FS CE T1-weighted (Figs. 1, 2), but multiple recurrent iliac lymphadenopathies were seen on DWI with b = 1000 (Fig. 3). Fusion images of T2-weighted and DWI (Figs. 4, 5) were useful in grasping the anatomical distribution of the lesions.

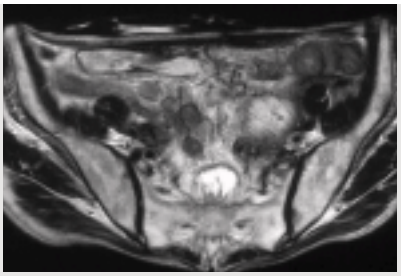

Figure 1 *T2-weighted image*

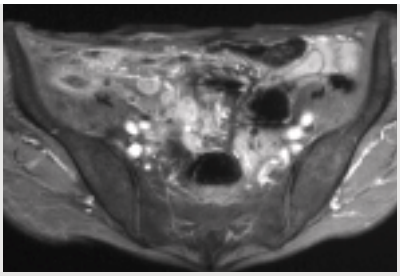

Figure 2 *Contrast-enhanced T1-weighted image with fat saturation.*

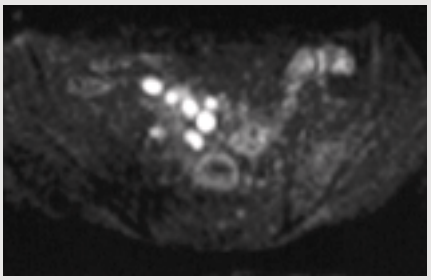

Figure 3 *Diffusion-weighted image – DWI (b = 1000)*

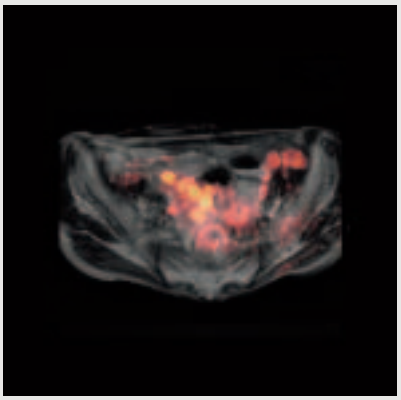

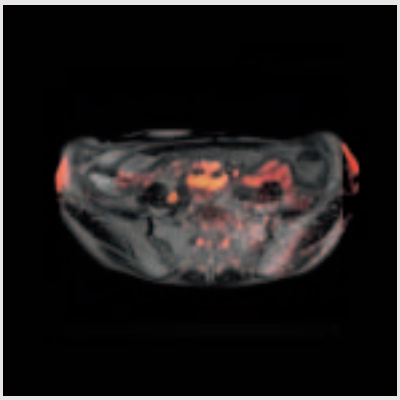

Figure 4, 5 *Fusion images.*

Case 8:
76-year-old male with bladder cancer

Thickening of the right wall of the urinary bladder can be seen on EPI-T2-weighted (Fig. 1, b = 0). There are high and low signal components in the lesion on DWI (Fig. 2, b = 1000); the former corresponds to malignant tumor and the latter to reactive inflammatory process. The bright spots on bilateral iliac walls are normal lymph nodes, proved by their symmetrical spherical shapes and typical location.

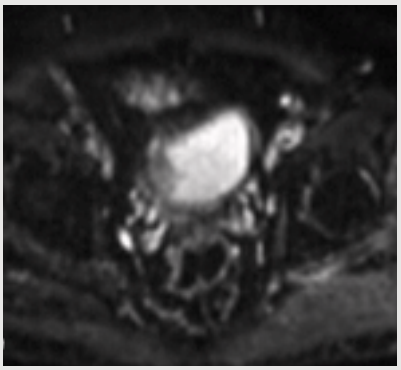

Figure 1 *T2-weighted Echo Planar Image (EPI) (b = 0)*

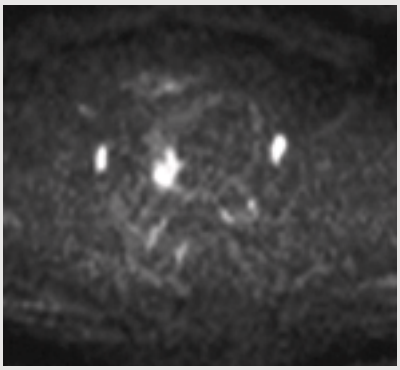

Figure 2 *Diffusion-weighted image – DWI (b = 1000)*

Case 9: 56-year-old male with prostate cancer

A low-signal mass in the inner gland of the prostate was seen on T2-weighted (Fig. 1). With DWI (b = 1000), the mass showed bright signal but the normal peripheral zone of the prostate was also bright (Fig. 2). On DWI with higher b value (b = 3000) shown in Figure 3, only the mass that showed bright signal, proving to be prostate cancer.

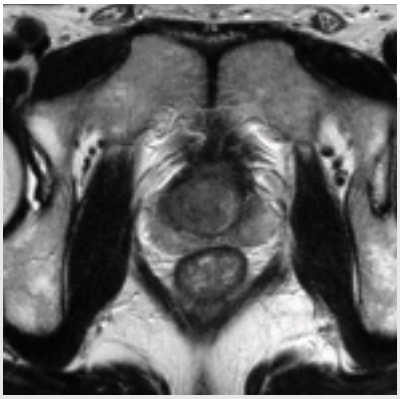

Figure 1 *T2-weighted image*

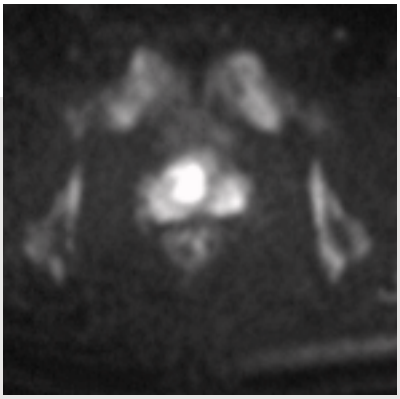

Figure 2 *Diffusion-weighted image – DWI (b = 1000)*

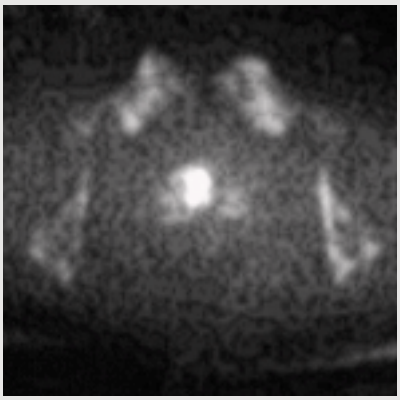

Figure 3 *Diffusion-weighted image – DWI (b = 3000)*

Case 10: 67-year-old male with recurrence of rectal cancer

Extensive post-operative change in the presacral region was seen on T2-weighted (Figs. 1-3). It was difficult to determine the presence of a recurrent tumor on these images, but DWIs (b = 1000) clearly revealed the recurrent tumor (Figs. 4, 5).

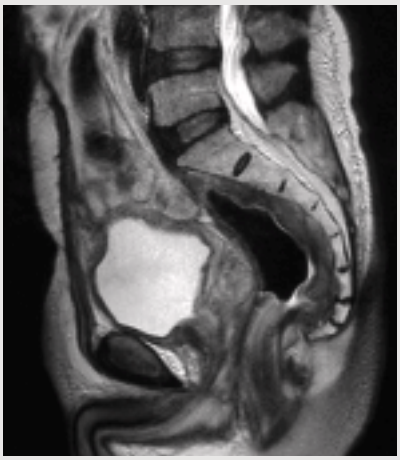

Figure 1-3 *T2-weighted images*

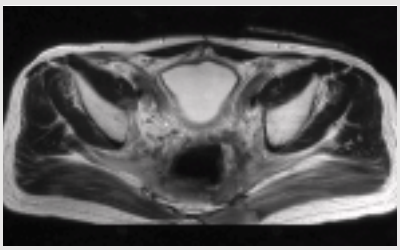

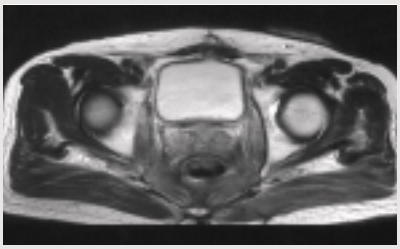

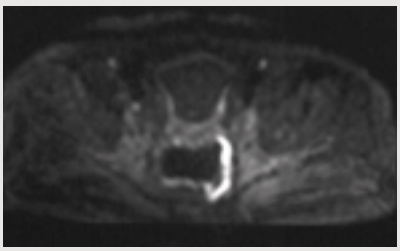

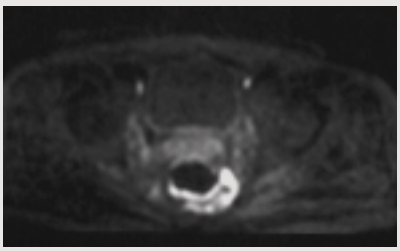

Figure 4, 5 *Diffusion-weighted images – DWI (b = 1000)*

Case 11: 39-year-old female with rectal cancer accompanied by liver metastasis

Rectal wall thickening and multiple liver nodules were seen on SPIO-T2-weighted (Figs. 1-4), but it was unclear whether the lesions were malignant. SPIO-DWIs (b = 1000) showed high signal in the corresponding lesions, revealing that they were malignant tumors (Figs. 5-8). Regional lymphadenopathy around the rectum can also be seen on DWI.

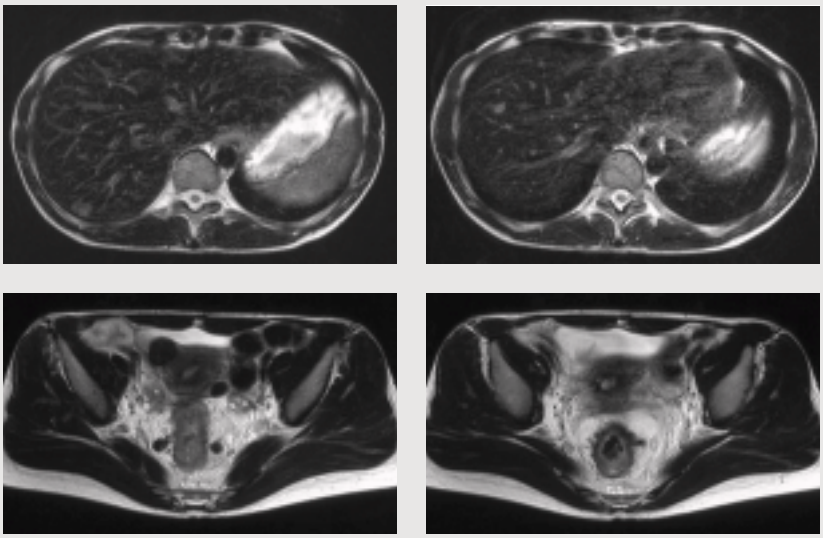

Figure 1-4 *SPIO T2-weighted image*

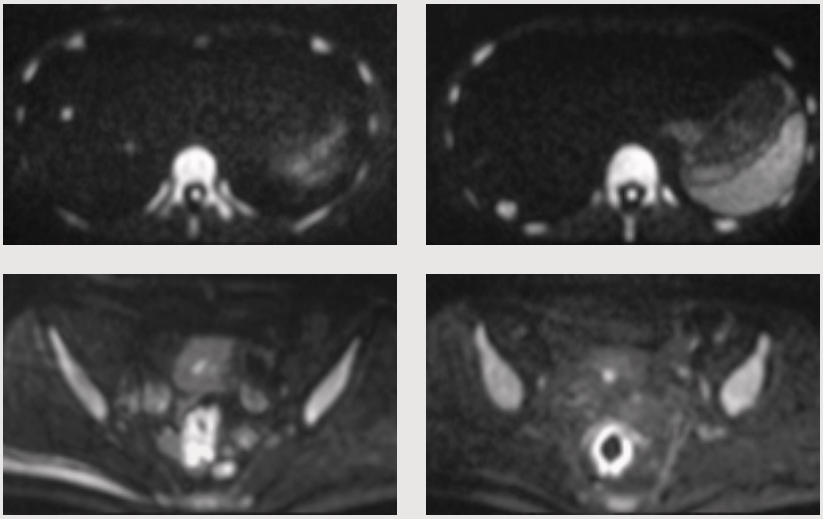

Figure 5-8 *SPIO diffusion-weighted images – DWI (b = 1000)*

SPIO, short for small particle iron oxide or superparamagnetic iron oxide. Used as darkening contrast agent for liver imaging.

Case 12: 70-year-old male with recurrence of rectal cancer

PET image showed mild uptake behind the urinary bladder (Fig. 1). There was an enhancing mass adjacent to the rectum (Figs. 2, 3), which showed high signal on DWI (b = 1000), turning out to be local recurrence (Fig. 4). Fusion image of contrast enhanced 3D VIBE and DWI (b = 1000) (Fig. 5) was useful in identifying the lesion.

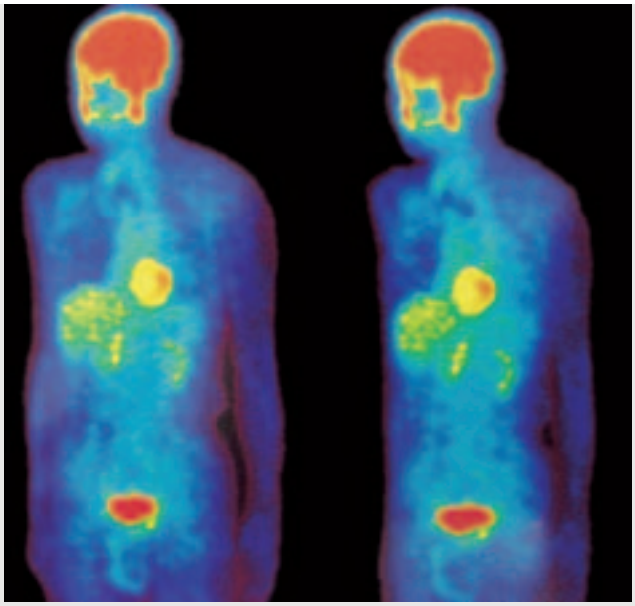

Figure 1 *PET image (Positron Emission Tomography)*

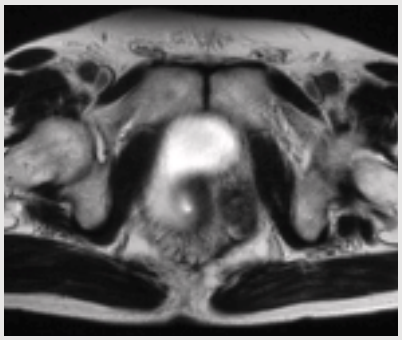

Figure 2 *T2-weighted image*

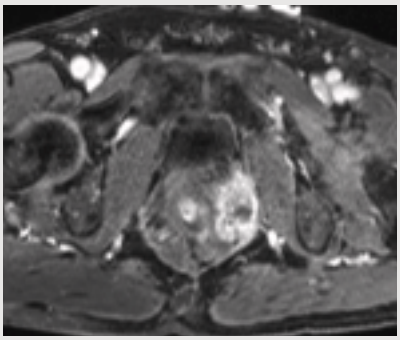

Figure 3 *Post-enhanced 3D VIBE (Volume Interpolated Breathhold Examination) with fat saturation.*

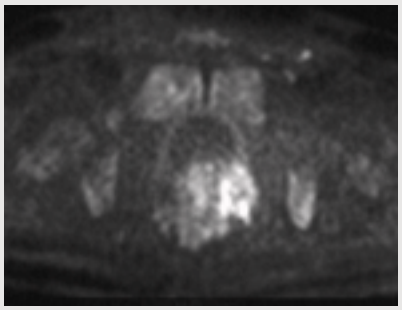

Figure 4 *Diffusion-weighted image – DWI (b = 1000)*

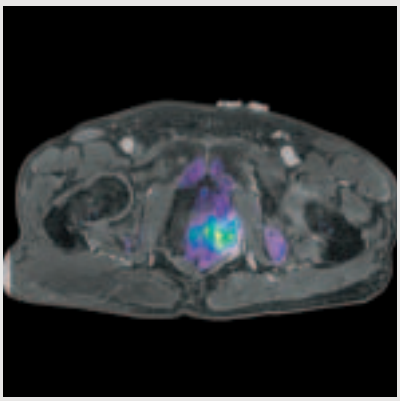

Figure 5 *Fusion image.*

Conclusion

The single-shot EPI with iPAT and CHESS fat suppression on MAGNETOM Avanto has produced very satisfactory body diffusion results.

Therefore, in Jikei University, we currently perform a body diffusion scan for all body patients. This adds only 3:30 min to the entire examination and has proven very useful for the detection of primary as well as metastatic malignant tumors, differentiation between benign and malignant tumors, and differentiation between post-operative inflammatory changes and recurrences. DWI significantly reduces the need for intravenous administration of contrast medium in evaluation of malignancies. Weighing up these features of DWI, we think that DWI should be performed to obtain additional useful information in detailed body examinations.

T2-Weighted 3D MR Imaging of the Torso – First Clinical Experiences with SPACE

M. P. Lichy, M.D.[1]
W. Horger[2]
J. P. Mugler, Ph.D.[3]
Marion I. Menzel, Ph.D.[2]
Berthold Kiefer, Ph.D.[2]
H.-P. Schlemmer, M.D.[1]

[1] Department for Radiological Diagnostics, University Tübingen, Germany
[2] Siemens AG Medical Solutions, MR Division, Erlangen, Germany
[3] University of Virginia, Radiology and Biomedical Engineering, USA

Introduction:

MRT provides the best soft tissue contrast of all imaging methodologies. Based on the technological advances (e.g. coil technology, parallel imaging), magnetic resonance is also able to image large body areals during an examination. The acquisition of larger anatomical regions is frequently the basis for an improved understanding of the pathologies involved. Oncology proves this point better than most. In addition to accurate diagnoses of local tumor expansion, both rather demanding with respect to resolution and contrast, large anatomical regions are required to fully acquire the actual tumor expansion.

This is the only way to provide for an exact as well as clinically useful planning of individual treatment strategies.

Until now, high-speed acquisition of large volumes with high resolution was the domain of multi-slice computed tomography (MS CT). The newest generation of Spiral MS CTs allows for a quick realization of 3D data records in the submillimeter range. But it is the possibility of retrospective reconstruction of random image planes that provides for an additional decisive advantage when dealing with complex relationships between anatomical structures and pathological changes. Based on the poor soft tissue contrasting when compared to MRT, MS CT as such rarely suffices for an exact evaluation of the pathology involved.

Using the newest generation of Spiral MS CTs, isotropic 3D data records in the submillimeter range can be realized within a short period of time. However, there is also the possibility of retrospectively reconstructing random image planes that represents a decisive advantage for complex relationships between anatomical structures and pathological changes.

Based on the poor soft tissue contrast obtained as compared to MRT, MS CT is frequently not capable on its own to provide satisfactory statements in regard to exact evaluations of the pathology involved. As a result, the necessity of combining different examination modalities – unfortunately this also leads to a delay in therapeutic treatments – increases overall treatment costs in the final analysis.

Therefore the demand for real three-dimensional imaging (that is, with the isotropy of the voxels) has been present in MRT for some time now. It was successfully resolved by using gradient-echo based (GRE) MR sequences for T1-weighted (w) imaging. For this reason, these techniques used in modern MRT are a permanent feature of examination protocols and an important part in the evaluation of pathologies. Even though T2-similar contrasts are possible with the help of GRE MR sequences (examples in this case are the MEDIC or DESS sequences), for optimal image contrast with T2-weighting, a Spin Echo or Turbo Spin Echo (TSE) is required. The introduction of SPACE sequence technology (Sampling Perfection with Application optimized Contrasts using different flip angle Evolutions; SPACE) is an important prerequisites for using T2-weighted 3D imaging:

1. T2-weighted image contrast (SPACE is a variant of TSE),
2. true isotropic 3D data records with high resolution (voxel size ≤ 1 mm³)
3. use of a large Field of View (FoV) and finally,
4. clinically acceptable measurement times [1, 2, 3].

Meeting these requirements is all the more important, because more questions will find their way into the clinical MR tomographic routine since the introduction of the Tim (Total imaging matrix) technology. These, based on the necessary acquiring of large FoVs, were previously the sole domain of MS CT. [4].

Application methods and their first clinical results

When using SPACE* for image generation in the torso, a number of factors have to be observed. Pulsations of large vessels and respiratory motion cannot limit image quality as compared to conventional MRT. In addition, the previously available patient preparation techniques have to be maintained. Since October 2004, SPACE is used within the framework of clinical routine for patients requiring high resolution T2-weighted 3D imaging as compared to conventional 2D MRT. Key emphasis are pathologies of the pelvis and the spine. Whenever necessary, (for example, for staging rectal carcinoma) an additional retrograde filling of the rectum with ultrasound gel is performed.To keep intestinal motion quiet as a function of the body weight, up to 1 or 2 vials of buscopan (n-butyle scopolamine) will be administered intravenously. The following were used as default values for previous routine applications of

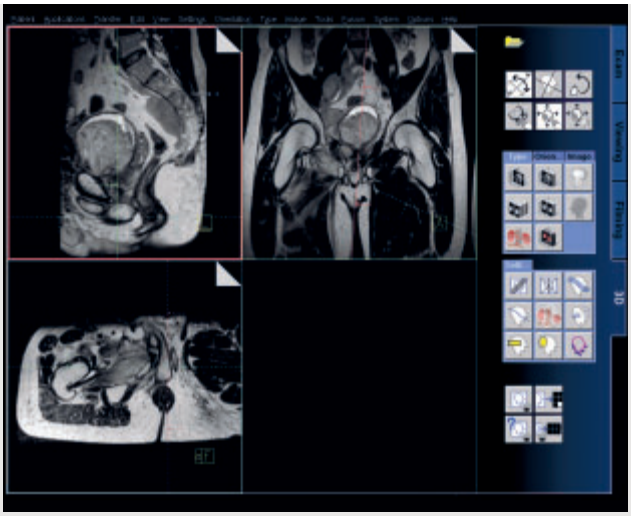

Figure 1 *T2 SPACE with PAT 3 of the pelvis.*
35-year-old patient with extended rhabdomyosarcoma invading into the bladder.
3D imaging with 1 mm³ isotropic spatial resolution allows retrospective slice prescription in any orientation needed.

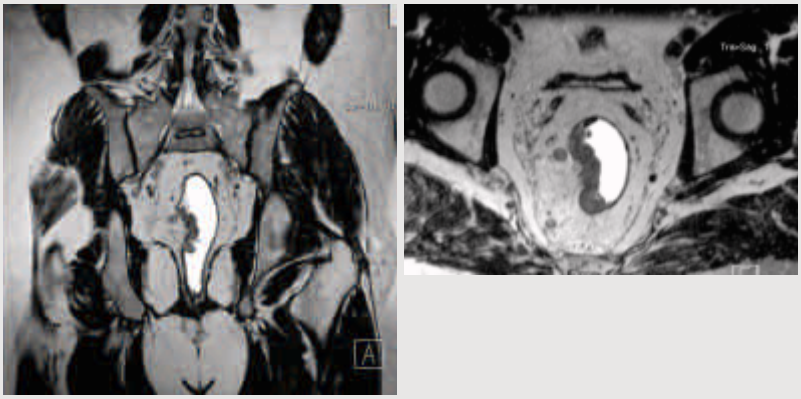

Figure 2 *T2 SPACE with PAT 3 of the pelvis 1 mm³ isotropic spatial resolution.*

43-year-old patient with rectum carcinoma with transgression of lamina propria /T3).
The 3D dataset was acquired in coronal orientation (left) and reconstructed in axial direction (right).

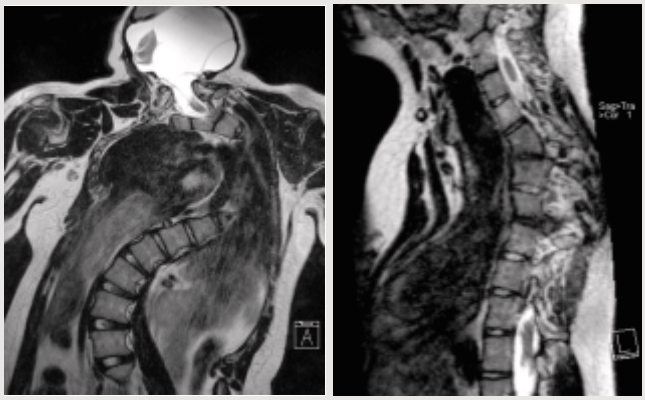

Figure 3 *T2 SPACE with PAT 3 of the spine. 1 mm³ isotropic spatial resolution.*

Female 13-year-old patient with
- *Arnold Chiari III*
- *Scoliosis*
- *Multiple segmentation disorders of the spine*

The isotropic 3D dataset acquired in coronal orientation (left) and a curved-cut reconstruction along the spine (right).

** The information about this application is preliminary. The application is under development and is not commercially available in the U.S., and its future availability cannot be ensured.*

SPACE: TR/TE = 1500/124 ms, 2 averages, Field of View (FoV) = 380 mm, 144 slices per slab, base matrix = 384, iPAT Factor = 3 (GRAPPA, 24 reference lines, triple matrix mode), Turbo Factor = 71, resulting isotropic voxel size $(1.0\ mm)^3$ (no interpolation), resulting measurement time 10 min, 32 seconds. It should be noted as well that the repetition time (TR) is shorter by using a restore pulse. All measurements are performed at a MAGNETOM Avanto system. Depending on the region to be examined, a variable combination of body and spine Matrix coils were implemented (when displaying the cervical spine/neck, an additional neck, head coil combination was used).

During the first 50 patients (21 females, 29 males, medium age 49 years, minimum 2 and maximum 79 years), the following regions were examined with SPACE: pelvis n = 30, lower spinal column n = 12, upper spinal column n = 6, extremities n = 4. Of 10 patients, the entire cohort was transferred for staging of a rectal carcinoma and a rectal filling with ultrasound gel was performed. In 2 cases, the entire spine was imaged using an automatic table feed followed by combining the images with a composing function of the scanner. Although it was possible to observe changes in the contrast characteristics of individual tissues to one another by using a restore pulse and variable flip angles (that theoretically led to a slight T1-dependency), the diagnostic quality obtained was not limited. Also, every case showed that the signal-to-noise ratio (SNR) was equivalent to conventional 2D T2-weighted imaging.

The same applies to the contrast-to-noise impression (CNR) of the SPACE sequence with respect to the diagnostic quality. Again, it can be considered equal to conventional T2-weighted imaging. We did not observe an increase in artifacts caused by e.g. metallic clips or implantations [5].

Conclusion and future considerations

What is decisive in using SPACE combined with Tim in the torso is the fact that the display of complex anatomical and pathological interactions and changes is possible in routine applications by means of MRT. It allows for the visualization of systemic disease aspects (for example, complete display of scoliosis) and enables at the same time a detailed view of the local situation (for example, proof of a small syrinx). In addition, this technology combines the advantages of T2-weighted MRT with high resolution and true 3D imaging.

Another critical point that deserves mentioning in our initial clinical experience is the fact that the diagnostic advantages are fully applied only in the presence of a widely available reconstruction software. This is especially important within the framework of interdisciplinary discussions. Our institute uses the SPACE sequence exclusively as required by the speciality – especially for planning large operative spinal column or pelvic interventions. Multiplanar reconstructions are dialog-driven via the radiologist or operator. Additional research is required to determine whether SPACE is suitable for replacing the previous 2D T2-weighted sequences used with previous examination protocols.

Bibliography

[1] *Mugler III JP, Kiefer B, Brookeman JR. Three-dimensional T2-weighted imaging of the brain using very long Spin Echo trains. Proceedings of the International Society for Magnetic Resonance in Medicine 687; 2000. Eighth Meeting, Denver.*

[2] *Mugler III JP, Wald LL, Brookeman JR. T2-weighted 3D Spin Echo train imaging of the brain at 3 Tesla: Reduced power deposition using low flip-angle refocusing RF pulses. Proceedings of the International Society for Magnetic Resonance in Medicine 438; 2001. Ninth Meeting, Glasgow.*

[3] *Mugler JP III, Meyer H, Kiefer B. Practical implementation of optimized tissue-specific prescribed signal evolutions for improved turbo-Spin Echo imaging. Proceedings of the International Society for Magnetic Resonance in Medicine 203; 2003. Eleventh Meeting, Toronto.*

[4] *Schlemmer HP, Schafer J, Pfannenberg C, Radny P, Korchidi S, Muller-Horvat C, Nagele T, Tomaschko K, Fenchel M, Claussen CD. Fast whole-body assessment of metastatic disease using a novel magnetic resonance imaging system: initial experiences. Invest Radiol. 2005 Feb;40(2):64-71.*

[5] *Lichy M, Wietek B, Mugler JP III, Horger W, Menzel M, Müller-Horvat C, Siegmann K, Martirosian P, Claussen C, Schick F, Schlemmer HP. WHole-body applications of isotropic high resolution T2-weighted MRI with a single slabe 3D-TSE based sequence optimized for high sampling efficiencies, called SPACE – initial clinical experiences. International Society for Magnetic Resonance in Medicine 2005. Thirtheenth Meeting, Miami.*

The information about this application is preliminary. The application is under development and is not commercially available in the U.S., and its future availability cannot be ensured.

We see a way to seamlessly image up to 100 cm FoV within a single exam

We see a way to position up to 4 coils simultaneously for true multichannel imaging

Small footprint giant steps

Results may vary. Data on file.

www.siemens.com/medical

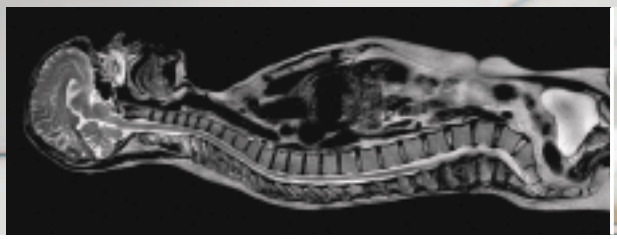

M-Z884-1-7600

Proven Outcomes in Magnetic Resonance.

MAGNETOM® C! distills years of experience and leading technical competence into a surprisingly compact and powerful, player in midfield MRI. The most compact C-shaped magnet with a pole diameter of only 137 cm assures easy, patient-friendly exams. Optimized components, high-field technology and superior workflow support deliver excellent image quality and high diagnostic confidence in a cost-friendly package. MAGNETOM C! – small footprint, small investment, giant steps in quality health care. Discover the changing face of midfield MRI.

Siemens **Medical Solutions** that help

SIEMENS
medical

Non-Contrast MRA of the Body Using Segmented 3D TrueFISP imaging

[1]Makoto Amanuma
[2]Takayuki Hoshino
[3]Atsuko Heshiki

[1]Department of Diagnostic and Interventional Radiology, Gunma University Hospital, Maebashi, Gunma, Japan

[2]Central division of Radiology, Saitama Medical School, Iruma, Saitama, Japan

[3]Department of Radiology, Saitama Medical School, Iruma, Saitama, Japan

Introduction

Contrast-enhanced magnetic resonance angiography (MRA) of the body is now firmly established in its clinical role for the evaluation of a variety of vascular-related abnormalities. However, the use of contrast media is undesirable for patients with compromised renal function, asthma, or a history of allergic reactions. Additionally, if an exam fails for technical reasons, repeating it within the usual examination time is usually difficult due to the limited optimal-contrast window.

Recently, the TrueFISP sequence has been introduced as a new fast gradient-echo technique. Due to its high blood signal-to-noise ratio, stable blood signal regardless of flow characteristics, and short acquisition time, this technique has been evaluated extensively in the field of coronary MRA. However, its use for vascular imaging in other areas has been relatively limited. Here, we present several trials of non-contrast MRA applications using the TrueFISP sequence.

Clinical methods

1. MR venography of a superficial venous system
Superficial veins of the extremities are surrounded mainly by fat tissue and muscles, a situation quite similar to that of coronary arteries. Therefore, use of the same imaging and reconstruction technique, i.e., a gated 3D segmented TrueFISP sequence followed by volume rendering, should likewise reveal superficial veins. (Fig. 1, 2, 3).

2. MR angiography of a deeply located arterial and venous system
Relatively high signal intensity of muscle on TrueFISP images reduces vascular conspicuity. Application of a proper T2-preparation pulse can decrease the muscle signal and significantly improve the demonstration of deeply located vascular structures (Fig. 4). While differentiation of artery and vein is difficult, large vascular structures such as the aorta or femoral vein are readily evaluated (Fig. 4, 5). Additionally, this technique can simultaneously demonstrate vascular abnormalities and associated lesions with long T2 relaxation times. Therefore, it is promising for the evaluation of hypervascular tumors such as hemangioma (Fig. 6, 7).

3. Selective arteriography and venography
As the TrueFISP technique is highly sensitive to the blood signal based on its relaxation characteristics, selective arteriography and venography are difficult to obtain. Although we have tried several methods using a saturation pulse, T2 preparation, and complex subtraction techniques, they are still under investigation, and a reliable method has yet to be established. However, results of these preliminary studies were promising (Fig. 8, 9), and further improvement is expected.

Figure 1 *TrueFISP MR venography of dorsal superficial veins of the hand.*

Figure 2 *TrueFISP MR venography of superficial veins of the right arm. Note abnormally developed draining superficial veins of the underlying hemangioma (same patient as Fig. 6).*

Figure 3 *TrueFISP MR venography of dorsal superficial veins of the foot.*

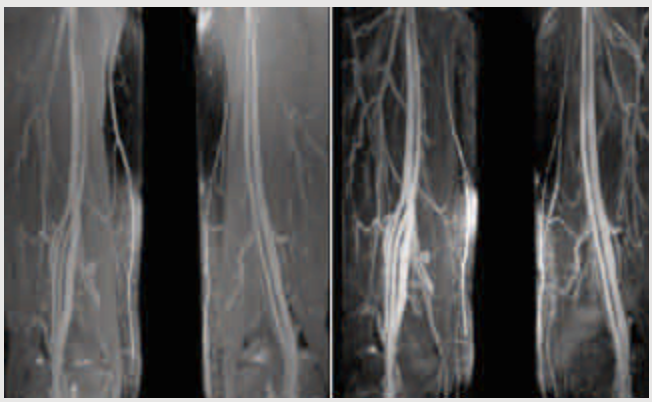

Figure 4 *TrueFISP MR angiography of superficial femoral artery and deep femoral vein with (left) and without (right) T2 preparation pulse. Note improved vascular conspicuity on the left image.*

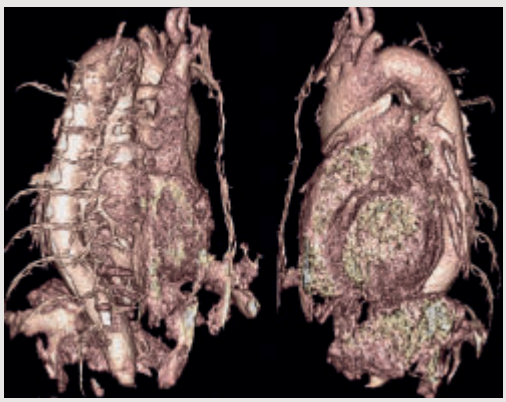

Figure 5 *TrueFISP MR angiography of dilated aorta.*

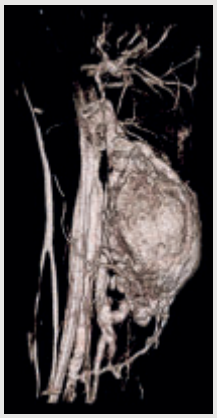

Figure 6 *TrueFISP MR angiography of deep-seated hemangioma in the arm.*

Figure 7a

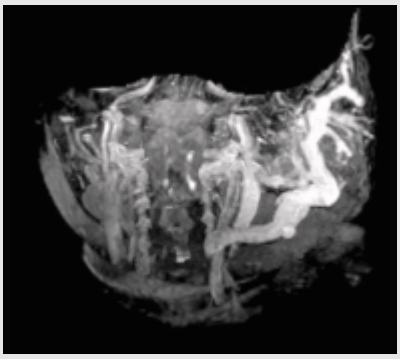

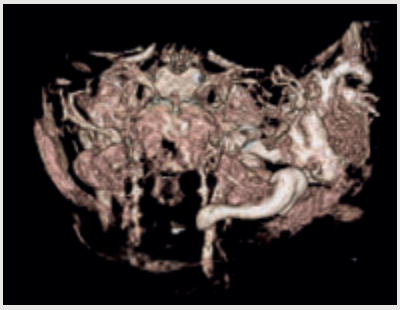

Figure 7b

Figure 7 *Hemangioma of the left parotid gland in 2-year-boy. (a) coronal T2-weighted image (b) MIP and VR reconstruction of the TrueFISP MRA. Note the dilated abnormal vein draining into the left internal jugular vein.*

Discussion

TrueFISP imaging has made a significant impact, not only on the field of coronary MRA, but also on diagnostic techniques for a variety of vascular-related abnormalities. As the sequence requires only a short acquisition time, breath-hold high resolution imaging of the chest and abdomen are also possible while maintaining a high vascular signal. In spite of these advantages, application to MRA other than that of the coronary arteries has been relatively limited. This may be due to difficulties such as relatively high fluid and soft-tissue signals, failure of selective arteriography or venography, and when applied without gating, inhomogeneous vascular signals related to blood flow.

Although ECG gating requires a relatively long preparation time, pulse gating is simple and fast. We use pulse gating for almost all gated TrueFISP MRA. In superficial areas of the extremities, major vascular structures are almost exclusively veins. Therefore, using volume rendering and masking of surrounding superficial structures, selective superficial venography is readily reconstructed.

As for MRA of deeply located vascular systems, surrounding muscles having relatively high signal on TrueFISP images obscure vascular structures on MIP images. Therefore, we applied a T2 preparation pulse for suppression of muscle signals. Signal loss of the blood was negligible, and the contrast-to-noise ratio between vessels and muscles was much higher than that obtained without a T2 preparation pulse. Although arteries and veins are simultaneously observed, large vessels are still easily evaluated. For excellent demonstration of vascular systems, uniform fat-signal suppression is mandatory. For this purpose we always use manual shimming for fat-water separation. The difficulty of obtaining a more complete suppression of the fat signal is also an important problem for TrueFISP MRA.

The final goal for this technique is selective arteriography and venography. While several trials showed promising results, a reliable method has yet to be established. Although there are still some problems to be solved, the clinical need for non-contrast MRA is large, and 3D TrueFISP has the potential to meet this need.

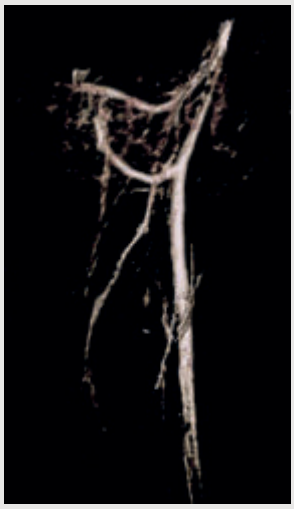

Figure 8 *Selective TrueFISP MR angiography of the right brachial artery using presaturation pulses.*

Figure 9 *Selective TrueFISP MR angiography of the right thigh using T2 preparation pulses.*

Sequence details

Sequence: 3D segmented TrueFISP
Plane: Coronal or sagittal
No. of slices: 33 - 80
(depending on the imaging area)
Slice thickness: 1.2 - 2.5 mm
TR/TE/FA: 3.2/1.6/65
Segmentation: 15 - 41
Gating: Pulse gating
FoV: 250 - 400 mm
No. of acquisitions: 1
Bandwidth: 890 - 975 Hz/pixel

Scanner model used

MAGNETOM Sonata
with Quantum gradient system

Coils used

8-channel head/6-channel surface array/body array/peripheral angiography coil

Diagnosis of Patent Foramen Ovale Using Contrast-Enhanced Dynamic MRI

Department of Cardiovascular MRI
Cardiovascular Center
Bethanien, Frankfurt/Main,
Germany

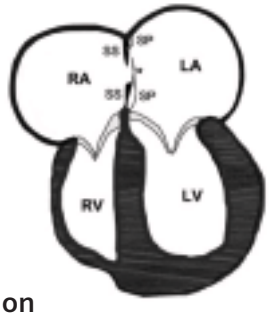

Figure 1

Introduction

The foramen ovale is a pivotal feature during intrauterine life. As depicted in figure 1, the interatrial septum primum on the left side and the interatrial septum secundum on the right side maintain a central hole after having grown from the periphery to the center. This hole is positioned caudally in the septum secundum and cranially in the septum primum, forming a slit valve that opens with pressure from the right. The blood from the umbilical vein entering through the inferior vena cava from the bottom of the right atrium keeps this door open until after birth. From then on, the left atrial pressure, slightly higher than the right atrial pressure, keeps the valve shut. In most individuals, the caudal portion of the septum primum on the left side and the cranial portion of the septum secundum on the right side fuse permanently, closing the foramen. In a minority of the population, however, the fusion does not take place and the foramen remains able to be opened (patent).

Patent Foramen Ovale (PFO) is a known cause of cerebral strokes or transient ischemic attacks due to paradoxical embolism. Diagnosis and treatment are required to prevent further cerebral events.

In patients without cardiac symptoms, the incidence of PFO is 34% during the first three decades and declines with age [1]. The annual recurrence rate of cerebral stroke or transient ischemic attacks for patients with PFO is about 3.5% [2, 3]. PFOs with large shunts have a higher risk than those with small shunts [4]. Recent studies show a higher incidence for cerebral strokes if the PFO is associated with an atrial septal aneurysm [5-8]. Therefore, an ideal method should show both diagnoses, PFO and atrial septal aneurysm.

Contrast-enhanced transesophageal echocardiography (TEE) is considered the clinical reference to detect PFO and atrial septal aneurysm. This method, however, is invasive. **Doctor Oliver Mohrs and his team at the Cardiovascular Center Bethanien (CCB) in Frankfurt/Main, Germany are working on a non-invasive new technique with MRI using MAGNETOM Sonata in the diagnosis of PFO and atrial septal aneurysm. Their results showing that contrast-enhanced MRI can be used to realiably detect PFO and atrial septal aneurysm have also been published in the American Journal of Radiology [9].**

Technique

Contrast-enhanced* MRI is performed on a 1.5T MRI system (MAGNETOM Sonata, Maestro Class). For signal detection, the combination of a 4-element CP Body Array coil and a 12-element CP Spine Array coil is used. ECG signal is received from an external system (Magnitude 3150, InVivo Research). An ECG-gated segmented true fast imaging with steady-state free precession (TrueFISP) – cine sequence (TR/TE: 2.7/1.2, temporal resolution: 34 ms, voxel size: 1.7 x 1.3 x 6.0 mm^3) serves for detection of atrial septal aneurysms in a stack of contiguous horizontal long-axis views and short-axis planes.

Contrast-enhanced perfusion analysis is performed during the Valsalva maneuver using 10 ml of gadopentetate dimeglumine (Magnevist, Schering) followed by a 20 ml saline solution, administered into an antecubital vein. The infusion rate is 6 ml per second. Two slices of a saturation-recovery TrueFISP sequence (TE: 2.7 ms, inversion time: 217 ms, flip angle: 50°, temporal resolution: 832 ms, matrix: 144 x 256, voxel size: 1.8 x 1.4 x 6.5 mm^3) are positioned in the horizontal long and short axis, which show the optimal view of the fossa ovalis chosen from the cine studies. For each slice, 40 consecutive images are acquired, one per heart cycle.

Signal-time curves are generated using Mean Curve. Two regions of interest (ROIs) are placed in a pulmonary vein and the left atrium. ROIs are manually fitted to every image without changing the size. The atrial ROIs are drawn close to the atrial septum, but inclusion of pixels from the right atrium is carefully avoided. The signal-time curves are normalized to baseline signal (second image) for each ROI. The single data points represented the percentage of the baseline signal. PFO grading for contrast-enhanced MRI is performed on the basis of the grading system as follows:

- **Grade 0:** no contrast enhancement in the left atrium before the contrast agent reached the pulmonary veins
- **Grade 1:** only slight contrast enhancement close to the atrial septum without enhancement of the entire left atrium before the contrast agent reached the pulmonary veins
- **Grade 2,** only slight contrast enhancement in the left atrium before the contrast agent reached the pulmonary veins
- **Grade 3,** bright contrast enhancement in the left atrium before the contrast agent reached the pulmonary veins.

Case Report

Patient History

61-year-old female who had a stroke 4 months prior to MRI. TEE results show ASA (Atrial Septal Aneurysm) and PFO (Patent Foramen Ovale) grade 3. Following MR examination also showed the same findings.

Image Findings

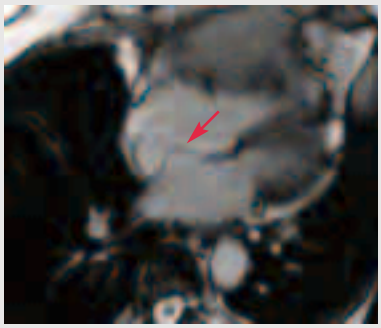

Figure 1a

Figure 1b

Figure 1 *Fig 1a and 1 b show bulging of the atrial septum in horizontal long axis (Fig. 1a) and in short axis (Fig. 1b)*

Figure 2a

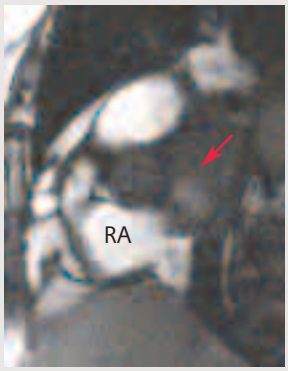

Figure 2b

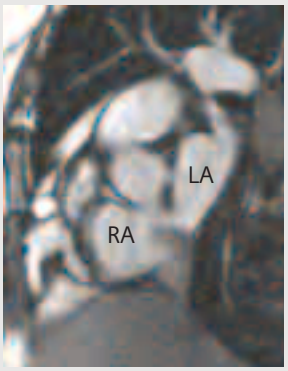

Figure 2c

Figure 2 *Fig 2a , 2b & 2c show contrast enhanced* dynamic perfusion imaging during Valsalva maneuver. Figure 2b shows enhancement of the left atrium due to right to left shunting before enhancement of the pulmonary vein.*

** The information about contrast enhanced dynamic perfusion is preliminary. The product is under development and not commercially available in the U.S., and its future availability cannot be ensured.*

The information presented in this case study is for illustration only and is not intended to be relied upon by the reader for instruction as to the practice of medicine. Any health care practitioner reading this information is reminded that they must use their own learning, training and expertise in dealing with their individual patients. This material does not substitute for that duty and is not intended by Siemens Medical Systems to be used for any purpose in that regard.

The drugs and doses mentioned herein are consistent with the approval labeling for uses and/or indications of the drug. The treating physician bears the sole responsibility for the diagnosis and treatment of patients, including drugs and doses prescribed in connection with such use. The Operating Instructions must always be strictly followed when operating the MR System. The source for the technical data is the corresponding data sheets.

References

[1] *Hagen PT, Scholz DG, Edwards WD. Incidence and size of patent foramen ovale during the first 10 decades of life: an autopsy study of 965 normal hearts. Mayo Clin Proc 1984;59:17–20*

[2] *Bogousslavsky J, Garazi S, Jeanrenaud X, Aebischer N, Van Melle G. Stroke recurrence in patients with patent foramen ovale: the Lausanne Study – Lausanne Stroke with Paradoxal Embolism Study Group. Neurology 1996;46:1301–1305*

[3] *Mas JL, Zuber M. Recurrent cerebrovascular events in patients with patent foramen ovale, atrial septal aneurysm, or both and cryptogenic stroke or transient ischemic attack: French Study Group on Patent Foramen Ovale and Atrial Septal Aneurysm. Am Heart J 1995;130: 1083–1088*

[4] *Stone DA, Godard J, Corretti MC, et al. Patent foramen ovale: association between the degree of shunt by contrast transesophageal echocardiography and the risk of future ischemic neurologic events. Am Heart J 1996;131:158–161*

[5] *Agmon Y, Khandheria BK, Meissner I, et al. Frequency of atrial septal aneurysms in patients with cerebral ischemic events. Circulation 1999;99:1942–1944*

[6] *Mattioli AV, Bonetti L, Aquilina M, Oldani A, Longhini C, Mattioli G. Association between atrial septal aneurysm and patent foramen ovale in young patients with recent stroke and normal carotid arteries. Cerebrovasc Dis 2003;15:4–10*

[7] *Bruch L, Parsi A, Grad MO, et al. Transcatheter closure of interatrial communications for secondary prevention of paradoxical embolism: single-center experience. Circulation 2002;105:2845–2848*

[8] *De Castro S, Cartoni D, Fiorelli M, et al. Patent foramen ovale and its embolic implications. Am J Cardiol 2000;86:51G–52G*

[9] *Oliver K. Mohrs, Steffen E. Petersen, Damir Erkapic et al. Diagnosis of patent foramen ovale using contrast.enhanced dynamic MRI; a pilot study; AJR 2005; 184:234-240*

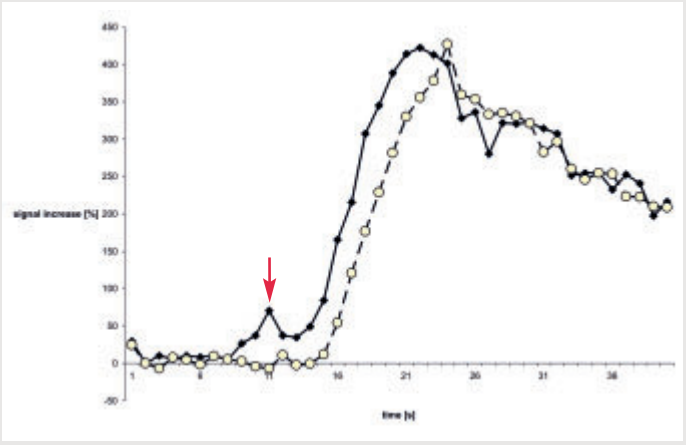

Figure 3a *Graph of signal-time curve shows early initial signal peak (arrow) in the left atrium (◆) followed by a second higher peak before the peak in the pulmonary vein (❍).*

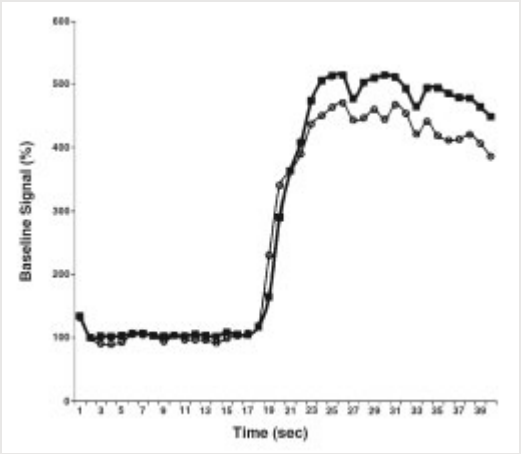

Figure 3b *Graph of a typical signal-time curve in a control patient without patent foramen ovale shows a single peak in the left atrium (■) at almost the same time as the peak in the pulmonary vein (❍).*

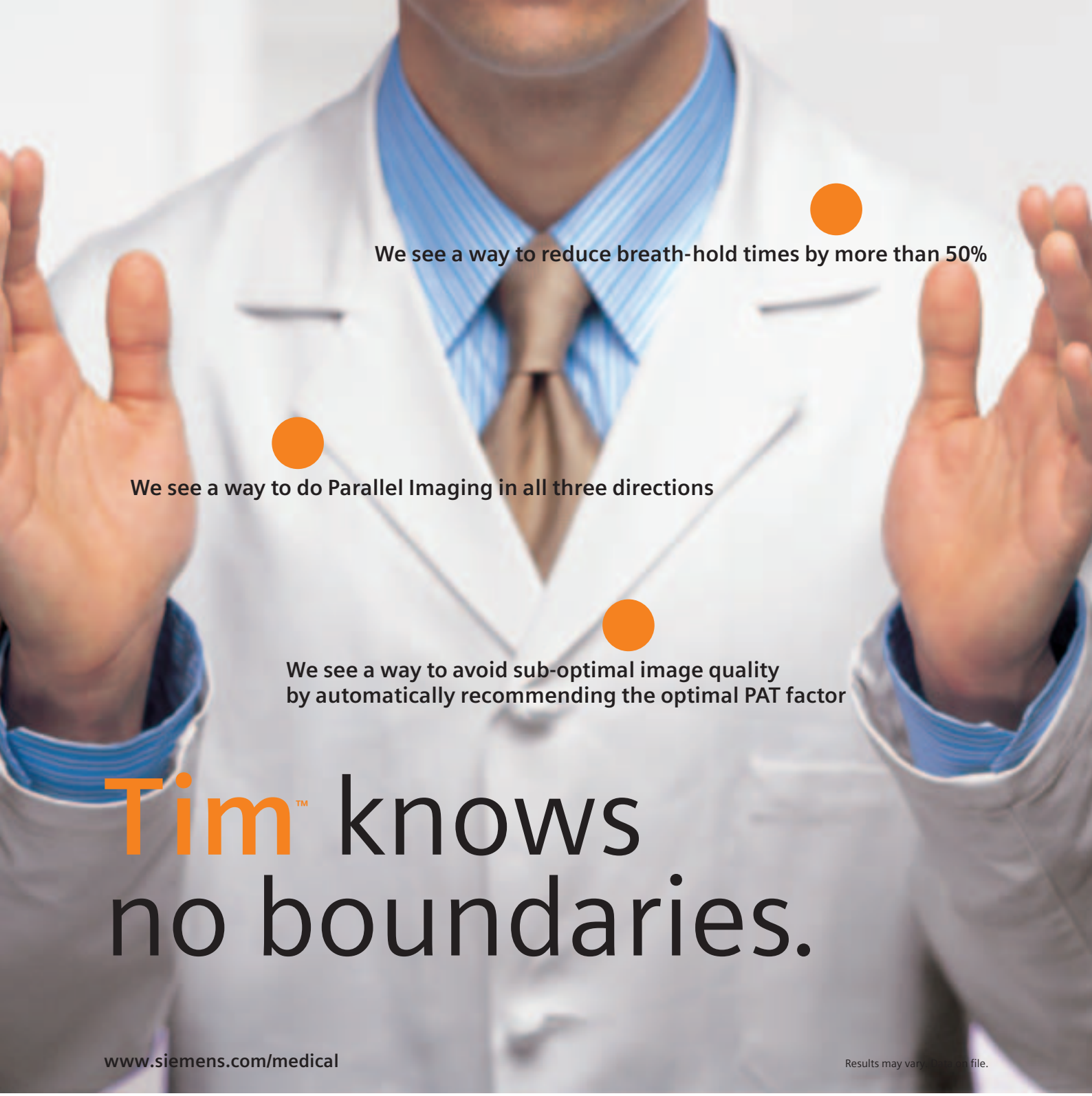

M-Z836-1-7600

Proven Outcomes in MR.

Imagine what's possible. And then think of Tim (Total imaging matrix). Tim brings together, for the first time ever, 76 matrix coil elements and up to 32 RF channels. All of which can be freely combined in any way. You are no longer restricted by a limited Field of View.

Tim enables unlimited Parallel Imaging in all directions – throughout the entire FoV of 205 cm (6' 9"). All while exploiting the highest signal-to-noise ratio possible today. For the highest image contrast, even with the highest PAT factors. Meet Tim for yourself at www.Siemens.com/Tim.

SIEMENS
medical

Siemens **Medical Solutions** that help

Whatever Happened to Cousin TR?

Gary R. McNeal

Cardiovascular MR R&D Team
Siemens Medical Solutions USA

Introduction

Long ago and far away, Cousin Boudreaux from the swamps of Southern Louisiana thought up something called a Spin Echo pulse sequence. It occurred to him about 3 am one night while the 'gator hunting was kind of slow. He was sitting there slapping mosquitoes and guzzling down a cold Dixie beer while contemplating what to call the repetition time between successive 90° excitation pulses. Right about then Cousin T.R. came along in his swamp boat to see how many 'gators had done been caught. Cousin Boudreaux lamented, "I ain't caught none of them ornery critters this whole night long." And after a brief, dull silence he added, "And I can't think of a good name for my new idea, either."

Cousin T.R. led the way to his favorite 'gator hunting pond and taught Cousin Boudreaux his favorite 'gator hunting trick. He pulled out his 'gator hunting call, which was really a mostly-broken duck hunting call. He warbled a few notes on it, and pattered the water with a mostly-broken boat paddle. In a few minutes three pairs of yellow eyes appeared in the high-beam, over near an old floating tree stump. As those eyes slowly advanced, sneaking up on that ol' lame duck, Cousin T.R. slowly lowered his noose over the side into the water and braced himself for the impending fray. In a moment it was all over. As usual, it was man over beast. Cousin Boudreaux flashed a big green-toothed, beer-smelling smile and declared, "Cousin T.R, you're the best 'gator hunter I ever seen."

And for many years thereafter we called the repetition time between successive excitation pulses "TR" to recall that fateful night when Cousin T.R. taught Cousin Boudreaux how to catch 'gators. But recently, various other definitions of TR have evolved as pulse sequences have grown in complexity. In some cases the original concept of TR seems to be lost. Many of you have asked, "Whatever Happened to Cousin TR?"

Definition #1

The conventional definition of TR is the repetition time between successive excitation pulses for the same slice. This is demonstrated by a single-slice Spin Echo (SE) pulse sequence in which each slice consists of a 90° excitation pulse, a refocusing pulse, and an echo (Fig. 1a).

This conventional definition of TR also applies to a multi-slice SE pulse sequence in which as many slices as possible are interleaved within the selected TR (Fig. 1b). For T1-weighting we typically select a relatively short TR (<1000 ms), or for T2-weighting a relatively long TR (>2000 ms).

Figure 1a *Single-slice Spin Echo pulse sequence.*

Figure 1b *Multi-slice Spin Echo pulse sequence.*

This conventional definition of TR also applies to a multi-slice Turbo Spin Echo (TSE) pulse sequence in which each slice consists of a single excitation pulse with multiple refocusing pulses and multiple echoes (Fig. 1c). Since there are more echoes per slice, a TSE sequence requires fewer repetitions than a SE sequence with the same TR, but accordingly fewer slices may be acquired within the selected TR.

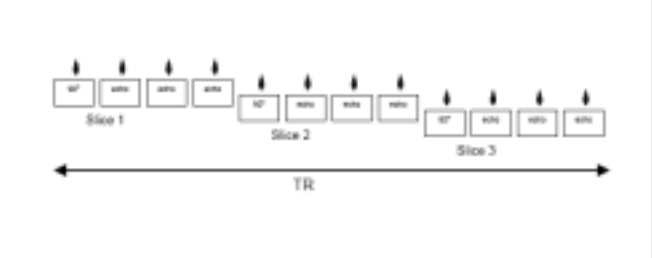

Figure 1c
Multi-slice Turbo Spin Echo pulse sequence.

This conventional definition of TR also applies to a multi-slice Gradient Recalled Echo (GRE) pulse sequence which contains no refocusing pulses at all (Fig. 1d). Each slice consists of a single excitation pulse and a series of gradient reversals to form an echo. TR is defined as the time between successive excitation pulses for the same slice in a GRE sequence, just like in SE and TSE sequences.

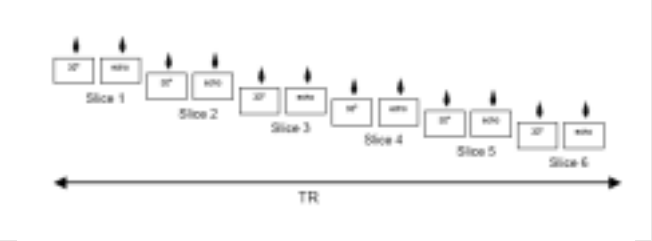

Figure 1d
Multi-slice Gradient Recalled Echo pulse sequence.

Definition #2
When a pulse sequence is cardiac triggered, the definition of TR can become a bit more complicated. Often the TR displayed in the user interface does not reflect the conventional definition of TR, but instead is used to define some other aspect of sequence timing relative to the cardiac cycle. In the discussion that follows, the TR displayed to the user will be denoted $TR_{protocol}$, while the effective TR, defined conventionally as the time between successive excitation pulses, will be indicated as $TR_{effective}$.

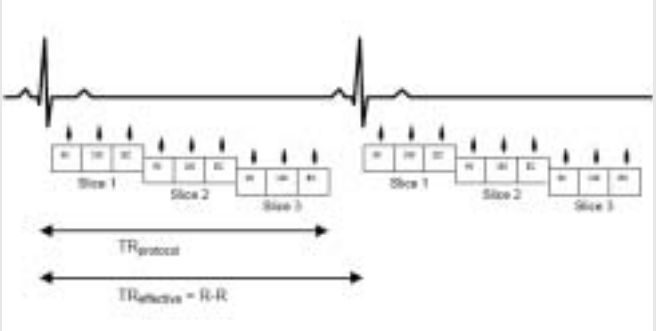

Figure 2a
Multi-slice, multi-phase pulse sequence. Cardiac triggered on every heartbeat.

When cardiac triggering is used in a multi-slice Spin Echo sequence, the $TR_{effective}$, according to the conventional definition, is the repetition time between successive heartbeats. This is demonstrated by a cardiac triggered multi-slice SE pulse sequence (Fig. 2a), but may apply as

well to multi-slice TSE and GRE pulse sequences. Each slice is excited only once per heartbeat, so $TR_{effective}$ equals the R-R interval. As the heart-rate increases, the $TR_{effective}$ decreases because the R-R interval decreases. Since each slice is acquired at a different phase of the cardiac cycle, this technique is often called a multi-slice multi-phase cardiac triggered pulse sequence. On the other hand, $TR_{protocol}$ for such a sequence is defined as the time actually used to acquire all the slices within the cardiac cycle.

A common method to increase the $TR_{effective}$ is to trigger the pulse sequence on every second or third heartbeat (Fig. 2b), in which case $TR_{effective}$ is twice or three times the R-R interval. This strategy is often used to control the image contrast for T2-weighted or IR-weighted pulse sequences.

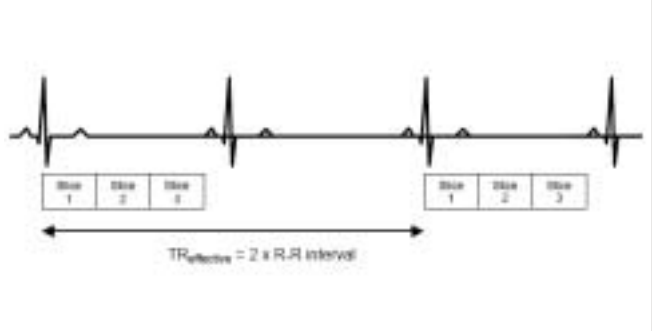

Figure 2b
Multi-slice, multi-phase pulse sequence. Cardiac triggered on every second heart-beat.

Definition #3
Cardiac triggered cine pulse sequences create a movie effect of the beating heart or flowing blood by acquiring a series of images at different phases throughout the cardiac cycle. Various types of cine techniques include TrueFISP, Flash, Phase Contrast, and Grid-Tagging pulse sequences. The $TR_{protocol}$ definition for a cine sequence is the repetition time between consecutive cardiac phases, also known as the temporal resolution of the sequence. This definition of TR is demonstrated by a simple cardiac triggered cine pulse sequence (Fig. 3a), in which only one echo is acquired per cardiac phase (non-segmented). In this non-segmented acquisition, the $TR_{protocol}$ represents both the repetition time between successive cardiac phases (temporal resolution) and the repetition time between successive excitation pulses ($TR_{effective}$).

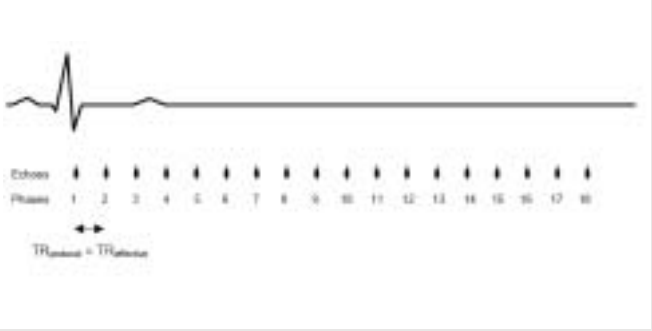

Figure 3a
Cardiac triggered cine pulse sequence. Non-segmented data collection.

Often, however, multiple echoes are acquired per cardiac phase to reduce the required number of repetitions (Fig. 3b), a scheme called "segmented" data collection. In a segmented cine pulse sequence the $TR_{protocol}$ represents the repetition time between the center echo of successive cardiac phases (temporal resolution) but no longer represents the repetition time between successive excitation pulses ($TR_{effective}$). The temporal resolution in Figure 3b is five times longer than in Figure 3a, although the echo spacing ($TR_{effective}$) is the same in both.

If the center echo is re-sampled between successive segments, and echoes are shared from the prior and next segments, the temporal resolution can be improved by reducing the center-spacing between successive phases (Fig. 3c). In an "echo-shared segmented" cine pulse sequence, $TR_{protocol}$ represents the repetition time between the center echo of successive cardiac phases (temporal resolution), and is always less than the comparable $TR_{protocol}$ without echo-sharing. In this example of an echo-shared segmented cine pulse sequence, the total number of echoes acquired per repetition is six (5 + 1), however the $TR_{protocol}$ (temporal resolution) after echo-sharing is only three echoes (6/2).

Figures 3d and 3e demonstrate an example of an echo-shared segmented GRE cine pulse sequence. In this example the total number of echoes acquired per repetition is twenty four (23 + 1), however the effective temporal resolution with echo-sharing is only twelve echoes (24/2) with a spacing of 43.32 ms between the centres of successive phases.

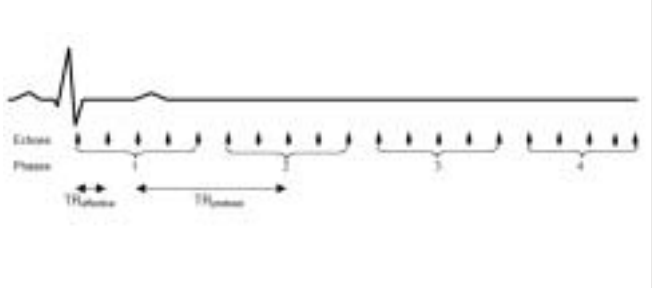

Figure 3b
Cardiac triggered cine pulse sequence. Segmented data collection.

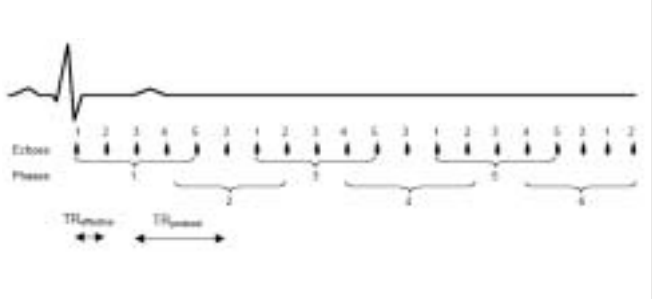

Figure 3c
Cardiac triggered cine pulse sequence. Echo-shared segmented data collection.

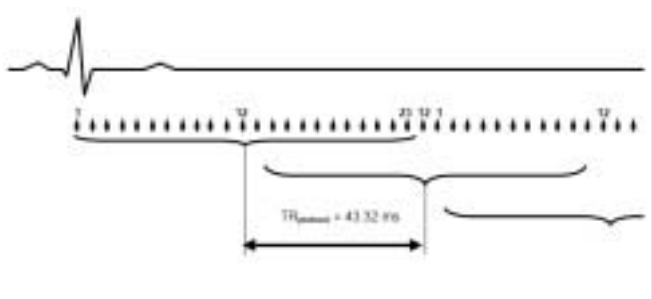

Figure 3d
Echo-shared segmented GRE data collection pulse sequence.

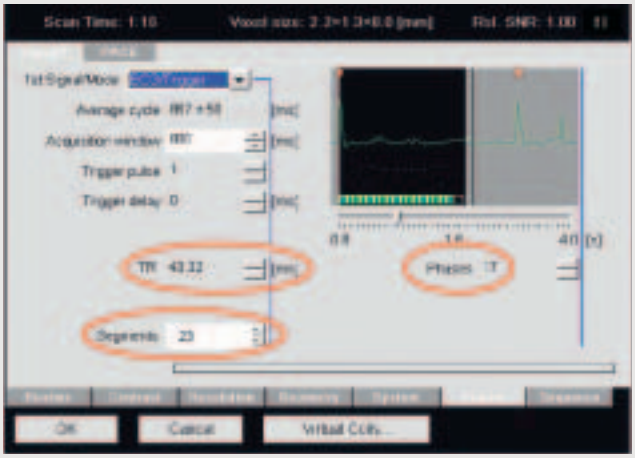

- The total number of cardiac phases is 17.
- The number of echoes per phase is 23.
- The temporal resolution per phase is 43.32 ms.

Definition # 4
Some cardiac triggered pulse sequences produce a single static image rather than cine images of the heart, and have yet a different definition of $TR_{protocol}$ (Figs. 4a & 4b). The $TR_{protocol}$ represents the minimum time needed to collect the train of echoes for a single diastolic-triggered segment. You should always set the $TR_{protocol}$ to its minimum possible value in this situation.
You can still think of the minimum $TR_{protocol}$ as the temporal resolution of the sequence, but there is only one image produced rather than a cine series. This applies to any non-cine cardiac triggered pulse sequence containing no Inversion Recovery (IR) or Saturation Recovery (SR) preparation pulses. Examples of cardiac triggered pulse sequences using this definition of TR include TrueFISP 2D localizers and Flash 2D angiography techniques.

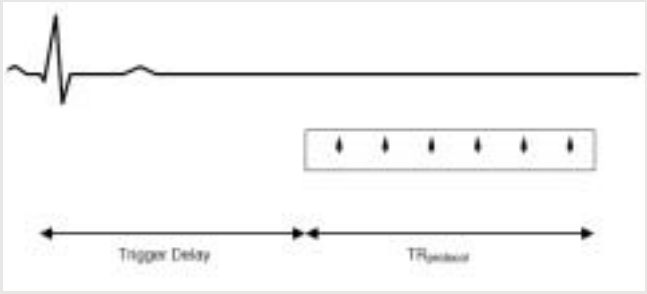

Figure 4a

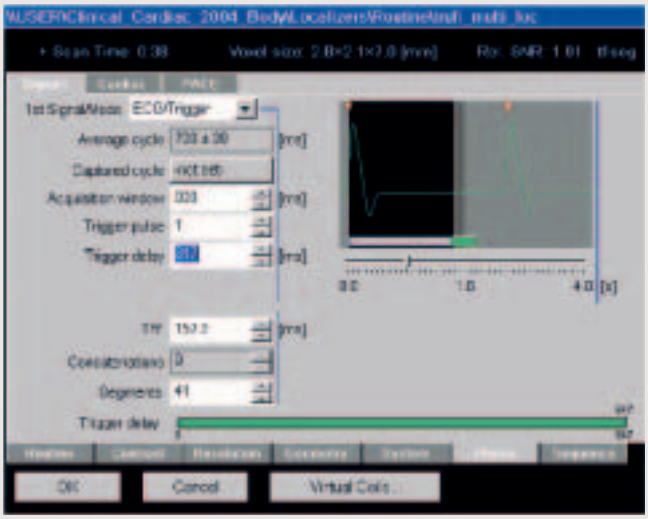

Figure 4b

As demonstrated in the *syngo* Physio Task Card for a segmented TrueFISP 2D localizer pulse sequence (Fig. 4b):

- The total number of echoes in the segment is 41
- The temporal resolution of the segment is 152.3 ms (green bar)
- The trigger delay prior to the segment is 647 ms (grey bar)

In the previous example of a TrueFISP 2D localizer pulse sequence (Fig. 4b) only 41 echoes were collected per heartbeat, so several heartbeats were required to completely create the image. Such a scheme is known as "segmented" data collection. However, the same pulse sequence could be slightly modified to operate as a "single-shot" data collection in which all the echoes needed to create the image are collected in one long segment within a single heartbeat (Fig. 4c). The temporal resolu-

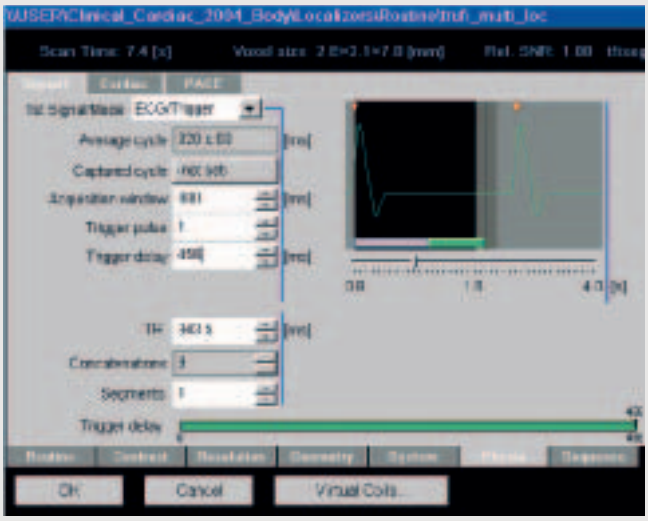

Figure 4c

tion is still defined as the minimum time to collect all the echoes (minimum $TR_{protocol}$), but it is much greater than in the previous example because many more echoes are collected in the segment.

As demonstrated in the *syngo* Physio Task Card for a single-shot TrueFISP 2D localizer pulse sequence (Fig. 4c):

- There is only 1 segment which contains of all the required echoes
- The temporal resolution of the segment is 343.5 ms (green bar)
- The trigger delay prior to the segment is 456 ms (grey bar)

Definition # 5
Yet another definition of TR applies to a cardiac triggered pulse sequence containing an Inversion Recovery (IR) preparation pulse (Figs. 5a & 5b). The $TR_{protocol}$ is defined as the time between the QRS trigger and the end of the data segment, and is used to adjust the timing of the data segment within the cardiac cycle. In an IR TSE pulse sequence the TI is defined as the time between the IR preparation pulse and the beginning of the data segment (Fig. 5a), and is typically adjusted for optimal fat nulling. In an IR GRE pulse sequence the TI is defined as the time between the IR preparation pulse and the center of the data segment (Fig. 5b), and is typically adjusted for optimal myocardial nulling. In these sequences the data segment is typically acquired every other heartbeat, so the $TR_{effective}$ is twice the R-R interval.

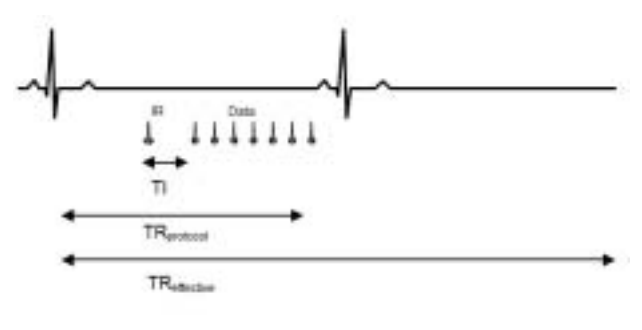

Figure 5a
Cardiac triggered IR TSE pulse sequence. Adjust TI for fat nulling.

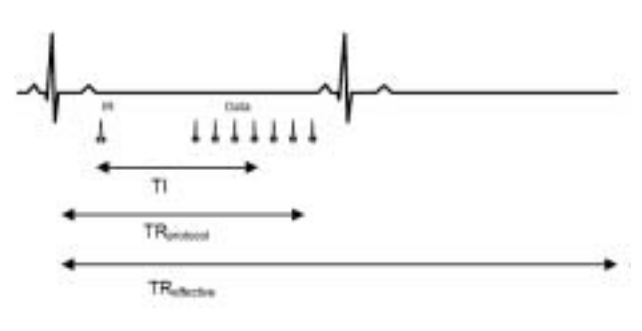

Figure 5b
Cardiac triggered IR GRE pulse sequence. Adjust TI for optimal myocardinal nulling.

In order to null the signal from flowing blood, we can apply a Double Inversion Recovery (DIR) preparation pulse at the QRS trigger and wait several hundred milliseconds to acquire the data segment in the late diastolic portion of the cardiac cycle (Fig. 5c). The DIR pulse, also known as a Dark Blood (DB) pulse, is available for Turbo Spin Echo, TrueFISP, and TurboFLASH pulse sequences. The TR in the protocol ($TR_{protocol}$) is defined as the time between the DB pulse and the end of the data segment. Since there is no TI available in a DB protocol, the $TR_{protocol}$ is used to adjust the location of the data segment for optimal blood nulling. Figure 5c demonstrates a cardiac triggered DB TSE pulse sequence in which the effective inversion delay time for blood nulling ($TI_{effective}$) is measured from the DB pulse to the beginning of the data segment. Figure 5d demonstrates a cardiac triggered DB GRE pulse sequence in which $TI_{effective}$ is measured from the DB pulse to the center of the data segment. In these sequences the data segment is typically acquired every other heartbeat, so the $TR_{effective}$ is twice the R-R interval.

In the following example of the *syngo* Physio Task Card for a DB TSE pulse sequence (Fig. 5e) the TR of 700 ms includes the DB pulse (at the ECG trigger), the inherent inversion delay time (dark-green bar), and the data segment (light-green bar). Trigger delay must be zero because the inversion delay is included within TR.

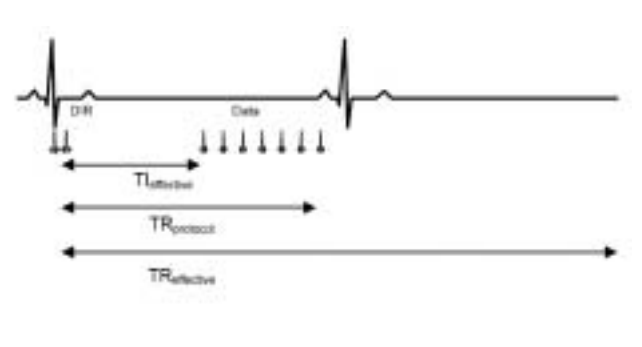

Figure 5c
Cardiac triggered DB TSE pulse sequence. Adjust $TR_{protocol}$ for optimal blood nulling.

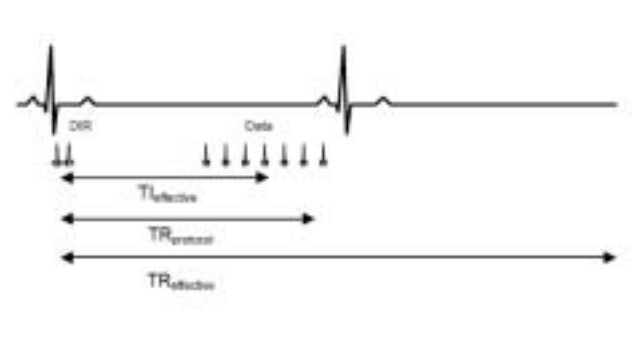

Figure 5d
Cardiac triggered DB GRE pulse sequence. Adjust $TR_{protocol}$ for optimal blood nulling.

Figure 5e

If we add a third IR preparation pulse to a double IR TSE pulse sequence, we have a Dark Blood STIR pulse sequence (Fig. 5f). $TR_{protocol}$ is adjusted for optimal blood nulling and $TI_{protocol}$ is adjusted for optimal fat nulling. In these sequences the data segment is typically acquired every other heartbeat, so the $TR_{effective}$ is twice the R-R interval.

Figure 5g is an example of the *syngo* Physio Task Card for a DB STIR pulse sequence. The dark-green bar within the TR includes the Double IR pulse and the inversion delay time for blood nulling. The light-green bar within the TR includes the single IR pulse and the inversion delay time for fat nulling, plus the data segment. Trigger delay must be zero because the inversion delay is included within the TR.

Another example is a FatSat IR FLASH 3D pulse sequence for coronary angiography, without a Navigator pulse (Fig. 5h) or with a Navigator pulse (Fig. 5i). The TI is measured from the IR pulse to the beginning of the data segment (centric ordering) and is adjusted for optimal myocardial nulling. The FatSat pulse immediately precedes the data segment. The navigator pulse immediately precedes the FatSat pulse. There is no double IR pulse for blood nulling.

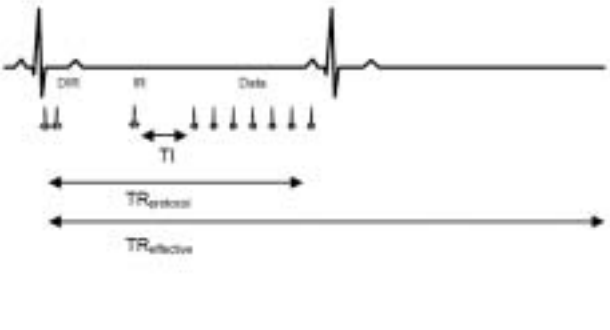

Figure 5f
Cardiac triggered DB STIR pulse sequence. Adjust $TR_{protocol}$ for optimal blood nulling. Adjust TI for optimal fat nulling.

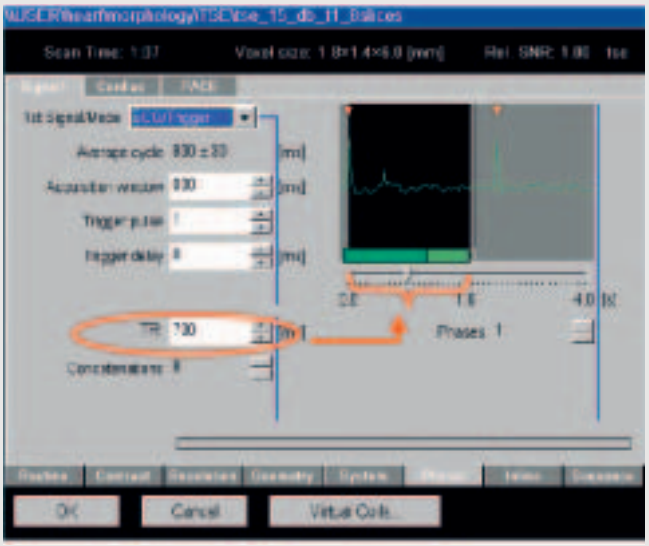

Figure 5g
Cardiac triggered DB STIR pulse sequence. Adjust $TR_{protocol}$ for optimal blood nulling. Adjust TI for optimal fat nulling.

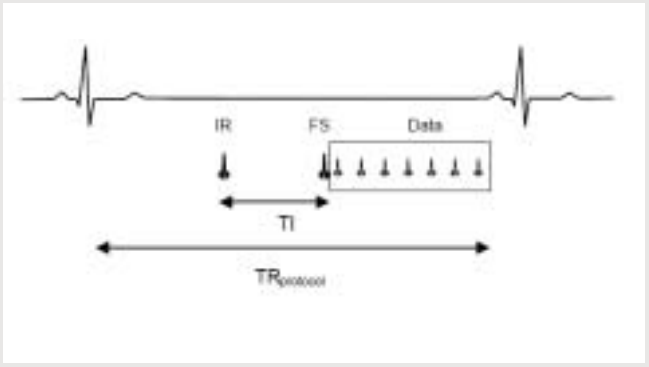

Figure 5h
Navigator FatSat IR Flash 3D pulse sequence.

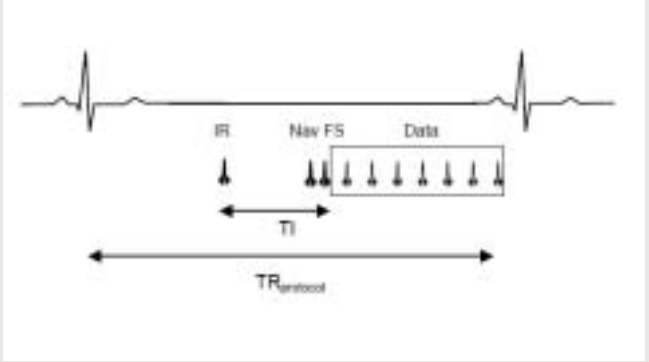

Figure 5i
Navigator FatSat IR Flash 3D pulse sequence.

Definition # 6
Yet another definition for TR is used in the IR- or SR-prepared GRE (Turbo-FLASH or TrueFISP) pulse sequences (Fig. 6a). These sequences can be used for T1-weighted single-shot imaging that requires multiple slices acquired within a single heartbeat with high temporal resolution. $TR_{protocol}$ consists of the minimum time duration needed for the SR preparation pulse, plus the delay period thereafter, plus the data segment. $TR_{protocol}$ can be thought of as the "time per slice." TI is measured from the IR- or SR-preparation pulse to the center of the data segment, and is adjusted for optimal myocardial signal.

SR Data

In an SR GRE pulse sequence the data segment is a "single-shot" of all required echoes for the entire slice. Typically, 3 to 5 slices can be acquired within each heartbeat (Figs. 6b & 6c).

Cousin TR had no idea how many different things Cousin Boudreaux was naming after him that fateful evening back in the swamp. While the physical definition of TR will always mean only one thing, the time between successive excitation pulses, a number of variations have cropped up out of the necessity of controlling a pulse sequence within the cardiac cycle. Hopefully, this brief explanation with diagrams will make it a little easier for everyone to understand.

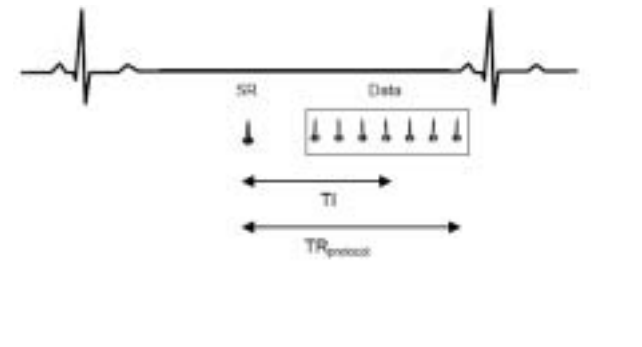

Figure 6a
Single-slice SR GRE pulse sequence.

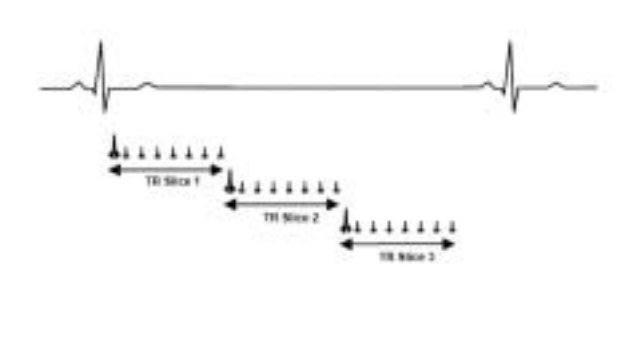

Figure 6b
Multi-slice SR GRE pulse sequence.

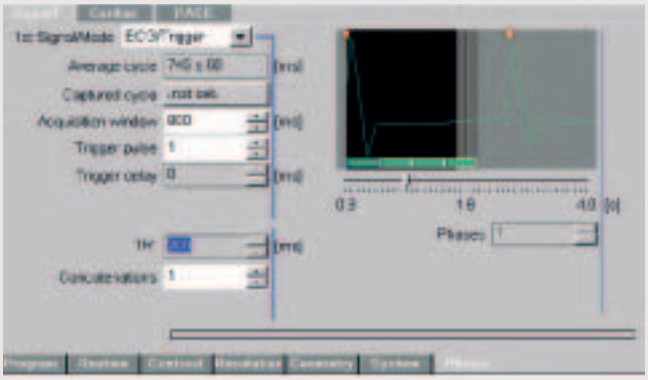

Figure 6c

M-Z899-1-7600

Proven Outcomes with Clinical 3T MRI.
Now MRI's most innovative new technology, Tim (Total imaging matrix) has been combined with the amazing power of 3T. Together, they go places no 3T has gone before. Now, what was only possible in research can be done daily in clinical practice. You'll see what couldn't be seen. And do things faster than they've ever been done before.

Imagine visualizing 0.4 mm cervical spine nerve roots in less than two minutes. Performing 3-D abdominal imaging with submillimeter resolution in 15 seconds. Or a full head protocol in less than three minutes. With 3T and Tim, the extraordinary will become routine. Everyday.

SIEMENS
medical

Siemens **Medical Solutions** that help

Tim Matrix Modes

Arne Reykowski, Ph.D.

Siemens AG
Medical Solutions,
Magnetic Resonance Division, Coil Development,
Erlangen, Germany

1. Why Matrix Coils?

Matrix coils are about flexibility, scalability and upgradability:

Flexibility, because Matrix coils can be combined to larger arrays to satisfy individual needs. For example, Head Matrix and Neck Matrix can be used together as Neuro-Vascular Array. By adding several Body Matrix coils with Spine Matrix and Peripheral Angio Matrix, the Field-of-View can be subsequently extended up to a whole-body range of 205 cm (6'9"). Furthermore, in order to accommodate head-first and feet-first exams, Body Matrix and Peripheral Angio Matrix can be rotated by 180° without loss in SNR (= signal-to-noise ratio – which is a measure of image quality).

Scalability, because Matrix coils are equipped with so called "Mode Matrix" combiners which allow a scalable use of RF channels. Depending on the Field-of-View chosen, the number of RF channels determines the iPAT (integrated Parallel Acquisition Technique) capability of a Tim (Total imaging matrix) system. No matter how many channels a Tim system has, the Mode Matrix will always guarantee maximum image quality in the important center region of the image.

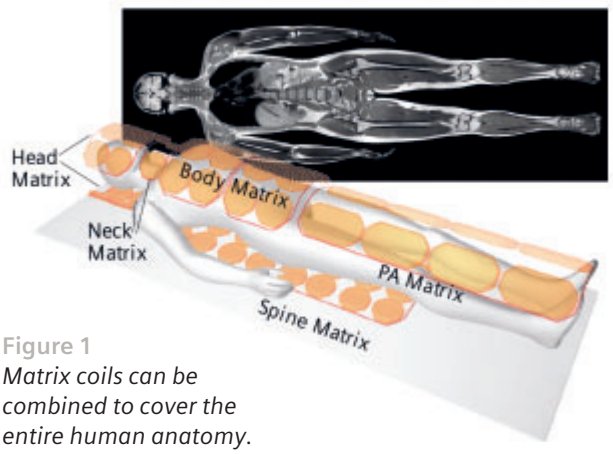

Figure 1
Matrix coils can be combined to cover the entire human anatomy.

Upgradability, because a Tim system upgrade towards a higher number of RF channels will not require exchange of any Tim coils. Tim and its Matrix Coils are 100% compatible with all upgrades. Not a single coil needs to be re-purchased in case of an upgrade, e.g. from Tim [32x8] to Tim [76x18] or Tim [76x32]. More importantly, with the different Matrix Modes (CP, Dual, Triple), the Matrix coils can be "scaled" to the Tim levels. The same coils can make full use of the higher number of RF channels with a higher Tim level.

2. What is a "Mode Matrix"?

The Mode Matrix is a smart combiner network which ensures RF channel scalability. It is a piece of hardware built into the Matrix Coils. A Mode Matrix has an identical number of input and output signals. Using all available output signals ("Mode signals") is equivalent to using the original input signals. However, when using less than the maximum number of output signals, the Mode Matrix ensures highest image quality, i.e. maximum SNR, at the center of the region-of-interest.

A good analogy to the Mode Matrix is broadcasting: First radio transmissions used single-channel mono broadcast signals. A mono signal contains all necessary information to listen to a broadcast. It can be described as the sum of the signals for left and right audio or simply L+R (left plus right).

With the advent of stereo broadcasting, a transmission format had to be designed which ensured compatibility with existing mono radio receivers. Therefore, stereo broadcast transmissions still transmit the mono L+R signal on a main channel. On a second channel, a differential signal L-R is transmitted. This is identical to transmitting L and R on two individual channels but at the same time ensures full compatibility with mono receivers.

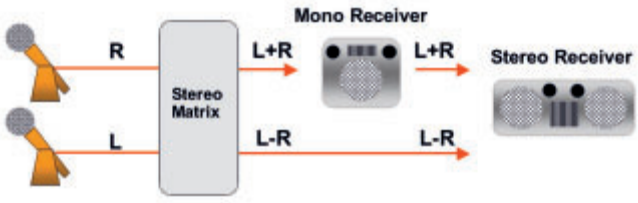

Figure 2 *Stereo broadcast consists of a mono broadcast signal plus a differential signal.*

The Mode Matrix combiner works in a similar fashion. All input signals are combined to a circularly polarized (CP) output signal on the main output channel. This CP Mode signal is the MR signal equivalent to the L+R mono signal in broadcasting applications. The higher-order output signals of the Mode Matrix contain differential information, designed to ensure RF channel scalability.

The sum of the three mode signals P, S and T (for Primary, Secondary and Tertiary) contains the same information as the original signals R, M and L (for Right, Middle and Left) from the coil elements.

The user selects CP, Dual or Triple Mode in the user interface. Primary, Secondary and Tertiary Modes are intermediate signals, invisible to the user.

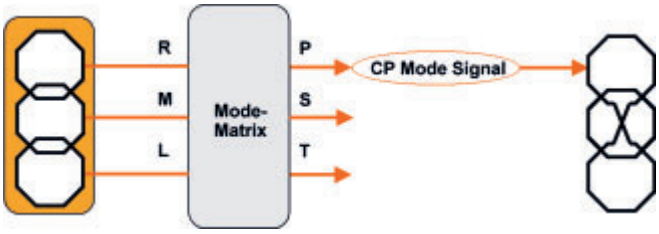

Figure 3 *In analogy to stereo broadcast, the Mode Matrix delivers high SNR, a circular-polarized signal plus additional differential signals for iPAT applications.*

3. What is a Ring? What is a Cluster?

Matrix coils allow the reception of high SNR signals from all regions of the human body. They are organized in multiple rings of up to 6 elements which surround the human anatomy and are stacked in head-feet direction (along the z-axis of the magnet).
Typically, a single ring of elements is divided into an anterior and a posterior cluster.

A cluster is a group of typically 3 coil elements with individual preamplifiers which are fed into a Mode Matrix combiner.

The output signals of this Mode Matrix combiner are termed Primary (CP), Secondary and Tertiary Mode Signals.

In CP Mode, only the Primary (also called CP) Mode signal is fed into a receiver channel.

In Dual Mode, the Primary and Secondary Mode signals are fed into two independent receiver channels.

In Triple Mode, the Primary, Secondary and Tertiary Mode signals are fed into three independent receiver channels.

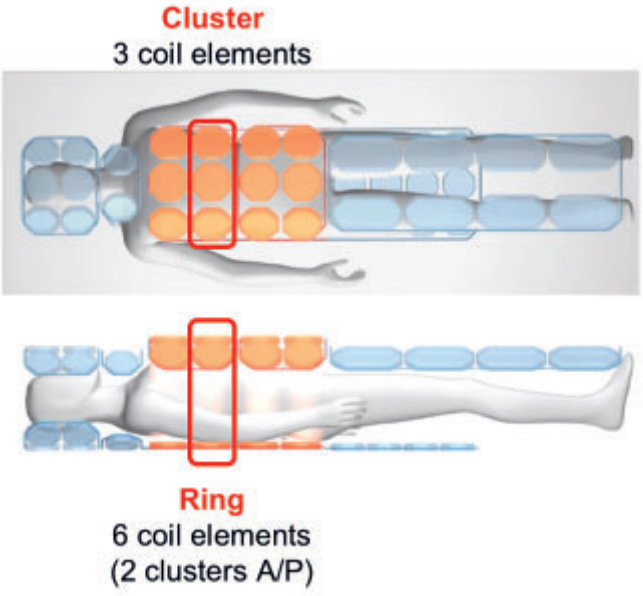

Figure 4 *The individual elements of Matrix coils are organized in rings and clusters. Each cluster is connected to a Mode Matrix combiner.*

4. What are CP, Dual and Triple Modes?

CP, Dual and Triple are the Matrix Modes for a Tim system.
In CP Mode, only the CP signal (also called Primary signal) from the output of the Mode Matrix combiner is used for data acquisition and image reconstruction. The CP Mode,

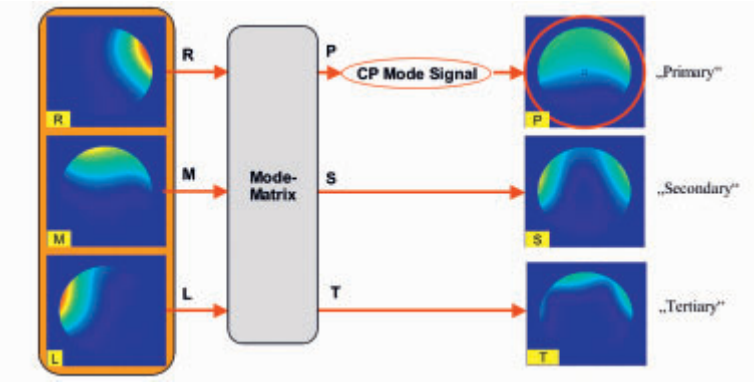

Figure 5 *The Mode Matrix combiner transforms the coil signals R,M,L into mode signals P,S,T. The primary mode signal P is equivalent to a high-SNR CP coil signal.*

with its circular polarization, already offers highest image quality in the center of the region of interest and is therefore used for standard imaging. CP Mode is the mode of operation which uses the smallest number of RF channels. Since the CP Mode generates less data compared to the other modes, shortest recon times can be achieved.

In Dual Mode, the CP signal as well a Secondary signal are used for data acquisition and image reconstruction. This Matrix Mode typically uses twice the number of RF channels as compared to CP Mode operation. Dual Mode improves iPAT with phase-encoding (PE) direction left-right in all regions of the human anatomy. Dual Mode also increases SNR in the image periphery.

Triple Mode is the highest Matrix Mode available. Triple Mode unfolds the full power of the Matrix coils in terms of iPAT capability and (peripheral) SNR. The Triple Mode uses the full number of mode signals available from all selected Matrix coils.

5. How do CP, Dual and Triple Modes relate to iPAT performance?

In general, for iPAT with phase-encoding directions anterior-posterior or head-feet, CP Mode is sufficient.

Dual Mode and Triple Mode offer additional benefits for iPAT with left-right phase-encoding direction. With the Head Matrix, the Spine Matrix and the Body Matrix coils, Dual Mode allows for a max. PAT factor of 2 in left-right direction, while Triple Mode allows for a max. PAT factor of 3 in left-right direction. The max. PAT factor for anterior-posterior direction and head-feet direction is fairly independent of the Matrix Mode.

There are also some cases, where PAT with left-right phase-encoding direction can be performed in CP Mode, e.g.:

a) The Peripheral Angio Matrix has individual elements for each leg, therefore permitting iPAT in left-right direction.
b) For the examination of obese patients it is possible to place two Body Matrix coils to the left and right of the patient. This setup allows the use of iPAT in left-right direction even in the CP Mode (and higher-than-normal PAT factors with Dual and Triple Modes).

6. Can I use all Matrix Modes (CP, Dual and Triple) with each Tim level?

Yes, all Matrix Modes are compatible with each Tim level. The differentiator between the various Tim levels is the maximum coverage in z-direction possible with different combinations of Tim levels and Matrix Modes.

For example, with Tim [32x8] you can select up to 4 Rings in CP Mode (about 60 cm* in z-direction), 2 Rings or 4 Clusters in Dual Mode (about 30 cm in z-direction), or 1 Ring or 2 Clusters in Triple Mode (about 17 cm in z-direction).

With Tim [76x18] you can select up to 4 Rings in CP Mode and Dual Mode (about 60 cm*), or 3 Rings or 6 Clusters in Triple Mode (about 45 cm* in z-direction).

Max. PAT Factors with Tim

	Tim [32x8]	Tim [76x18]	Tim [76x32]
head - feet	4 Head + Neck + Spine + Body 2 PA		
ant - post	3 $Head_{T\ 1\,ring}$ 2 others	3 $Head_T$ 2 Neck, Body+Spine, PA+Spine	
left - right	3 $H.S.B_{T\ 1\,ring}$ 2 $N_{\square}$, PA	3 $Head_T$, $Spine_T$, $Body_T$ 2 $Neck_{\square}$, PA	
max.	9 (3x3 $iPAT^2$) $_{1\,ring}$	12 (4x3 with $iPAT^2$)	

Table 1 *Possible iPAT factors for different Tim configurations and phase encoding directions. For example, with phase-encoding left-right, Tim [32x8] allows iPAT factors of 3 with Head-, Spine- or Body Matrix and iPAT factors of 2 with Neck- or PA Matrix.*

	Tim [32x8]	Tim [76x18]	Tim [76x32]
CP Mode	$FOV_z \geq 50$ cm (4 rings)		
Dual Mode	$FOV_z \geq 50$ cm (4 clusters) $FOV_z = 30$ cm (2 rings)		
Triple Mode	$FOV_z = 30$ cm (2 clusters) $FOV_z = 15$ cm (1 ring)	$FOV_z \geq 50$ cm (4 clusters) $FOV_z \leq 50$ cm (3 rings)	$FOV_z \geq 50$ cm (4 rings) + 8 spare channels

Table 2 *Possible FoV in z-direction for different Tim configurations and Matrix Modes. For example, Tim [32x8] allows a $FoV_Z \geq 50$ cm in Dual Mode if 4 clusters in z-direction are selected (e.g. spine imaging) or a $FoV_Z = 30$ cm if 2 complete rings in z-direction are selected (e.g. abdominal imaging with Body Matrix and Spine Matrix).*

And finally, with Tim [76x32] you can select up to 4 Rings in all 3 Modes (about 60 cm*).

7. What is Auto Mode?

Auto Mode is the smart operational mode. Depending on the Tim configuration, Field-of-View and iPAT factor, the Auto Mode selects the optimum Matrix Mode (CP, Dual or Triple) to get the job done.

The Auto Mode function, together with Auto Coil Detect and remote patient table positioning, are designed to minimize user-system interactions in order to maximize the focus of attention onto the exam itself.

In the current implementation of Auto Mode, Triple Mode is chosen most of the times when iPAT is selected and CP Mode is chosen if iPAT is deselected.

When selecting Auto Mode, the Auto Mode switch indicates which Matrix Mode will be used.

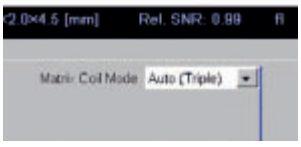

Figure 6 *When selecting Matrix Coil Mode "Auto", the user interface indicates the Matrix Mode chosen by the system (in this example Triple Mode).*

8. Is a Tim system limited to Matrix coils?

Not at all!

All MAGNETOM systems, including our new Tim systems, offer a host of coils for dedicated applications, like Wrist, Knee, Shoulder etc.

The MAGNETOM Avanto has two coil plugs that are compatible with coils from MAGNETOM Symphony and MAGNETOM Sonata. Most Symphony/Sonata coils can be connected to the system.

* *This is the FoV of the coil rings/clusters for RF signal reception. The max. FoV of MAGNETOM Avanto is 50 cm.*
4 rings/clusters with an "RF field" of 60 cm allow the flexible positioning of the coils with regard to the max. 50 cm FoV.
3 rings/clusters are just sufficient for covering the max. 50 cm FoV, but care has to be taken that the 3 rings/clusters exactly cover the FoV.

9. What is the meaning of Tim [32x8], [76x18] and [76x32] ?

Every Tim system is characterized by two numbers: The total number of coil elements which can be seamlessly connected to the system and the maximum number of true independent RF receiver channels available on the system.

Three Tim Levels

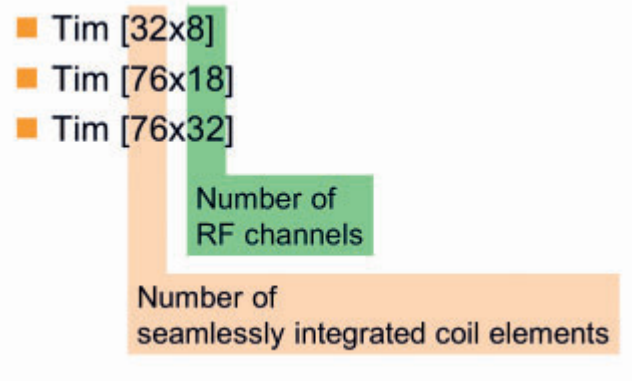

A necessary and unique component of a Tim system is the full RF channel switching matrix which allows free control over which of the up to 76 coil elements or mode signals are fed into the receiver chain with up to 32 receivers.

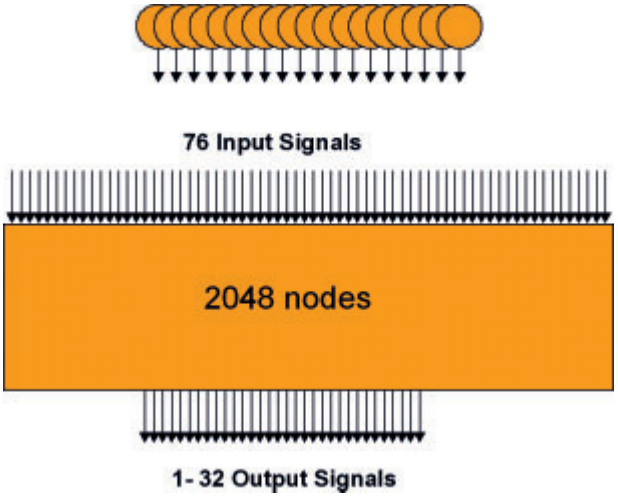

Figure 7 *Each Tim system contains a powerful and unique piece of hardware which allows free selection of up to 32 out of 76 Matrix coil elements.*

This concept is completely workflow-driven: During an exam, there is no need for manual patient repositioning and/or exchange of local coils. Everything can be done right from the user console. Auto Mode, Auto Coil Detect and remote patient table positioning minimize user-system interaction in order to maximize the focus of the attention onto the exam itself.

10. Which Tim configuration is the right one?

First, keep in mind that, whatever your initial choice, there is a clear and simple upgrade strategy from Tim [32x8] all the way up to Tim [76x32]. So, if today you are hesitant about going for the most advanced Tim [76x32] and for example instead decide to buy a Tim [32x8], you will not get penalized later when you change your mind and upgrade to Tim [76x18] or [76x32]. The exact same set of coils is available to all three Tim system configurations and there are no built-in obstacles that will make such a later upgrade difficult or highly expensive. The only hardware that is needed for this RF channel upgrade are the additional receivers. This is the major economical benefit from Tim's scalability!

Tim [32x8]: Tim performance for the high-end professional clinical routine. Whole-body examinations can be performed with up to 32 CP coil elements (i.e. using all Tim coils in CP Mode). Tim [32x8] allows true whole-body and local MRI in highest quality. It allows Parallel Imaging for the whole clinical routine. Note that Tim [32x8] already offers a performance level far beyond anything that is currently available elsewhere on the market. And this is not only due to a clear and simple upgrade path to higher Tim performance but also and especially due to the Parallel Imaging performance already in place with 8 channels.

Tim [76x18]: With its 76 seamlessly integrated coil elements and 18 independent RF receiver channels, it is the technology of choice for superior quality MRI, from clinical routine up to demanding research. Anatomically optimized for unlimited iPAT in large Field-of-Views, in all three dimensions.

Tim [76x32]: The top-of-the-line performance level, for all clinical areas including the most demanding research. This level is prepared for all new applications like MR-guided intervention where you might need further receiver channels for catheters or further antennas/coils.

11. Is there a need to buy new coils for upgrades within the Tim Technology (e.g. Tim [32x8] to Tim [76x32])?

No! This is one of the big advantages of Tim.
Tim and its Matrix Coils are 100% compatible with all upgrades. Not a single coil needs to be re-purchased in the event of an upgrade, e.g. from Tim [32x8] to Tim [76x18] or Tim [76x32]. More importantly, with the different Matrix Modes (CP, Dual, Triple), the Matrix coils can be "scaled" to the Tim levels. The same coil can make full use of the higher number of RF channels with a higher Tim level.

With a competitive system, you need to purchase new dedicated multi-channel coils to make full use of an RF receiver channel upgrade. Of course, the old coils would still be compatible – but what's the use of an RF channel upgrade when there are no coils to utilize the additional channels?

12. How does Tim help to handle the additional complexity?

You do not need to select coils on a Tim system – simply select the exam.
Auto Coil Detection will automatically determine the relative positions of all available coils (Matrix or other) in the Field-of-View. These relative coil positions are then

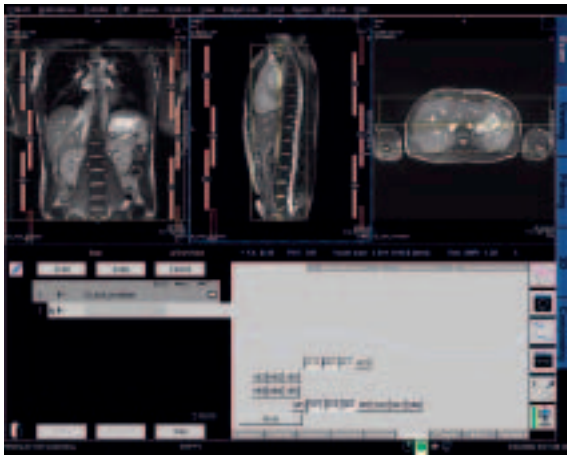

Figure 7 *The relative positions of the various Matrix coil clusters are visualized in the scout view as well as on the coil card in the user interface. In addition, Matrix clusters can be selected via mouse click from the scout view as well as through the coil buttons.*

shown as graphic superposition on the initial body scout views, where they can easily be selected with a mouse click.

With the Mode switch set to "Auto", the system will decide for you which Mode (CP, Dual or Triple) will be used during the exam. Non-iPAT exams are usually run in CP Mode, while iPAT exams may be run in CP, Dual, or Triple, depending on the phase-encoding direction and acceleration factor.

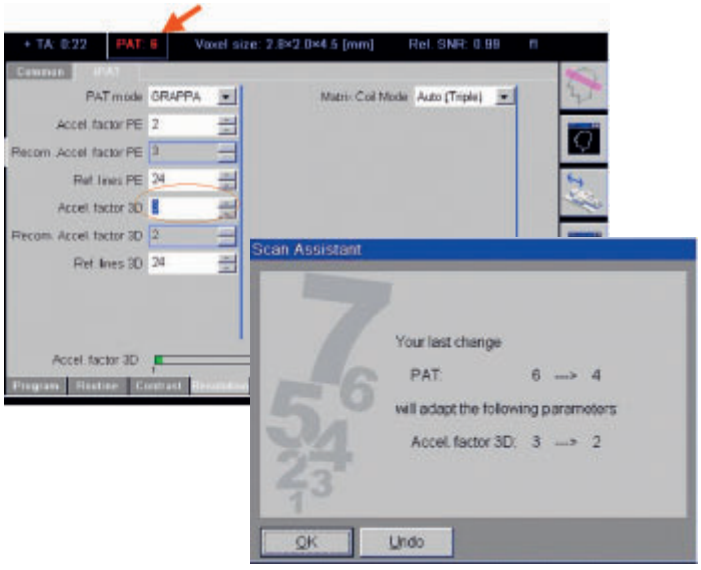

Figure 8 *The Scan Assistant will guide you through the entire setup procedure and will make recommendations where necessary.*

13. Why do uncombined Matrix images look different?

Advanced users who select "save uncombined images" in the user interface will notice that in Dual Mode and Triple Mode the uncombined images from Matrix coils differ from conventional coil images.

Only the uncombined CP Mode signal from a Matrix coil resembles a traditional coil image. Higher order mode signals only contain information from the periphery of the region-of-interest since the CP Mode signals already contain the full SNR at the center region of the images.

In analogy with stereo broadcasting, where L+R and L-R signals are used, a higher order Matrix mode signal is equivalent to the L-R signal in broadcast applications. In the same way the L-R signal would never be received and processed alone, higher-order mode signals are only received and processed in conjunction with lower-order mode signals.

The user selects CP, Dual or Triple mode in the user interface. Primary, secondary and tertiary modes are intermadiate signals invisible to the user.

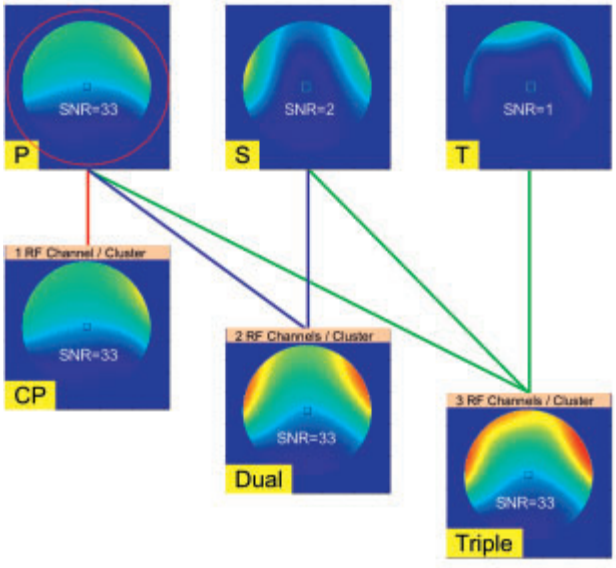

Figure 9 *The uncombined secondary and tertiary Mode signals S and T contain only differential information needed for iPAT, therefore these signals do not resemble conventional coil maps. Nevertheless, the combined array image from all mode signals P, S, T is identical to the array combination of the original coil signals R, M, L.*

MR Safety and Cerebrospinal Fluid (CSF) Shunt Vales

Frank G. Shellock, Ph.D.
FACC, FACSM

Adjunct Clinical Professor of
Radiology and Medicine
University of Southern California
and
Institute for Magnetic Resonance
Safety, Education, and Research

Hydrocephalus is the accumulation of cerebrospinal fluid in the brain, resulting from increased production, or more commonly, pathway obstruction or decreased absorption of the fluid. Cerebrospinal fluid (CSF) shunts have been used for decades for the treatment of hydrocephalus. A CSF shunt involves establishing an accessory pathway for the movement of CSF in order to bypass an obstruction of the natural pathways.

The shunt is positioned to enable the CSF to be drained from the cerebral ventricles or sub-arachnoid spaces into another absorption site (e.g., the right atrium of the heart or the peritoneal cavity) through a system of small catheters. A regulatory device, such as a valve, may be inserted into the pathway of the catheters. In general, the valve keeps the CSF flowing away from the brain and moderates the pressure or flow rate. Some valves are fixed pressure valves (i.e., monopressure valves) and others have adjustable settings. The drainage system using catheters and valves enables the excess CSF within the brain to be evacuated and, thereby, the pressure within the cranium to be reduced.

There are several different types of CSF shunt valves and associated accessories used for treatment of hydrocephalus. Information for certain CSF shunt valves is provided in this monograph. In general, for shunt valves that utilize magnetic components, highly specific safety guidelines must be followed in order to perform MRI procedures safely in patients with these devices.

CODMAN HAKIM Programmable Valve

The CODMAN HAKIM Programmable Valve (Codman, a Johnson and Johnson Company, Raynham, MA, USA) offers the ability to optimize the opening pressure of a shunt system before and after implantation. This is considered to be an important feature because the shunted patient's condition will often change over the course of treatment. The use of a programmable valve allows the surgeon to non-invasively change the opening pressure, negating the need for revision surgery to alter the valve pressure. Furthermore, the programmability of the valve may allow for the development of specialized treatment regimes.

The opening pressure of the CODMAN HAKIM Programmable Valve is changed through the use of an externally applied, magnetic field. The "spring in the ball and spring mechanism" of the valve sits atop a rotating spiral cam that contains a stepper motor. Applying a specific magnetic field to the stepper motor will cause the cam to turn slightly, increasing or decreasing the tension on the spring and ball, thus changing the opening pressure of the valve.

With regard to MRI, the product insert for the CODMAN HAKIM Programmable Valve states: "Note: Remember to verify valve pressure setting after an MRI."

Delta Shunt Assembly

The Delta Shunt Assembly (Medtronic Neurosurgery, Goleta, CA, USA) combines the Delta valve with an integral, open-end, radiopaque peritoneal catheter. All Delta shunt assemblies incorporate the same product features as the Delta valves. These include injectable reservoir domes, occluders for selective flushing, and a completely non-metallic design. The valves are fabricated of dissimilar materials – polypropylene and silicone elastomer – reducing the chance of valve sticking and deformation. The normally closed Delta chamber mechanism minimizes over-drainage by utilizing the principles of hydrodynamic leverage. Because of the non-metallic design, the Delta shunt is safe for patients undergoing MRI procedures.

POLARIS Adjustable Pressure Valve

The POLARIS Adjustable Pressure Valve (Sophysa USA, Inc., Costa Mesa, CA, USA) has magnets made of Samarium-Cobalt, which are specially treated to preserve permanent magnetization, even after repeated exposure to MRI at 3 Tesla. The principle of the POLARIS Adjustable Pressure Valve is based on the variation in pressure exerted on a ball by a semicircular spring at different points along its curvature. The flat semicircular calibrated spring determines an operating pressure. Because of the unique design of the POLARIS Adjustable Pressure Valve, it is considered to be safe for patients undergoing MRI procedures at 3 Tesla or less.

Pulsar Valve

The Pulsar Valve (Sophysa USA, Inc., Costa Mesa, CA, USA) for CSF drainage is a monopressure valve. Its principal is based on the play of a silicone membrane, calibrated in low, medium, or high pressure, ensuring a proximal regulation of CSF flow through the shunt system. The Pulsar Valve is safe for patients undergoing MRI procedures.

Sophy Mini Monopressure Valve

The Sophy Mini Monopressure Valve (Sophysa USA, Inc., Costa Mesa, CA, USA) for CSF drainage has a ball-in-cone mechanism. This device is safe for patients undergoing MRI procedures.

Strata Valve

The PS Medical Strata valve (Medtronic Neurosurgery, Goleta, CA, USA) is an adjustable flow control valve in which the resistance properties of the valve can be changed non-invasively by the caregiver. It is designed to minimize over-drainage of cerebrospinal fluid (CSF) and maintain intraventricular pressure (IVP) within a normal physiologic range, regardless of patient position.

Extensive testing of the Strata valve was conducted using MRI with a static magnetic field of 1.5 Tesla. Results of the testing indicated that the valve is "MR-Safe." That is, exposure of the valve to MRI scanning will not damage the valve, but it may change the valve's performance level setting. Therefore, after MRI exposure, the valve performance level setting needs to be confirmed and adjusted as necessary. From a diagnostic standpoint, the presence of the Strata valve in a patient may disrupt or impair the use of MRI if the area of interest is near the location of the valve (Personal Communication, 9/17/04, Karen Rhodes, Manager, Medtronic Neurosurgery, Goleta, CA, USA).

SOPHY Adjustable Pressure Valve

The principle of the SOPHY Adjustable Pressure Valve (Sophysa USA, Inc., Costa Mesa, CA, USA) resides in the variation in pressure exerted on a ball by a semi-circular spring at various points along its circumference. The spring is attached to a magnetic rotor whose position can be noninvasively altered using an adjustment magnet. A series of indentations allows a variety of positions to be selected, each position representing a different pressure setting. The valve's ball-in-cone mechanism maintains the selected pressure constant without significant drift through the time.

Because a magnetic component is associated with this device, special MR safety precautions exist for scanning patients with the SOPHY Adjustable Pressure Valve, as follows:

- The pressure settings should always be checked in case of shock on the implantation site.
- Changing pressure settings must only be performed by a neurosurgeon.
- The patient must be advised that carrying his Patient Identification Card is important and necessary for the follow-up of the clinical conditions.
- Patients undergoing MRI exposure should be advised that they might feel a small yet harmless effect due to MRI.
- The pressure settings should always be checked before and after MRI exposure, or after strong magnetic field exposure.
- The patient must be advised that in the case of implantation on the skull, vibrations due to CSF flow may be perceived.
- Patients with implanted valve systems must be kept under close observation for symptoms of shunt failure.

[For these devices, MRI healthcare professionals are advised to contact the respective manufacturer to ensure that the latest information is obtained and carefully followed in order to ensure patient safety.]

References

Codman, a Johnson and Johnson Company, Raynham, MA, USA; Cerebral Spinal Fluid Shunt Valves and Accessories, http://www.codmanjnj.com/CSFshunting.asp

Codman, a Johnson and Johnson Company, Raynham, MA, USA; Cerebral Spinal Fluid Shunt Valves and Accessories, http://www.codmanjnj.com/PDFs/Prog_ProcedureGuide.pdf

Medtronic Neurosurgery, Goleta, CA, USA; Cerebral Spinal Fluid Shunt Valves and Accessories, http://www.medtronic.com/neurosurgery/shunts.html

Sophysa USA, Inc., Costa Mesa, CA, USA; Cerebral Spinal Fluid Shunt Valves and Accessories, http://www.sophysa.com

A Success Story for Clinical Services and for MAGNETOM Trio

Hong Kong Sanatorium and Hospital

Dr.Gladys Lo, Radiologist-in-Charge, at the opening ceremony for MAGNETOM Trio.

Hong Kong Sanatorium and Hospital Limited (HKSH) is a private sector enterprise with more than 400 beds, and having been founded in 1922 are in operation for over 80 years. Since the inception of the hospital it has provided patients with excellence in service, use of the best equipment available combined with the support of highly trained staff. Recent examples in diagnostic imaging include HKSH as one of the first sites worldwide to put 16-slice multi-detector CT into early clinical practice with the release of Siemens SOMATOM Sensation 16. 16-slice CT is now considered at the high end of clinical service and widely used at prestigious institutions over the world. Even more recently HKSH introduced combined PET and CT imaging with Siemens Biograph PET/CT scanner. This was significant as the first installation worldwide of a PET/CT system with the revolutionary new Lutetium Oxyorthoscilicate crystal (LSO) detector technology – Siemens Biograph LSO. So the introduction of 3T MRI to clinical services in December of 2003 continued in the tradition of this hospitals' leadership model to provide state-of-the-art equipment for its patient services. It is also a first for hospitals in Hong Kong to see and experience clinical examinations being done locally at this field strength.

Exciting for MR users in the Asia region is the next generation of 3T technology. HKSH will be the first site in Asia and one of the very first in the world to use the Total imaging matrix – Tim at 3T. This comes in recognition by Siemens of the excellence and commitment of HKSH in 3T MRI, and the manner which HKSH has worked with others to provide access and educational value to users within Hong Kong and the greater Asia region. This should prove to be of significant value to patients and patient confidence, to clinicians for diagnostic sensitivity and accuracy, and to the business of diagnostic imaging – by providing workflow efficiencies not seen before at 3T and a new range of MR applications.

Early 3T sites face a challenge

3 tesla MRI scanner installations had predominantly been the domain of scientists and researchers and most often these sites confined themselves to neuroscientific work. While 3T MRI clinical services do exist worldwide it remains uncommon for 3T MRI to be targeted at the provision of specialist clinical diagnostic services throughout all regions of the body while not still dedicating a major component of service time to scientific endeavours. In contrast to the conventionally applied field strength of 1.5T MRI which has had many years of protocol maturation in clinical service and in understanding the contrast mechanisms, 3T on the other hand has not had the same benefit of time for protocol optimisation. Contrast mechanisms at 3T change – so re-education of staff is necessary to align themselves to operate with the specialties of 3T MRI. Moreover, often these 3T systems are supported strongly by scientists, physicists or engineers. These are the new challenges for institutions such as HKSH whose ambition is to explore and exploit the benefits to patients of 3T MRI.

State-of-the-art MRI for clinical services

HKSH have a highly experienced radiographic operator and diagnostic services required from the 3T MRI cover the full spectrum of patient examinations which are routinely delivered from 1.5T MRI – this group does not confine them to imaging of the brain, as is often the case at other 3T centres. Upon installation HKSH personnel immediately underwent specialist training programs for 3T MRI and initiated their own internal investigation comparing 3T diagnostic images with 1.5T to validate clinical services.

1.5T 3T

Figures: Initial examples comparing 1.5T and 3T MRI:

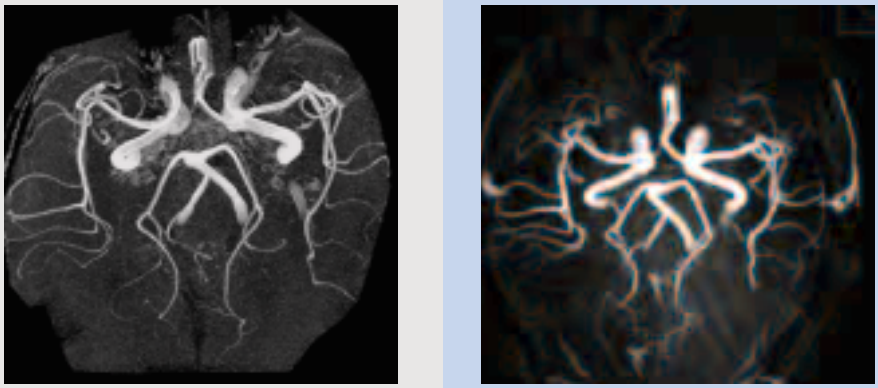

Figure a *MR Angiography with 3T showed smaller vessels and more distal branches compared to 1.5T.*

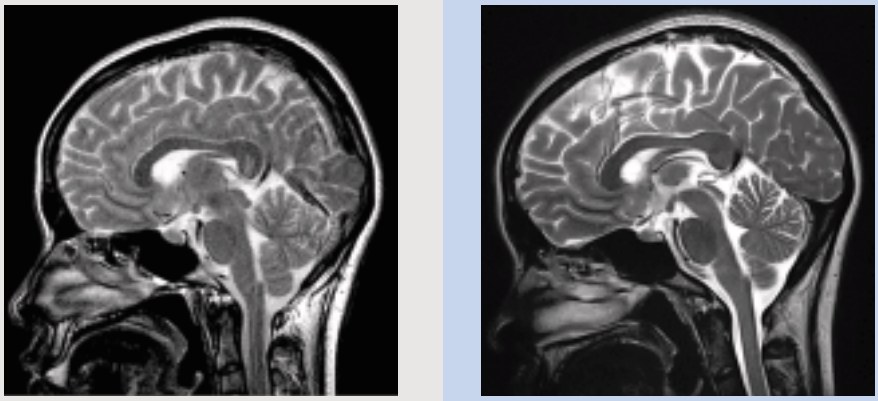

Figure b *Showing exquisite detail of the midline structures compared with the comparable acquisition protocol at 1.5T (left image).*

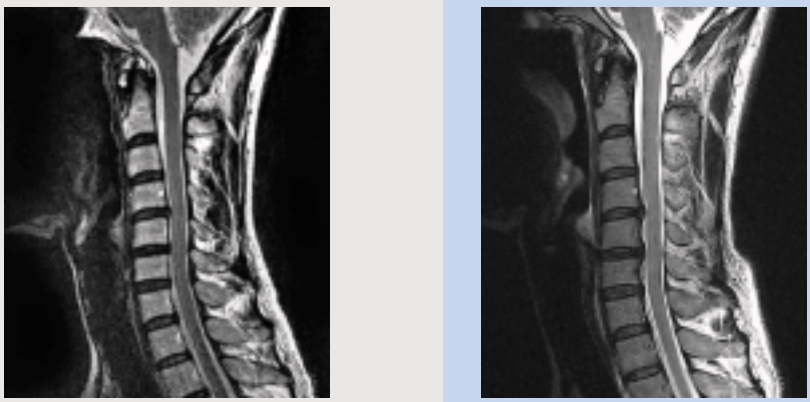

Figure c *A more clearly defined disk herniation C4/5 and disc bulges at C5/6 and C6/7.*

1.5T 3T

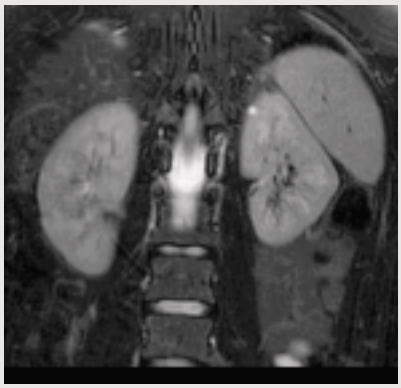


Figure d *Differences in image definition shown here for the kidneys and liver,*

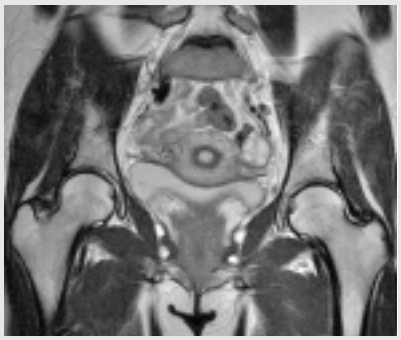
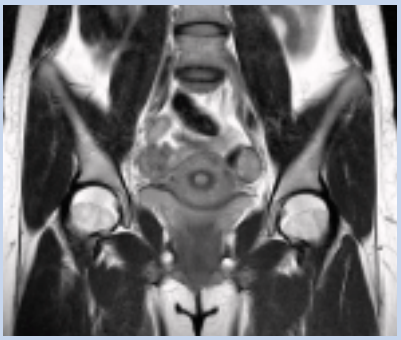

Figure e *for the pelvis,*

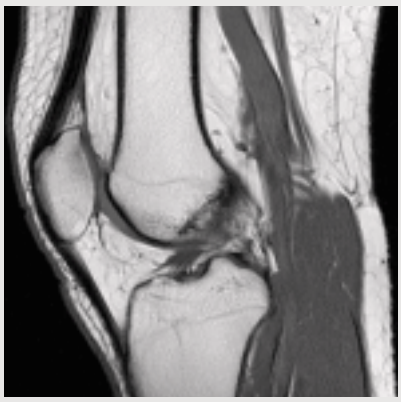
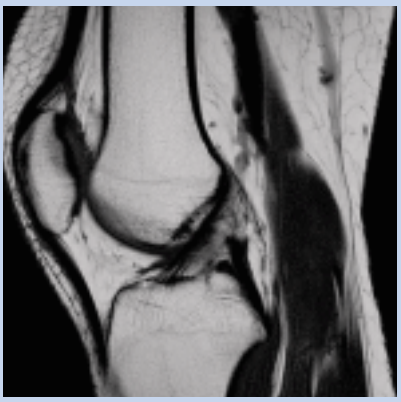

Figure f *and an example of orthopaedic imaging.*

HKSH routine patient cohorts for 3T MRI are spine, abdomen, brain, angiography, orthopaedics, breast and even cardiovascular services are possible. For some examinations the comparisons made between 1.5T and 3T have now led to a migration of applications to 3T.

Building on the strengths of 3T MRI

There are clear advantages to many MR examinations by taking advantage of improvements in resolution. HKSH have capitalised on the strengths of 3T MR in angiography, neuro imaging paediatrics, orthopaedics, and others.

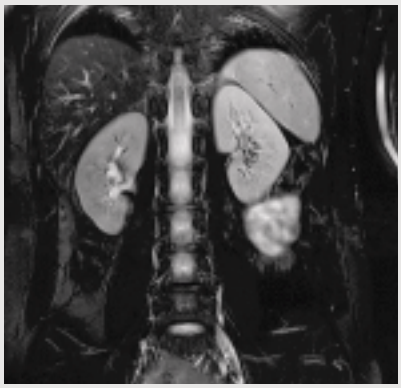

Figure a

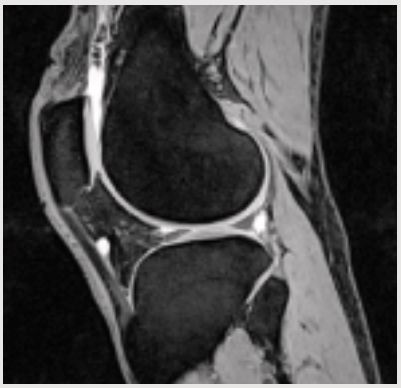

Figure b

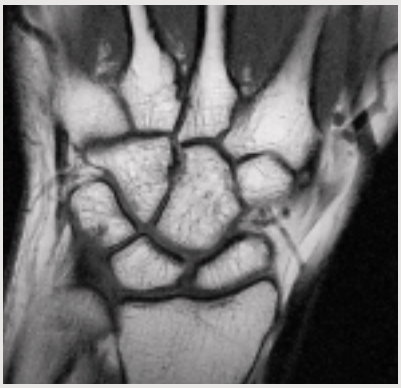

Figure c

Figures
Examples where HKSH have been able to realise the benefits of 3T: a) Large FoV abdominal imaging with fat saturation, b) orthopaedic imaging using 3D-DESS imaging with water excitation, c) wrist imaging.

For example, an unexpected result where HKSH have been doing breast examinations on their 1.5T, they now perform these at 3T because of the clear benefits to patients from greater resolution. Furthermore, with Siemens' VIEWS technique for bi-lateral breast imaging they are able to image both breasts at the same time whereby they had previously been required to image each separately. On top of this, new clinical services have now been made possible with 3T.

New clinical services

While the quality of MR imaging at 3T is well known, what is not so well defined is what new clinical services are possible from this field strength by leveraging the higher signal-to-noise and the new contrast mechanisms. This has been a discovery for HKSH. Early in their experience new applications and referrals were found. For example, it is now possible for the neuro department to refer to 3T MRI for aneurysm, previously the domain of DSA. What 3T MRI offers using the Time-of-Flight technique is a non-invasive examination of aneurysm, without x-ray radiation, and without the need to administer
a contrast agent.

Figure
Early example of an aneurysm of the carotid siphon imaged at 3T using Time-of-Flight angiography (4 mm aneurysm, no contrast required).

As the resolution from 3T MRI can be increased there is now greater interest to move away from examinations using invasive techniques or x-ray radiation, particularly in paediatric cases. So now the conventional diagnostic boundary between modalities is blurring. Non-invasive examinations combined with 3T image quality and without x-ray radiation is testing these boundaries.

New referrals

Imaging at higher field strengths can offer improved diagnostic accuracy and image quality. After installing MAGNETOM Trio, HKSH experienced a positive influx of referrals from outside the hospital itself, particularly from neurologists who wish to examine more challenging diagnostic cases – such as can be found in paediatric neuro and spine diseases.

"There has been much interest in what 3T offers clinical services as compared with the more routine 1.5T MRI scanners. This has contributed to the new referrals." In doing so HKSH also provides an educational opportunity for other groups within Hong Kong to experience 3T and compare for themselves first hand the clinical value with respect to the more widely used 1.5T scanners.

HKSH contributing to research programs in Hong Kong

Within a few weeks of 3T operation, HKSH were quick to realise new and advanced techniques available for functional imaging of the brain. Multi-directional diffusion-weighted imaging sequences combined with specialised fibre tractography software from Massachusetts General Hospital in Boston, USA allowed HKSH to demonstrate the white matter fibres in the brain, and the brain's enormous connectivities. HKSH has specialised sequences for acquisition of the diffusion tensor from up to 99 different directions in a single examination. The initial application for HKSH was to study the integrity of fibre tracts affected by stroke.

BOLD (**B**lood **O**xygen **L**evel **D**ependent) imaging is available for real-time demonstration on the operator's console at HKSH. Specialised sequences are installed that allow a spiral acquisition for increases in resolution, improved susceptibility effects at 3T, and to use shorter echo times (TE).

Combining these specialised areas of diffusion tractography and BOLD imaging allows researchers to study the connectivity of the brain, localising cognitive processes across the brain, and relating this with communicating white matter fibres.

Since taking these initial steps researchers from Hong Kong University are now using the new HKSH facilities and undertaking their neuroscientific programs based on data collected from Siemens MAGNETOM Trio 3T MRI. Dr. Li Geng from Hong Kong University department of Electrical and Electronic Engineering investigate the use of functional MRI (fMRI) at 3T as a means to predict the effects/benefits acupuncture may offer patients paralysed by stroke.

Stroke is the second most common cause of death in China and the third most common cause of death in Hong Kong. According to Dr. Li many stroke patients do try acupuncture to promote functional recovery, despite a lack of compelling evidence for its effectiveness. However, his co-workers indicate that stimulation of certain acupoints on stable stroke patients, with specific types of persistent functional deficits, can activate specific and relevant brain areas during functional magnetic resonance imaging. This is a new and potentially significant discovery.

Figures
Study of connectivity in the brain: Examples from Diffusion Tractography of the*
a) Corpus Callossum,
b) Internal Capsule, and
c) Forceps. Each tractography image was constructed from diffusion imaging of 72 independent directions.

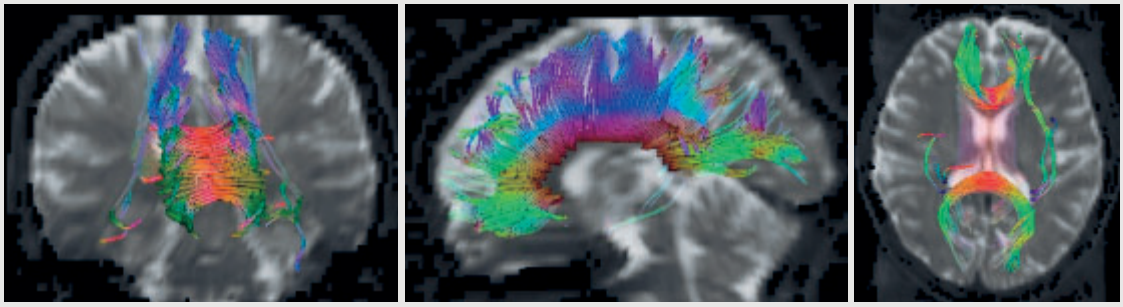

Figure a *Corpus Callossum*

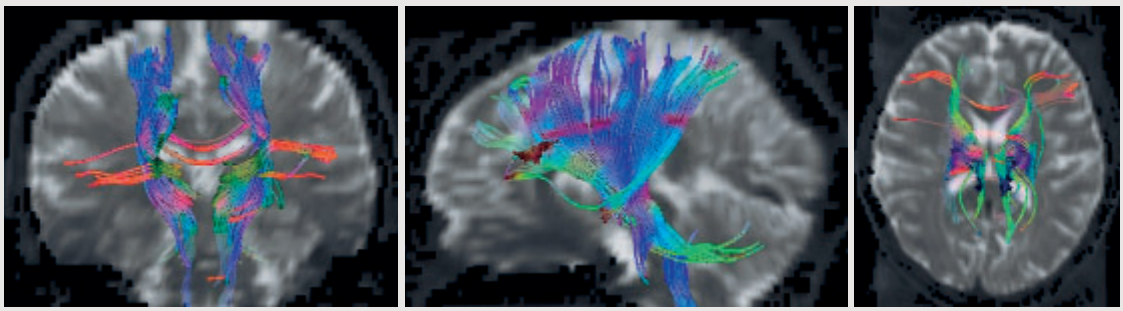

Figure b *Internal Capsule*

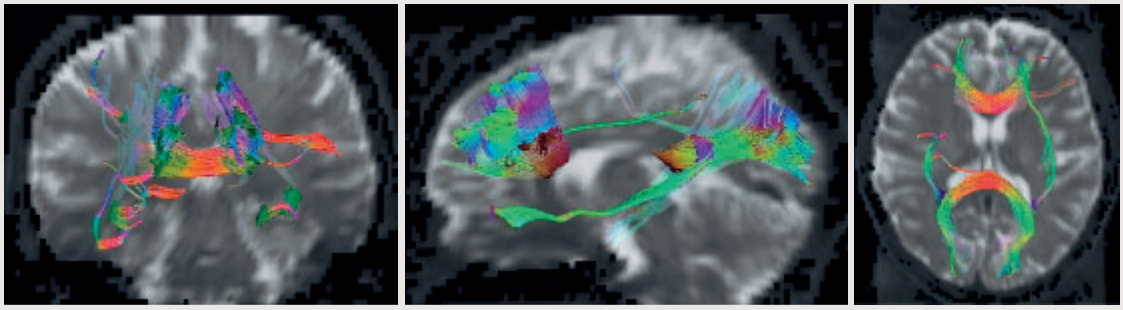

Figure c *Forceps*

**The information about this application is preliminary. The application is under development and is not commercially available in the U.S., and its future availability cannot be ensured.*

Dr. Khong Pek Lan, an associate professor at the department of diagnostic radiology of the University of Hong Kong proposes to use two new techniques at 3T, Diffusion Tensor Imaging (DTI)* and functional MRI (fMRI), to study behavioral development, specifically response inhibition of the maturing brain. Response inhibition is an important step in cognitive development for the maturing brain whereby we adopt and apply behavioural rules that prevent us from inappropriate behaviour. By combining these two sets of DTI, fMRI and cognitive testing into one study, the question on how response inhibition develops in relation to brain maturation can be investigated.

At HKSH diffusion imaging has been extended beyond examination of the brain and to the spinal cord. While conventional MR imaging allows the physical compression to be seen clearly on the image, no internal damage to the white or grey matter can be seen. Dr. Ng Man Cheuk however sees the possibility that diffusion tensor imaging (DTI) in the spinal cords may localise the structurally damaged fibres in patients with spinal dysfunctions. Positive results to date have been shown which suggests that DTI is likely to be a possible diagnostic tool. In their initial studies, they are using DTI to localize the damaged regions in cervical myelopathy patients. Myelopathy exists as the most common cause of spinal cord dysfunction in the elderly. This information may facilitate the surgeons to decide which kind of surgeries will be the most suitable for patients. As a result, the risk of surgery can then be lowered.

"This sort of study is still quite unique at 3T. While the application of DTI in the spinal cord has its challenges at 3T with the inherent increase in susceptibility effect associ-

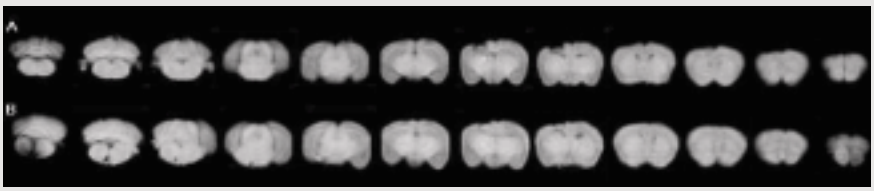

Figure *Stroke model for mouse imaged on MAGNETOM Trio.*

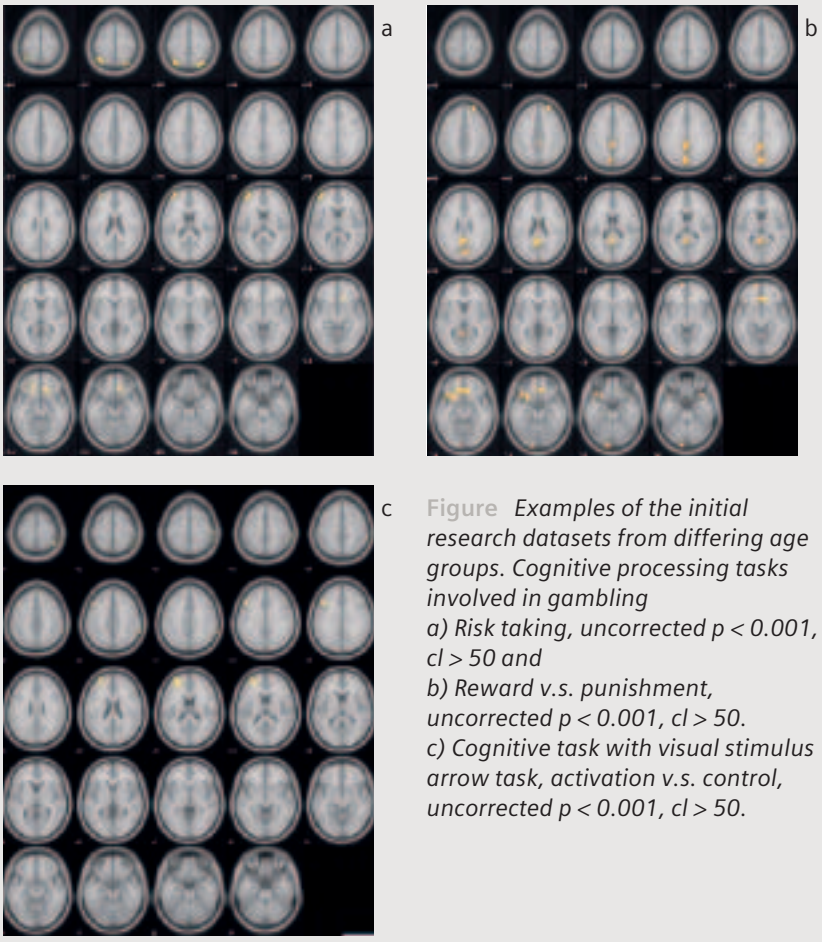

Figure *Examples of the initial research datasets from differing age groups. Cognitive processing tasks involved in gambling*
a) Risk taking, uncorrected p < 0.001, cl > 50 and
b) Reward v.s. punishment, uncorrected p < 0.001, cl > 50.
c) Cognitive task with visual stimulus arrow task, activation v.s. control, uncorrected p < 0.001, cl > 50.

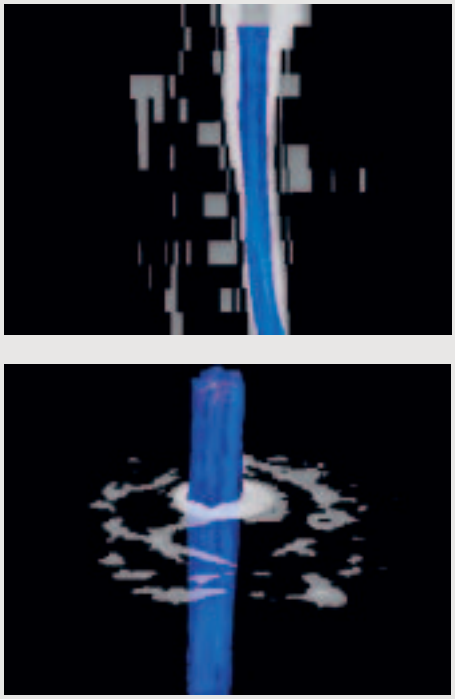

Figure *Example of Diffusion Tractography* results from imaging of the cervical spine.*

ated with higher field strength, this is somewhat overcome by Siemens iPAT technologies (integrated Parallel Acquisition Technology) available on MAGNETOM Trio . Parallel imaging from the spine array is a key design ingredient for image quality by reducing the susceptibility effect around the spine."

The future of MRI services at HKSH

In July HKSH will be the first institute in the Asia Pacific region to install Tim technology, the **T**otal **i**maging **m**atrix at 3T. Although Tim technology has created a revolution at 1.5T now proven with over 360 clinical installations worldwide, it has even more to offer at higher field strengths where the power of Tim can be extended towards the extreme of current MR applications. In fact you could say that "3T and Tim was meant to be". Tim offers further SNR gains for 3T applications, allows MR to operate with parameters not seen by conventional MRI in speed and resolution, and of course with its very high density of coil elements the Parallel Imaging of Siemens iPAT can reach acceleration factors as high 16 – with the standard coils delivered. At HKSH we aim to see 3T and Tim coming together delivering "undreamed of clinical performance".

The future is brighter than ever for their patients, the clinicians reporting on MRI, associated research programs, and the business of radiology at HKSH. Tim technology has much to offer all of these areas.

**The information about this application is preliminary. The application is under development and is not commercially available in the U.S., and its future availability cannot be ensured.*

The information in this document contains general descriptions of the technical options available, which do not always have to be present in individual cases.

The required features should therefore be specified in each individual case at the time of closing the contract.

Siemens reserves the right to modify the design and specifications contained herein without prior notice. Please contact your local Siemens sales representative for the most current information.

Original images always lose a certain amount of detail when reproduced.

This brochure refers to both standard and optional features. Availability and packaging of options varies by country and is subject to change without notice. Some of the features described are not available for commercial distribution in the US.

Siemens AG
Wittelsbacherplatz 2
D-80333 Muenchen
Germany

Headquarters
Siemens AG, Medical Solutions
Henkestr. 127, D-91052 Erlangen
Germany
Telephone: +49 9131 84-0
www.siemens.com/medical

Contact Addresses

In the USA
Siemens Medical Solutions USA, Inc.
51 Valley Stream Parkway
Malvern, PA 19355
Telephone: +1 888-826-9702
Telephone: +1 610-448-4500
Telefax: +1 610-448-2254

In Japan
Siemens-Asahi
Medical Technologies Ltd.
Takanawa Park Tower 14F
20-14, Higashi-Gotanda 3-chome
Shinagawa-ku
Tokyo 141-8644
Telephone: +81 3 5423 8411

In Asia
Siemens Medical Solutions
Asia Pacific Headquarters
The Siemens Center
60 MacPherson Road
Singapore 348615
Telephone: +65 6490-6000
Telefax: +65 6490-6001

In Germany
Siemens AG, Medical Solutions
Magnetic Resonance
Henkestr. 127, D-91052 Erlangen
Germany
Telephone: +49 9131 84-0

Siemens **Medical Solutions** that help

Order No. A91100-M2220-F691-9-7600
Printed in Germany
CC MR 66214 WS 040520.